Individual-based movement model of mule deer (*Odocoileus hemionus*) contacts and application to artificial attractants

by

Kelsey M. Gritter

A thesis submitted in partial fulfillment of the requirements for the degree of

Master of Science

in
Ecology

Department of Biological Sciences
University of Alberta

Abstract

Chronic wasting disease (CWD) is an emerging prion disease in Canada that infects mule deer, white-tailed deer, elk, and moose by direct and environmental transmission and is invariably fatal. CWD spread can be promoted at "hotspots" that attract deer, such as attractants that are created in fields by hay bales and grain bags, and attractants such as grain bins and agricultural storage at farm sites. An individual-based model was created to investigate the effects of different densities and arrangements of hotspots on contact rates between- and within-groups. The model tracks contacts (when two individuals come within five meters of one another), which are defined as between- or within-group depending on the group membership of the two individuals. Simulations are run in Netlogo on a heterogeneous landscape and include behaviours such as grouping and home ranges. Using a two-hour time step, deer are moved across the landscape based on both step-selection movement rules relative to resources and group behaviours. The integrated step-selection function utilizes GIS layers for environmental weights and GPS-collar movement data for calculating step-selection coefficients, and step length distributions. Sensitivity analysis was performed on the model and revealed a greater sensitivity of within-group contacts to changes in model parameters, particularly group cohesion. Following model analysis, simulations were run to assess the effect of artificial attractant (AA) density and configuration using two strategies for initial placement of attractants, random and clustered around farms, and two strategies for removing them, random and by proximity to woody cover. Simulations revealed that reducing the number of attractants on the increases between-group contacts as well as unique contacts between deer. Additionally, reducing AA density generally increased overall unique visits per site indicating potentially greater environmental contamination at remaining sites. Although having no attractants produced the

lowest contact rates, management must take into consideration the feasibility of eliminating all attractants and the potentially negative impacts if sufficient reduction of AAs is not achieved. Additionally, the strategy used to eliminate attractants must be considered because although removal by proximity to woody cover and random removal showed similar patterns, removing by proximity to woody cover caused a greater increase in contacts for field attractants. For removal at clusters around farms, removing individual attractants versus all attractants in a cluster resulted in different trends as removing individually had a limited effect on contacts, whereas removing by cluster caused an increase in between-group contacts. If feasible, management should aim to eliminate attractants via mitigation strategies and enforcement; however, if insufficient resources are available for enforcement, then management strategies should be taken with caution because insufficient reduction of attractants could worsen contact rates.

Preface

This thesis is an original work by Kelsey Gritter. The research project, of which this thesis is a part, received research ethics approval from the University of Alberta Research Ethics Board for both time periods, project name “Chronic Wasting Disease: Mule Deer Contact Rates”, AUP00001461 and AUP00001369, 2007-2011 and 2017-2021.

Acknowledgements:

I would like to thank both the Lewis and Merrill-Boyce lab members for their support and feedback throughout my thesis. My lab and office discussions/environment have been invaluable in the completion of my thesis. I'd particularly like to thank Maria Dobbin who worked closely on the CWD project with me and gave valuable input and support throughout. I would also like to thank my supervisors Mark Lewis and Evelyn Merrill for their support, feedback, and guidance throughout my thesis, this thesis would not be what it is without you. I'd also like to thank my committee member Margo Pybus whose perspective, resources, and input were key in helping to shape this project to be a better product that is more useful for management. Thanks also to Scott Nielsen for agreeing to be part of the examination committee. Additionally, I'd like to thank my parents for their love and support throughout this process, celebrating the highs and supporting me through the difficult times.

Table of Contents

List of Tables

List of Figures

Chapter 1: Introduction

Disease is an ecologically important problem in populations because it can cause increased mortality and population declines (Cotterill et al., 2018; McCallum et al., 2009). This in turn can affect ecosystem function as population declines or extinction of species can disrupt natural functioning (Herrera and Nunn, 2019). A variety of modelling techniques have been useful in investigating the effects of disease, as well as certain conservation and management strategies. These models include top-down models such as compartments models and ordinary different equations, and bottom-up models such as individual-based models (Croft et al., 2020; Wells et al., 2019; White et al., 2018a). These models can shed light on the influence of factors such as connectivity, landscape heterogeneity/fragmentation, social behaviours, and vaccinations, and give information on elements such as disease risk, spread, persistence, outbreak size, and outbreak duration (Ramsey and Efford, 2010; Silk et al., 2019; White et al., 2018b, 2018a). Models can enable one to test multiple scenarios and strategies, without requiring manipulation of the landscape or large-scale experiments, making them useful tools in conservation disease management.

Chronic wasting disease (CWD) is a transmissible spongiform encephalopathy (TSE) first discovered in Colorado in 1967, and was classified as a TSE in the 1970s (Miller and Williams, 2004; Williams and Young, 1982, 1980). Currently found in 3 Canadian provinces, CWD first spread into wild deer in Saskatchewan in 2000 before spreading to wild deer in Alberta in 2005 (Miller and Williams, 2004; Smolko et al., 2021). In Alberta, continued surveillance occurs via submission of cervid heads by hunters in wildlife management units (WMUs) along the front edge of spread (https://www.alberta.ca/chronic-wasting-disease-surveillance-and-response.aspx). In 2020, CWD was found in 12 new WMUs along the south

and southwestern fronts (https://www.alberta.ca/chronic-wasting-disease-updates.aspx). Overall, in Alberta the total prevalence exceeds 10% with some areas, such as some WMUs along the Saskatchewan border, having a prevalence as high as over 50% in male mule deer (https://www.alberta.ca/chronic-wasting-disease-updates.aspx). Social interactions impact spread because the disease is transmitted both directly and indirectly, and season will change the ratio of between- and within- group contacts, and the number of contacts (Schauber et al., 2007; Silbernagel et al., 2011). For example, higher contacts are observed during gestation (Dec. 16-May 16), and contacts are more often between deer of the same sex, except in rut (Silbernagel et al., 2011). Additionally, the ratio of within:between group contacts is higher in the spring/autumn, but this ratio did not differ from 1 in the summer (Schauber et al., 2007).

At present there is no cure or vaccine for controlling CWD and management actions have focused primarily on harvest strategies or using sharp-shooters to remove groups around infected animals (Heberlein, 2004; Manjerovic et al., 2014; Mateus-Pinilla et al., 2013) or removing the group of individuals with the highest prevalence levels, i.e., males (Heberlein, 2004; Potapov et al., 2013). These efforts have been relatively effective at slowing progression as a retrospective study by Conner et al. (2021) showed that number of male deer harvested or number of hunters 1-2 years prior was an explanatory variable for male CWD prevalence in all competitive models.

A third key strategy common in most CWD management plans is the reduction of artificial attractants (AA) such as supplemental feeding sites and grain spillage (Heberlein, 2004; Peterson et al., 2002; Western Association of Fish and Wildlife Agencies, 2018). Many governmental jurisdictions in North America, including Wisconsin, Michigan, Illinois, Colorado, Ontario, Alberta, and others have banned feeding deer as part of their initial management strategy. Banning baiting has been and is a strategy for managing other diseases where

transmission is facilitated by congregation such as bovine tuberculosis among white-tailed deer in Michigan, where bans have been in place for a long time, though issues with compliance still arise (Cosgrove et al., 2018; O'Brien et al., 2011, 2006). Apparent prevalence of bovine tuberculosis did decrease overall; however, bait management was in conjunction with other management strategies such as density reduction so the bans cannot be isolated as the cause (O'Brien et al. 2011). Baiting bans for CWD have varied in their longevity as in places such as Wisconsin the bans were not received well and received pushback from businesses selling bait due to lost revenues, hunters because of reduced harvest opportunities, and the public who feed wildlife to view them (Bartlett et al., 2003; Heberlein, 2004; Holsman et al., 2010; Peterson et al., 2002; Western Association of Fish and Wildlife Agencies, 2018). This pushback has led to the removal of bans in the long run when political action opposing the bans has been strong (Heberlein, 2004). While the bans aiming to reduce supplemental feeding are still in place in Alberta, other places such as Norway have found that a ban has not been successful in removing all supplemental feeding sites (Mysterud et al., 2019).

Previous modelling for CWD has investigated disease elements such as potential transmission methods, hunter-harvest strategies, relative importance of direct and indirect transmission, frequency- versus density-dependence, and transmission coefficients (Almberg et al., 2011; Belsare et al., 2020; Conner et al., 2021; Potapov et al., 2013, 2015). Although less modelling has been done on CWD and AA, the work that has been done, in combination with previous research on AA in relation to bovine tuberculosis, has revealed the importance of habitat in which the AA is located, type of attractant, and layout of feed at the AA (Cosgrove et al., 2018; Mejía-Salazar et al., 2018; Miller et al., 2003; Thompson et al., 2008).

In this thesis, I develop an individual-based model for mule deer movement that accounts for grouping, home range, and resource selection behaviours and use this model to assess direct contact rates of deer, particularly in the context of artificial attractants. In Chapter 2, I develop the model and then assess model sensitivity and performance. In Chapter 3, I use this model to evaluate different densities and configurations of attractants and their impact on model outputs including within-group and between-group contacts, unique contacts between deer, number of attractants used by deer, and the number of unique deer visiting each site. Attractants were placed to represent either a) grain bags and hay bales left in the fields or b) crop storage and grain bins at farm sites. Two AA removal strategies were investigated including random removal and removal by proximity to woody cover. This model gives unique insight into the effects of removal strategies and density/configuration that can be difficult to obtain experimentally and adds key knowledge to the existing work on AA and wildlife disease.

Chapter 2: Individual-based movement model of mule deer (*Odocoileus hemionus*) contacts

Introduction

Disease can negatively affect populations and ecosystems by causing mortality directly or by lowering individual fitness (Cotterill et al., 2018; McCallum et al., 2009). In turn, declines in some species due to disease can alter ecosystem functioning (Herrera and Nunn, 2019). A range of modelling tools from top-down**,** compartmental and ordinary differential equations models to bottom-up, individual-based models (IBMs) have been used to gain insight when addressing the impact of diseases on species and ecosystems (Croft et al., 2020; Wells et al., 2019; White et al., 2018a). Epidemiological studies using compartment models and ordinary differential equations can address questions related to pathogen invasion, disease dynamics and persistence, and population thresholds. However, because they employ population averages and do not let each individual have unique values and combinations of parameters (Mortensen et al., 2021; Murphy et al., 2020), they provide less insight on the effect that small-scale, individual variation in host responses to heterogeneity in environmental conditions has on disease dynamics.

In contrast, bottom-up IBMs are advantageous in that they have the advantage of allowing spatial and, uniquely, individual heterogeneity, allowing for variation between individuals in behaviour and state variables (An et al., 2020; Kerr, 2019; White et al., 2018a). For example, Scherer et al. (2020) found that predicted probabilities of disease persistence were up to eight times higher when the underlying habitat structure was accounted for in individual movement. Responses to environmental heterogeneity may be particularly important for wide-ranging hosts, such as large mammals, where the behavioral interaction with the environment, such as habitat selection while moving, can influence host interactions and alter disease spread (Accolla et al., 2021; Scherer et al., 2020). Further, IBMs facilitate the incorporation of host

grouping patterns and their correlated movements, which can influence rates of contacts and disease transmission (Schauber et al., 2007; Tosa et al., 2015). As a result, IBMs lend themselves to assessing management strategies and the sensitivity of model outcomes to changes in individual behaviors and in different environmental conditions (Kerr, 2019; Maloney et al., 2020; Ramsey et al., 2014). This is particularly useful for assessing disease management strategies that focus on altering host densities or the spatial pattern in resources influencing their movement and distribution. At the same time, IBMs require a large amount of data to parameterize and can be highly computationally expensive (Crooks et al., 2008; White et al., 2018a). To combat these challenges, I used data collected over many years to parameterize and perform sensitivity analysis on non-data-driven parameters to assess their influence on the model outputs. I also used servers with high computational power to avoid the limitations of computation.

In this Chapter, I present an IBM to predict contact rates of mule deer (*Odocoileus hemionus*) in a heterogeneous environment as a surrogate of animal-to-animal disease transmission. The model can be used to address questions such as how the density and spatial distribution of natural and artificial resources (e.g., food items) influence sex-specific contact rates (Chapter 3), the degree to which frequency- and density-dependent transmission influence disease dynamics, and how different placement strategies of oral vaccine baits influence their rates of encounter (Manlove et al., 2017; Ramsey and Efford, 2010; Smith et al., 2009; Thulke and Eisinger, 2008). I include realistic, sex-specific behaviors of mule deer such as home ranges, where individuals select the location of their home ranges based on landscape characteristics, and selection of preferred habitats while moving within a home range. I include these two scales of resource selection because they may promote conspecifics contacts when deer are attracted to

resources and use the same areas (Herrera and Nunn, 2019; White et al., 2018b). I incorporate social group structure to be able to assess how within- and between-group contacts change with group size and environmental conditions. I do not include demographic changes in the population (i.e., birth/death; immigration/emigration). Instead, the model focuses on mule deer contact rates in winter when mule deer are generally more concentrated and form larger, mixed-sex groups (Lingle, 2003), and assumes winter home range size and habitat selection patterns during movement remain constant. However, the model could be extended to include more seasons with seasonally changing behaviors within a year.

Simulations were conducted across a real landscape representing habitats in eastern Alberta, where chronic wasting disease (CWD) was first detected in 2005 and has since been rapidly increasing. Chronic wasting disease is a transmissible spongiform encephalopathy caused by prions that is 100% fatal in cervids including mule deer (Saunders et al., 2012; Williams et al., 2002). Prevalence of CWD in harvest mule deer submitted for testing in Alberta was 14.8% in 2020. CWD transmission occurs both directly through contact between individuals and indirectly through the environment (Williams and Miller, 2003); however, transmission during establishment is likely dominated by animal-to-animal contact whereas environmental transmission is likely a major route of transmission after CWD becomes well-established (Almberg et al., 2011). To parameterize the model, I used data from mule deer in this region. Winter deer densities, group size, and composition of groups were based on winter aerial surveys during 2008, 2009, 2018, and 2020, whereas 81 GPS-collared mule deer, monitored over two periods (2006 - 2009, 2017 - 2020), provided the basis for home ranges sizes, home range resource selection function, and movement integrated step selection functions. Outputs of the

model include between- and within-group contacts by dyad type (male-male, male-female, female-female).

I first give an overview of the model details in a standard presentation format for IBMs (Grimm et al., 2010, 2006). I assessed model performance by comparing a map of the simulated contacts across the landscape to a map of the probability of contacts occurring in a location, which was derived statistically based on known contacts of GPS collared deer (Dobbin 2022). I also performed a sensitivity analysis on model parameters to identify model output patterns in response to parameter changes, model robustness, and key parameters driving outputs (Cariboni et al., 2007; Manlik et al., 2018; Prieto and Ibarguen-Mondragon, 2019; ten Broeke et al., 2016). Sensitivity analysis can be done using local methods, such as one-at-a-time testing where each variable is tested and varied individually, or using global methods, such as variance- or regression-based methods that test the influence of covarying parameters (Ligmann-Zielinska et al., 2020; ten Broeke et al., 2016). In this work I used Latin-hypercube sampling to sample the parameter space, which takes equal samples across the parameter range, and then used regression-based analysis to evaluate the results. Partial correlation coefficient values were used to identify linear effects whereas partial rank correlation coefficient values were used to look for non-linear effects (Helton and Davis, 2003).

Methods

Overview

Purpose

The purpose of this work is to use an IBM to simulate seasonal within- and between-group contacts of mule deer on a real, heterogeneous landscape and to record contact rates by deer and

by patch, where a patch is a 30 x 30-m cell. The model was programmed, and simulations were run in Netlogo 6.1.1. (Wilensky, 1999). The IBM incorporates key deer behaviours including seasonal grouping, home ranges, and resource selection, with the aim of producing a depiction of potential contact rates and locations that may be representative of disease transmission on a heterogeneous landscape. This model can be used to assess how sensitive the rates and distribution of contacts among the sexes are to landscape heterogeneity, and to evaluate disease management scenarios such as removal of artificial food attractants (Chapter 3).

State Variables and Scales

There are two key sets of state variables for the model -- those belonging to the patches, and those belonging to the deer (Appendix A). The patches are characterized by attributes which consist of input values representing landscape features derived from GIS layers (Table 2.1), proportional selection weights for the integrated step-selection functions, as well as outputs of cumulative between- and within-group contacts and cumulative contacts by deer dyad type. Landscape covariates include vegetation features, topography, and distance to linear features, which are described in Table 2.1. Patches represent a 30-by-30-meter area for consistency across GIS layers.

Individual deer variables include the movement variables of step length, turning angle, and the proportional weight at end point destination of the step. Each deer has its own turning angle distribution, a von Mises distribution, which depends on the *vm-length* that represents the agreement between the direction of persistence and the direction towards the home range centroid, as well as *sine* and *cosine* which are used to define the mean turning angle. Deer also have variables defining their sex, group number, the ID of the group leader, and the x and y

coordinates of their home range centre. Lastly, deer and patches have variables defining their cumulative and step-specific number of contacts by group type (within- or between-group) and dyad type (male-male, female-female, female-male).

Timesteps represent two hours and the simulation was run for a period representing winter-spring (16 December 16 – 9 May, modified Silbernagel et al. 2011, Dobbin 2022) plus a 100-timestep burn-in period yielding 1840 timesteps. This temporal extent was chosen so as to limit the need for incorporating population dynamics such as reproduction and mortality; however, the model could be parameterized for other seasons. The total simulation area is 1440 km^2, which represents the largest square extent that can fit in the study area, i.e., Wildlife Management Unit 234 in eastern Alberta.

Process Overview and Scheduling

Within each two-hour timestep, movement occurs in 4 stages in the order presented in Figure 2.1. For each module, individuals and patches are processed in a random order.

Design Concepts

The general concepts considered in this model include home range, social grouping, and resource selection at the movement scale because they influence contact rates. Sex-specific home-range placements and size are dictated by landscape resources and deer preferences that will influence the overlap between groups. The more that groups overlap, the more between-group contacts will increase (Schauber et al., 2007). Home range size and placement differ by sex (Silbernagel, 2010).

How deer are grouped also influences contact rates because group-membership is used to define between- versus within-group contacts, and group size and spatial proximity within a

group will influence within-group contact rates (Habib et al., 2011; Tosa et al., 2015). Group sizes of mule deer are larger in winter than in summer and have a mixed-sex composition in winter (Lingle, 2003).

Resource selection is incorporated into individual deer movement via the integrated step-selection functions and represents the link between landscape features and how deer move (Avgar et al., 2016; Fortin et al., 2005). Resource selection influences contact rates because, if the deer have strong selection for a resource, this can put deer in close proximity to each other (Kjær et al., 2008). Habitat selection is also different for each deer sex (Rodgers et al., 2021).

Emergence

The contacts between deer are a focal output that emerges from the model, which are affected by the environment and submodels describing the deer's behaviour. Spatial use patterns are an emergent output that depends on the environmental input as well as the turning angle, and step length distributions. Home range size and shape also are emergent outputs as they are the product of a step length distribution, a turning angle distribution modified for a bias to the home range centroid, habitat selection, and grouping behaviour. Other elements, such as group size, are less emergent as they are dictated simply by deer density and allocation to home ranges.

Sensing

Deer are assumed to sense their environment, responding to resource covariates in the placement of their home ranges and their step selection process. They are assumed to 'know' the resources covariates and the corresponding selection weight at the end point of every drawn step, which determines whether or not they accept the step (Fortin et al., 2005; Thurfjell et al., 2014). The deer also have an intuitive sense of the direction of their home range centre, incorporated as a

bias towards their home range centre in calculating their turning angle parameters (Duchesne et al., 2015; Moorter et al., 2009). Deer within a group sense leadership status and consider it in their movements as the "followers" are required to move within a defined angle on either side of the direction of the group leader (Kjær, 2010).

Stochasticity

Stochasticity is included in the home range placement and movement of the deer. Deer are randomly placed on the landscape at the beginning of a simulation at one of the predetermined home-range centroids. Because each individual deer, rather than a group of deer, is located at a centroid, the exact group size and composition may vary slightly and differ with each iteration, although mean group size will stay the same because the number of groups correspond to the number of home range centroids. Stochasticity is also included in deer movement within a home range as steps are randomly drawn from turning angle and step length distributions at every timestep. A sequential movement of deer proceeds via the acceptance-rejection method for each step (Appendix H), with the probability of a step being accepted proportional to the patch weight, adding stochasticity to the model. I do not include stochasticity in resource weights of a patch.

Collectives

Deer form groups, corresponding to home range centroids, and exhibit grouping behaviour in their movement. Groups move using an approach of a leader moving and the other group members following the leader (Kjær, 2010). Groups will average ~6.6 individuals, which corresponds to a mixed-sex group in winter (Lingle, 2003; Merrill, unpublished data). The model does not allow fission and fusion in group membership during an iteration.

Observation

The data collected from simulations for each deer and patch include dyad-specific total within- and between-group contacts. The number of contacts is cumulative throughout an iteration of the simulation.

Details

Initialization

All model iterations were run with a sex ratio of 70:30 females to males and a density of 1 deer/km^2, which is within the ranges observed for mule deer in winter deer ground surveys in the study area (Merrill, unpublished data). Number of potential deer home ranges were determined by dividing deer population size by target group size (~6.6) and location of home range centroid was chosen based on a sex-specific, resource selection function derived from field data (see below). At the beginning of an iteration, each deer had a 0.7 probability of being female and 0.3 probability of being male. Deer were randomly placed at one of the potential home range centroids to create a mixed-sex group associated with each of the home range centroids, and group number was assigned based on centroid.

Input

Home-range Placement

Home-range centroids were placed with the probability of a location being picked being proportional to the value of its resource selection function weight (Lele et al., 2013; Manly, 2002). More than the required number of home ranges were placed on the landscape, and then rarified to be no less than 200 meters apart (Comer et al., 2005). Sex-specific RSFs were

developed for home range placement based on field data in 3 seasons (Appendix B), but only the sex-specific RSF for winter/spring (16 December – 9 May) was used in this Chapter. The winter home-range selection function was derived using movement data from 54 female and 21 male GPS-collared mule deer that had between 309 and 584 fixes for the winter when including only one fix from each quarter of the day. Then home ranges were delineated base on 95% utilization distributions calculated with the `adehabitatHR` software package (Calenge, 2006). Home ranges (used units, 1) were compared to randomly placed circular areas (0, available units), where available units were equal in area to the median home range size (16.05 km^2 for males,14.36 km^2 for females). I used the median home range size instead of the mean due to some large outliers due to early seasonal movement. Five available units were generated for each used unit (Gustine et al., 2006; Ladle et al., 2018).

Covariate values for each used and available home range unit (Table 2.1) were derived as the average covariate value in the home range. Covariates were assessed for collinearity and variables correlated with $| r^2 | > 0.7$ were not simultaneously input to the same model. Models were fit using a generalized linear model with a logistic function, using the `lme4` package in R, for a standard set of models plus the model including covariates that did not overlap zero in the global model (Bates et al., 2015; Boyce et al., 2002). I initially fit home range RSFs separately for male and female mule deer; however, males and females needed to be combined if possible, because mixed groups needed to be placed with one home-range centroid for all members (Lingle, 2003; unpublished data). Therefore, the top 5 models from males and females were taken as the candidate models for the winter-spring category and male and female data were pooled to parameterize a winter RSF for both sexes. Spatial weights on the landscape were then calculated using home-range-sized moving window layers. Separate male and female RSF

layers were calculated as the sexes have different home range sizes, and then an RSF layer for both sexes was created by averaging the separate female and male layers with a 70:30 weights for females: males.

We used a model selection approach to select the most supported models of home range selection based on Akaike's information criterion (AIC) and parsimony. AIC is based on using maximum likelihood estimates to approximate Kullback-Liebler information (Burnham and Anderson, 2002). The log-likelihood is then corrected for upward bias by penalizing the estimate for the number of parameters (i.e., AIC = 2[log-likelihood] + 2K) where K is the number of parameters (Burnham and Anderson, 2002). A model is considered to have more support if its AIC is lower than the next best model by at least 2. The combination of the lowest AIC score and the most parsimonious model among competing models ($\Delta AIC < 2$) is considered to be the top model to avoid overfitting (Burnham and Anderson, 2004). An extension of AIC is AICc, where AIC corrected for small sample size by adding $\frac{2k^2+2k}{n-k-1}$, where n is the sample size and k is the number of parameters (Burnham et al., 2011; Burnham and Anderson, 2002). Information criterion, such as AICc, are relative, not absolute, meaning they do not tell one how well the model fit the data, only how well it performs compared to other models in a candidate set (Burnham and Anderson, 2002). As a result, I assessed model performance using k-fold cross validation that used a circular moving window to calculate covariate values for each cell.

Submodels

At the beginning of each time step deer are moved to a new location in four stages (Figure 2.1).

Turning Angles

First, at each time step, a turning angle distribution for each individual (leader or follower)

within each group is calculated. The turning angle distribution was derived based on the consensus method in Duchesne et al. (2015). Mean turning angle of the distribution was an angle between the direction of persistence (θ) and direction of home range (ψ) with the position being determined by κ values defining how much the deer favors persistence versus home range (Equation 1).

$$\mu = atan\big(\kappa_1 sin(\theta) + \kappa_2 sin(\psi), \kappa_1 cos(\theta) + \kappa 2 cos(\psi)\big). \qquad (1)$$

The spread of the turning angle distribution is defined by the agreement between the direction of persistence (θ) and direction of home range (ψ), defined by equation 2.

$$\kappa = \sqrt{\big(\kappa_1 sin(\theta) + \kappa_2 sin(\psi)\big)^2 + \big(\kappa_1 cos(\theta) + \kappa_2 cos(\psi)\big)^2}. \qquad (2)$$

κ values for simulation were derived via simulation experiment and are not empirical.

Selection and movement of group leader

The leader of the group was the first individual to move at each time step and moved independently of every other individual in the group. A new group leader was randomly chosen with equal probability and designated as the leader, whose movement influences all other individuals in the group. This assumed both male and female deer could be leader of the group. The leader moved according to an integrated step-selection function (iSSA, Avgar et al., 2016), where the step length and turning angle are randomly chosen from their respective distributions to move the leader to a new location. The sex-specific, exponential step length distribution was derived from empirical 2-hour GPS data pooled from GPS-collared mule deer whose movements were monitored in 2006-2009 (M=11, F=20) and 2017-2020 (M=16, F=34) in eastern Alberta. Data used to parameterize the step length distribution were restricted to be above 20 meters to

avoid including spurious turning angles due to GPS error (Hurford, 2009). However, when simulating movements, deer could select below 20 meters because GPS error is not a concern when simulating movements. Turning angle was randomly chosen from the distribution of turning angles calculated for the individual animal as described above.

Integrated Step Selection Functions

Once the leader selected a location, the location was either accepted or rejected by comparing the proportional weight of selection of the patch at the end of the step to a random number between 0 and 1 (von Neumann, 1951; Appendix H). If that number was above the proportional weight, the step was rejected, and a new step was taken by redrawing from the step length and turning angle distribution until the step is accepted. Steps also were rejected if the target patch is occupied by more than 7 deer, which is the average group size, and two groups were constrained in occupying the patch at the same time. Once the leader moved, other group members followed the leader but were required to select an angle that made them move within 30 degrees on either side of the leader (Belsare et al., 2020; Kjær, 2010).

Proportional weights of rejecting and accepting a step were derived based on sex-specific iSSA (Avgar et al. 2016). I modeled the iSSA weight by comparing covariate values associated with the end point of each step of a GPS-collared deer (1) to those at the end point of 15 random steps (0), initiated at the same location but whose direction and step length were chosen at random from the empirical distributions of the GPS-collared deer (F = 52, M = 25, selection for inclusion described in Appendix E). I drew step lengths from an exponential distribution fit to data pooled across individuals for each sex, and a step-specific modified turning angle distribution with empirically determined κ. I measured the attributes in Table 2.1 at the end

point of a step as opposed to the beginning point of the step or an average over the step because step origin implied current position determining future location, and the latter assumes the individual travelled in a straight line Models were fit using a conditional logistic regression, using the `amt` package in R (Signer et al., 2019). The candidate models included a set common to both sexes plus the model including only variables in the global model that did not overlap zero for each sex. The top model for each sex/season was selected using AICc and parsimony.

Contacts

A contact was defined for a current step when two deer came within 5 meters of each other. I used 5 m to be consistent with contacts that were used for model assessment (Dobbin 2022). The contact is classified as a between-group contact if the group number of the two individuals is different and otherwise as a within-group contact. At every time step, I recorded the number of conspecifics of each sex within 5 m. I summarized the total, cumulative winter contacts by group type (within or between) and by dyad type (female-female, FF; male-male, MM; female-male, MF) by deer and for each patch in the landscape where a contact occurred. I counted contacts only after 100 timesteps to allow for a burn-in period that allowed the individuals to spread out and take a more natural positioning on the landscape.

Sensitivity Analysis

We conducted a sensitivity analysis of 3 key model parameters while holding all other parameters constant. I varied the magnitude of *kappa-1* value from 0 to 1, which influences the restriction angle for individuals following the leader to represent social cohesion in movement of group members; while holding density constant I varied the number of groups from 196 to 240 to represent how aggregated deer were across the landscape; and I varied the restriction angle for

the followers to represent varying group cohesion. I employed a Latin hypercube sampling procedure using the `nlrx` package in R (Salecker et al., 2019). One hundred iterations, each running for 1840 timesteps, were used. I present partial correlation coefficients as well as partial rank correlation coefficients to look for non-linear effects. Confidence intervals for the correlation coefficients were calculated using bootstrapping.

Model Assessment

We compared the spatial distribution of contacts output by the model for patches in the study area to the predicted relative contact probabilities (RCP), which were statistically derived from contact rates of deer collared with proximity loggers in the study area (Dobbin 2022). The RCP were derived by modelling actual contact (1) and random locations within the overlap of 2 mule deer (0) as function of landscape covariates (Table 2.1) where high values indicated a high probability of deer contact. RCP values were scaled between 0 and 1 by dividing by the maximum value. Output values for a patch from the simulations were averaged across 10 simulations using ten different random seeds. A t-test was used to compare the mean RCP of cells where contacts occurred in the simulations to the mean RCP at the equivalent number of random points. This allowed us to see if the model simulated contacts occurring in cells with a higher probability of contact, as one would expect, compared to random.

Results

Home-range resource selection functions

There were 4 competing models (ΔAICc <2) for mule deer selection of home range locations, and there was considerably more support for these models than the null model (Table 2.2). The top models all included distance to river, streams, well sites, and extent of woody cover,

although models differed with respect to the linearity in the selection for woody cover. A negative effect of distance to road was also in 3 of the top models. I selected as the top model the one that reflected that home ranges were located in areas generally closer to large rivers and well sites, but further from streams and had more woody cover, with woody cover having the greatest influence on home range placement (Table 2.2).

Model predictions across the study area indicated that there was one large cluster of high RSF values in the center and one on the western portion of the study near Chauvin, with a few other clusters scattered throughout the study area (Figure 2.2), which corresponded to areas of high woody cover (Appendix J). Five-fold cross validation revealed a correlation of 0.82±0.08 (±SD) for the winter RSF (Appendix B).

Integrated Step Selection Function

Empirical step length distributions of males and females had exponential rate coefficients of -0.0037 and -0.0041, respectively (Figure 2.3). Turning angle distributions were unique to every step of each individual (Figure 2.1) due to the influence of persistence and bias to the home range centroid. I derived the value of the κ_1 parameter, which influenced the persistence, and the κ_2, which influenced home range centroid bias using simulation as 0.4 and 0.5, respectively (Appendix F). When simulating, the same κ values and target home range size were used for both sexes as their home range sizes were less than one standard error different (target home range size was 14.87 km^2, a 70:30 weighted average of female and male home range sizes).

There were two competitive iSSF models (ΔAICc <2) for female and one iSSF model for males (Table 2.3). I chose the model for males without the interaction between ruggedness and distance to the nearest river as the top model due to parsimony as the addition of an interaction term did not considerably improve the model. Male iSSF models differed from that of females

in that female step selection increased at high extents of woody cover whereas males selected high and low values of woody cover. In contrast, female movement was less influenced by the distance to well sites compared to males. The distribution of step selection values in the study area did not differ significantly between males and females (KS test $D = 0.291$, $p < 0.001$; Appendix I). Values of selection were generally high in the central-west and along the eastern edge of the study area. Although males and females select for similar areas, the male higher selection values, especially in the center-west of the map, appear more diffuse than the females, likely because they also select for low woody cover values (Figure 2.4).

Sensitivity

Partial correlation coefficients (PCC) revealed an extreme sensitivity of within-group contacts to group cohesion, a sensitivity of between-group contacts to the number of groups, while none of the other parameters have a substantial impact (all other confidence intervals overlap zero; Figure 2.6a). PCC of within-group cohesion was -0.93, indicating that as the restriction angle controlling group cohesion increased and the group became less restricted in following the group leader, resulting in fewer overall contacts within a group, but not between-group contacts. As the number of groups got larger, the number of between-group contacts decreased as indicated by a PCC of -0.29. This resulted because, as the number of groups increases, group size decreases with fewer individuals contacting each other for the groups that overlap more. Persistence, which influences home range size, did not significantly affect within- or between-group contacts.

Partial rank correlation coefficients (PRCC) reveal non-linear influences not seen by looking at partial correlation coefficients (Figure 2.6b). Within-group contacts remained extremely sensitive to group cohesion (PRCC = -1.00), but were also sensitive to both number of

groups (PRCC = -0.62) and movement persistence (PRCC = -0.29) in a non-linear manner. Between-group contacts were only slightly sensitive to the number of groups (PRCC = -0.26). Some of these non-linear relationships can be seen by graphing contacts against parameter value (Appendix D); however, these plots cannot display the effects of covariation and therefore some relationships may not be visible.

Comparison to Statistical Contact Risk Map

The simulation outperforms randomness in all but the male-male, within-group scenario where randomness was not significantly different from simulation results (Table 2.4). Contacts occur in higher RCP areas (Figure 2.5). In every other simulation the model was significantly better with very small p-values.

Discussion

Males and females selected similarly at the step scale as well as the home range scale, with woody cover being particularly important in both cases. Woody cover was associated with selection for both sexes at the home range and step scales, while both sexes selected rivers at the home range scale and avoided them at the step scale. Woody cover was also found to be selected for at both scales in previous studies (Habib et al., 2011; Nobert, 2012; VerCauteren and Hygnstrom, 2004). The difference in selection of rivers at the two different scales could be due to rivers being associated with other characteristics that deer select for home ranges, such as woody cover, which can be riparian, and being able to capture a wider range of values with each home-range sample unit as it has a bigger area than simply a point when the sample unit is a step. Deer's avoidance of areas near rivers at the step scale may be simply because major rivers are relatively uncommon with only one major drainage in the upper corner of the study area (Battle River). Surprisingly deer avoided streams at both the step and home range which is contrary to

previous knowledge about deer preferring riparian areas in the winter (Edmunds et al., 2018; Walter et al., 2011). The similarity of selection and strong dependence on a patchy resource could increase contacts as it leads to concentrated areas of home ranges and attracts individuals to similar areas (Bonnell et al., 2010; White et al., 2018b). For example, Bonnell et al. (2010) used an IBM with resource selection to show that resource heterogeneity can increase contacts between individuals and therefore facilitate disease transmission. Patches of a selected resource effectively increase local density and facilitate more contacts between deer (Joly et al., 2006; Storm et al., 2013). This indicates that a more homogeneous landscape, where woody cover is more evenly distributed, could help to reduce contacts as it would spread the deer out more over the landscape and not keep them all in the same few areas (Dion et al., 2011; Dion and Lambin, 2012; Habib et al., 2011; Real and Biek, 2007). Using an IBM, White et al. (2018b) found that more fragmented landscape, with stronger resource selection, and lower resource availability had the highest change of disease persistence and higher outbreak peaks. This is consistent as it points to a few patches of woody cover, which the deer strongly select for, facilitating disease persistence and transmission.

Within-group contact rates were more sensitive to model parameters than between-group contact rates. Contact rates have been found to be higher within groups, and to vary with factors such as home range overlap and density (Schauber et al., 2007; Vander Wal et al., 2014). Greater home range overlap resulting in increased contact rates was found by both Schauber et al. (2007) and Vander Wal et al. (2014) who used GPS collars and proximity loggers to analyze this relationship. Although the sensitivity of within-group is notable, the lack of sensitivity in between-group contacts is key as between-group contacts are particularly important for disease, since they allow disease to spread through the population instead of being contained to a group,

and are therefore an essential output (Cross et al., 2007, 2005; White et al., 2017). Between-group contacts are also sensitive to number of groups/group size, although when looking at PRCC, they are not as sensitive as within-group contact rates. Group size is known to correlate with disease risk, which is consistent with this result (Rifkin et al., 2012; White et al., 2017). A meta-analysis by Rifkin et al. (2012) revealed a significant, positive correlation between group size and measure of parasitic risk. Group characteristics such as size can vary in response to predation risk and habitat (Bowyer et al., 2001; Leuthold and Leuthold, 1975; Ruckstuhl and Neuhaus, 2000). More cohesive groups had individuals contacting each other more, indicating a key target for reducing within-group contacts. Group cohesion can vary with factors such as environment; for example, white-tailed deer were more tightly grouped in more open areas (Seagle, 2003).

Simulation and statistical models agree, which is expected given that the simulation should be modelling natural deer behaviour, and supports my model in all except the male-male within-group case, where the simulation does not outperform randomness. This could be because upon validation of the RCP model, the male-male within-group model was the worst performing model and did not outperform randomness (Dobbin 2022). Although the statistical model can be used for some evaluations such as environmental variables and to determine the areas at the highest risk for contacts, the IBM has the ability to analyze multiple scenarios in a quick manner on factors such as environmental variables, but additionally can evaluate scenarios regarding management factors such as artificial attractants (Chapter 3) and vaccine baits (Ramsey and Efford, 2010). In all these scenarios the model can also analyze the effect of the environment and other scenarios on the relative proportion of between- and within-group contacts and therefore the degree of density- versus frequency-dependent disease transmission

when considered at the population level. Within-group contacts typically drive frequency-dependency, whereas between-group contacts typically drive density-dependence and therefore looking at their relative proportions can tell us which may dominate at the population level (Manlove et al., 2017).

This model could be extended in several important ways. First, although contacts are an appropriate proxy of transmission, the addition of a transmission coefficient would allow for the visualization of geographic spread. This implementation could be done with a constant transmission coefficient as is often done in epidemiological models, but could also be done with a statistical distribution of transmission coefficients to represent variation in contact duration that cannot be modelled due to the 2-hour timescale (Aiello, 2018; Aiello et al., 2018; Rakowski et al., 2010). Contact duration can influence transmission probability and a distribution of contact duration can be fit to a statistical curve such as a lognormal distribution, as shown by Aiello (2018). Second, the model could be extended to multiple seasons to encapsulate seasonally-varying attributes such as group size, group composition, home range size, and selection (Lingle, 2003, unpublished data Merrill et al.). Fission-fusion grouping dynamics can impact group size and cohesiveness which both can influence contact rates and transmission between individuals and subgroups (Aureli et al., 2012; Body et al., 2015). Lastly, the model could be applied to attractant and vaccine scenarios to investigate management strategies. Attractant and vaccine management focus on minimizing and maximizing contacts, respectively, and this model, given its ability to model and record contacts, can be used to evaluate the most ideal and detrimental distributions and densities for these elements.

Chapter 2 Tables

Table 2.1. State variables, units, and analysis scale characterizing 30-m patches in a landscape of east central Alberta, Canada used in simulating mule deer contact rates

Variable	Unit	Analysis scale	Description	Source
Distance to wells	m	--	Distance to nearest well site as an exponential decay function: Distwell = exp(-0.001*distance). (Appendix G)	(Alberta Energy Regulator, 2020; Governement of Saskatchewan, 2015)
Distance to rivers	m	--	Decay distance to nearest river calculated as an exponential decay function: exp(-0.001*Euclidean distance) Rivers were all primary or secondary rivers in Alberta; in Saskatchewan rivers were the Battle River, North and South Saskatchewan River (Appendix G).	(Altalis, 2018a; Government of Canada, 2017)
Distance to streams	m	--	Decay distance to nearest stream calculated as an exponential decay function: exp(-0.001*Euclidean distance) Streams included all permanent linear water feature besides Battle River, North Saskatchewan River, and South Saskatchewan River in Saskatchewan, and all perennial and indefinite streams in Alberta. (Appendix G)	(Altalis, 2018a; Government of Canada, 2017).
Distance to roads	km	--	Distance to nearest road, paved and unpaved, as an exponential decay function: Distroad = exp(-0.001*distance). (Appendix G)	(Altalis, 2020; Governement of Saskatchewan, 2019).
Agriculture	%	250 m	Proportion agriculture land cover from Landsat imagery (Appendix G).	(Latifovic, 2019; Merrill et al., 2013)
Woody cover	%	250 m	Proportion woody cover from TM Landsat imagery. (Appendix G)	(Latifovic, 2019; Merrill et al., 2013)
Woody cover edge	km/km^2	250 m	Linear density of woody cover edge. (Appendix G)	(Latifovic, 2019; Merrill et al., 2013)
Ruggedness	unitless	30m	Terrain ruggedness (Riley et al., 1999; Appendix G)	(Altalis, 2018b; Government of Canada, 2016).

Table 2.2 Top models for winter, mixed-sex home range resource selection function predicting the selected locations of the 95% utilization home ranges of mule deer in eastern central Alberta, Canada based on pooled movement data of (54 female and 21 male GPS-collared mule deer). Edge density is not listed as it was not present in any top model. See Appendix B for full model. * indicates that the confidence interval does not overlap zero.

Int	Distance to rivers	Distance to roads	Rugged Terrain	Distance to streams	Woody cover	Woody cover^2	Distance to wells	ΔAICc
-4.64 ± 0.44*	**1.21 ± 0.36***			**-1.34 ± 0.65***	**7.48 ± 0.87***		**0.91 ± 0.31***	**0**
-5.59 ± 0.77*	0.97 ± 0.41*	-0.59 ± 0.58	0.91 ± 1.16	-1.33 ± 0.64*	16.94 ± 5.30*	-10.44 ± 5.70	1.09 ± 0.41*	0.462
-4.61 ± 0.44*	1.18 ± 0.36*	-0.60 ± 0.59		-1.30 ± 0.65*	7.46 ± 0.87*		1.17 ± 0.40*	0.962
-4.56 ± 0.45*	0.94 ± 0.41*	-0.63 ± 0.60	1.22 ± 1.16	-1.45 ± 0.65*	7.53 ± 0.88*		1.18 ± 0.41*	1.865
-4.19 ± 0.39*	0.85 ± 0.39*		1.28 ± 1.16	-1.21 ± 0.62*	6.91 ± 0.81*			6.953
-1.61 ±0.13*								128.16

Table 2.3. Parameter values for the top 3 sex-specific integrated step-selection functions for mule deer in winter in east central Alberta, Canada. Bolded is the selected model which was chosen as a combination of AICc and parsimony. * indicates that the confidence interval does not overlap zero.

	Agriculture	Edge density	Distance to rivers	Distance to roads	Rugg x Rivers	Rugged Terrain	Distance to streams	Woody cover	Woody cover^2	Distance to wells	ΔAICc
Males	**-0.70 ± 0.09***	**0.09 ± 0.02***	**-0.10 ± 0.02***	**-0.16 ± 0.01***	**-0.11 ± 0.04***	**0.28 ± 0.02***	**-0.12 ± 0.02***	**-0.73 ± 0.26***	**0.73 ± 0.25***	**-0.03 ± 0.01***	**0**
	-0.69 ± 0.09*	0.09 ± 0.02*	-0.08 ± 0.02*	-0.16 ± 0.01*		0.28 ± 0.02*	-0.11 ± 0.02*	-0.70 ± 0.26*	0.70 ± 0.25*	-0.03 ± 0.01*	10.70
	-0.68 ± 0.09*	0.06 ± 0.01*	-0.08 ± 0.02*	-0.17 ± 0.01*		0.28 ± 0.02*	-0.12 ± 0.02*	0.03 ± 0.06		-0.03 ± 0.01	56.12
Females	-0.31 ± 0.06*	0.07 ± 0.008*	-0.05 ± 0.007*	-0.12 ± 0.009*	-0.02 ± 0.008*	0.25 ± 0.01*	-0.12 ± 0.01*	0.46 ± 0.04*			0
	-0.31 ± 0.06*	**0.07 ± 0.008***	**-0.05 ± 0.007***	**-0.12 ± 0.009***		**0.25 ± 0.01***	**-0.12 ± 0.01***	**0.46 ± 0.04***			**1.87**
	-0.31 ± 0.06*	0.06 ± 0.01*	-0.05 ± 0.007*	-0.12 ± 0.009*		0.25 ± 0.01*	-0.12 ± 0.01*	0.59 ± 0.17*	-0.13 ± 0.16	0.003 ± 0.007	5.01

Table 2.4. Two-sided t-test results for comparing mean values of relative contact probability (RCP, Dobbin 2022) at locations where simulated contacts occurred and at random locations. Sample size (n) indicates the number of cells where contacts occurred and the number of random points. Separate t-tests were done for each group and dyad type.

	Simulated Contact Location	Random locations	t	P value	n
Within group					
Female-female	0.65	0.59	64.046	<0.001	13823
Male-female	0.47	0.35	87.562	<0.001	10852
Male-male	0.24	0.25	-0.208	0.835	2578
Between groups					
Female-female	0.45	0.40	28.766	<0.001	2002
Male-female	0.91	0.69	36.423	<0.001	1564
Male-male	0.26	0.24	5.5328	<0.001	379

Chapter 2 Figures

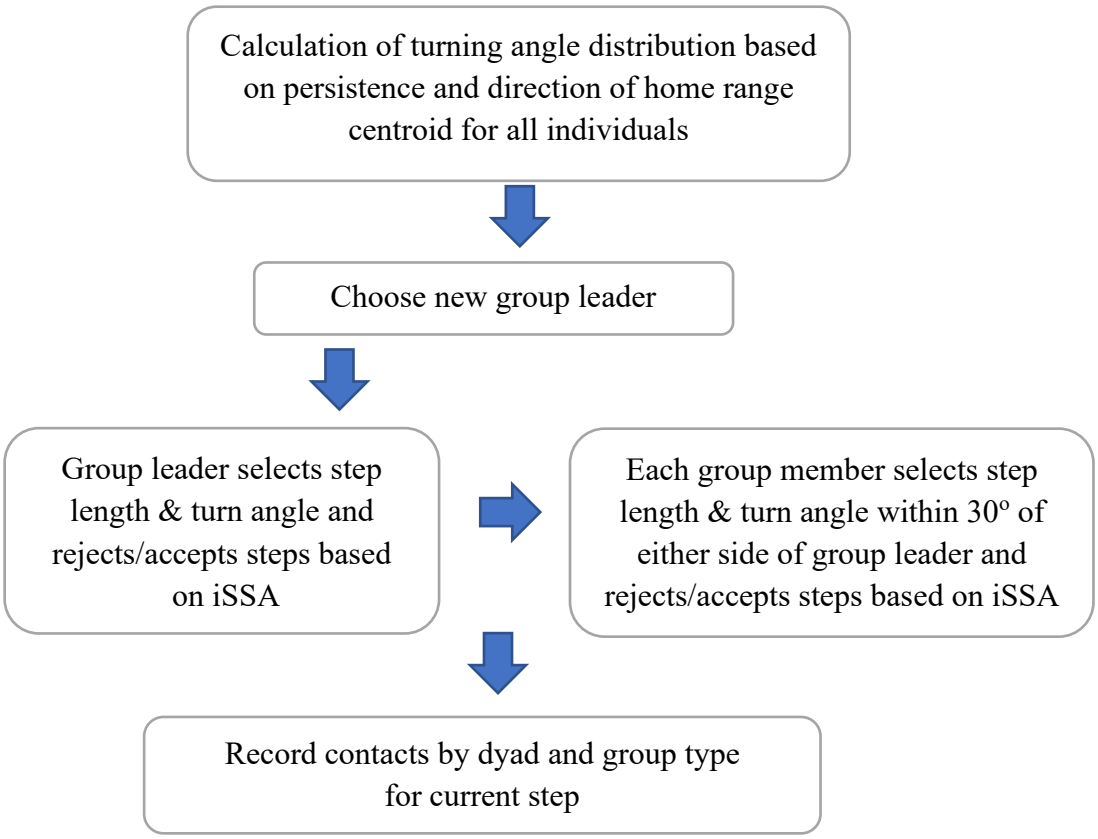

Figure 2.1. Flow chart depicting order of scheduling for the 4 major movement stages to recording contacts at each time step.

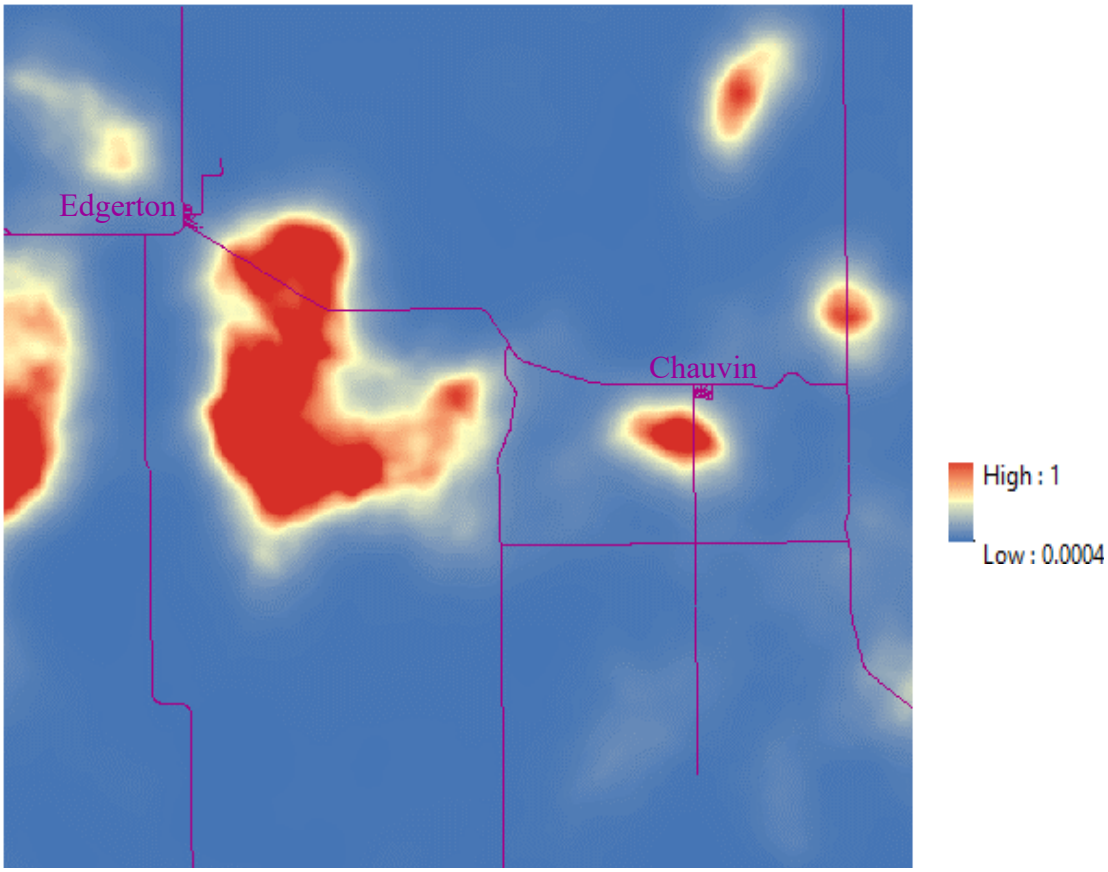

Figure 2.2. Scaled, calculated winter home range RSF weights in simulation area based on weighted average of male and female calculated RSF layers. Purple lines represent all four-lane undivided paved roads, two-lane undivided paved roads, and divided paved roads in the study area.

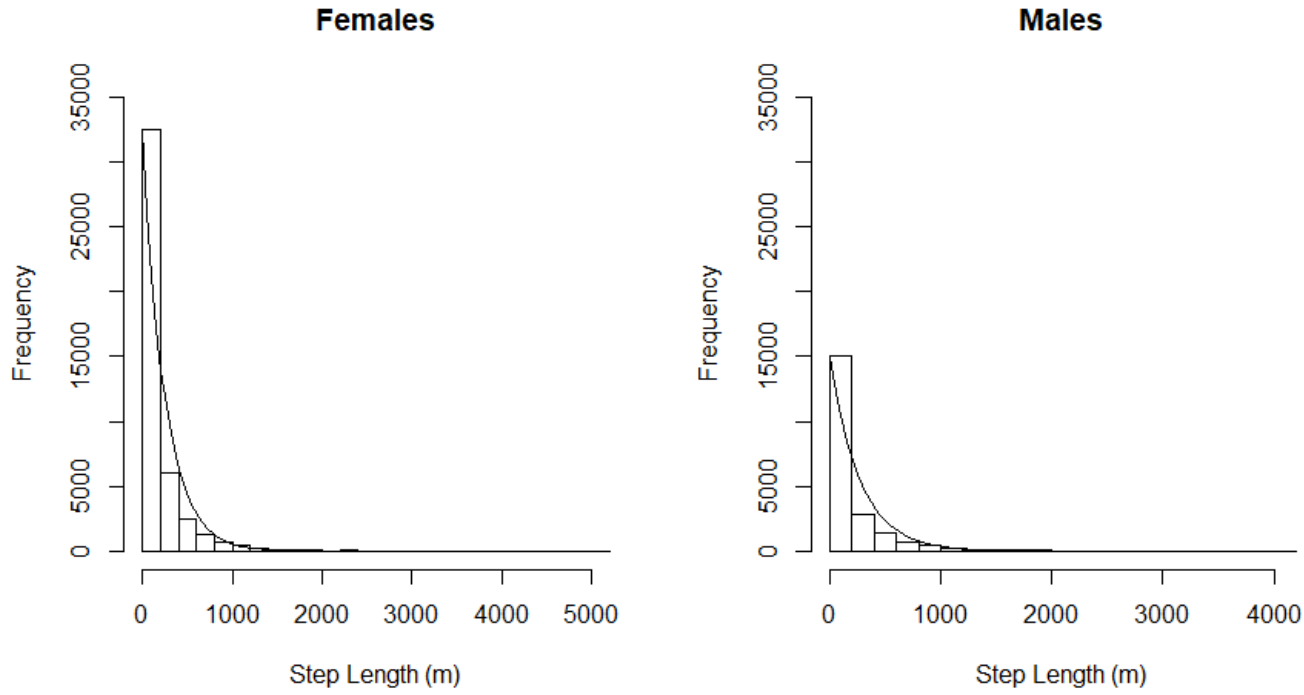

Figure 2.3. Empirical step length distributions derived from mule deer movements in central eastern Alberta, Canada with exponential distribution fit lines overlaid.

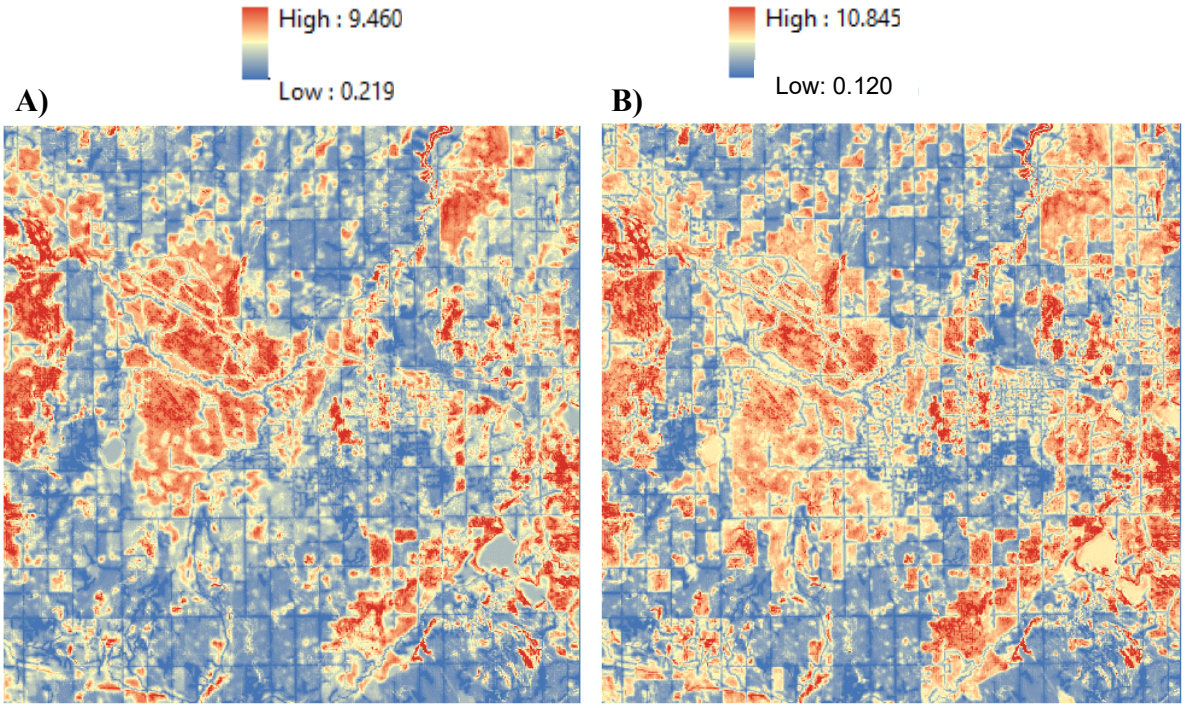

Figure 2.4. Winter selection weights derived from empirical iSSF for a) female (n = 52) and b) male (n = 25) mule deer predicted for study area in east central Alberta, Canada.

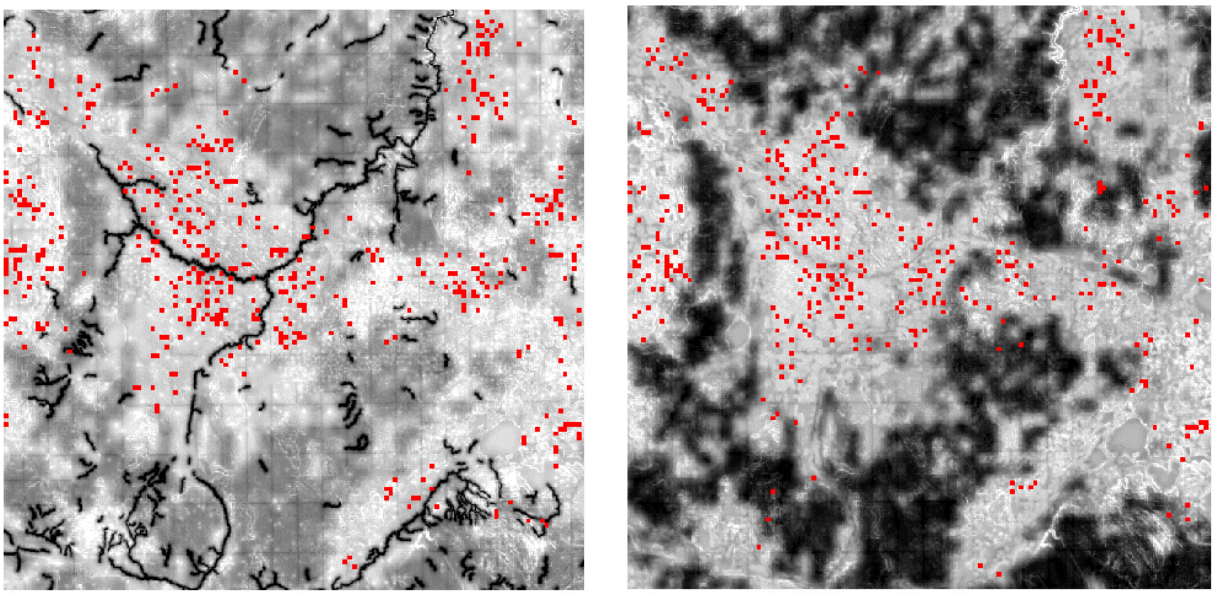

Figure 2.5. Simulation contacts overlaid on relative contact probability layers (Dobbin 2022) for Within Female-female (left) and Within Male-female (right). Simulation contacts were averaged across runs from 10 random seeds and resampled bilinearly to 300 m by 300 m from 30 m by 30 m for visibility. Red represents where contacts occurred in the simulation. Lighter indicates a higher value for the relative contact probability layers. Remaining overlays are in Appendix C.

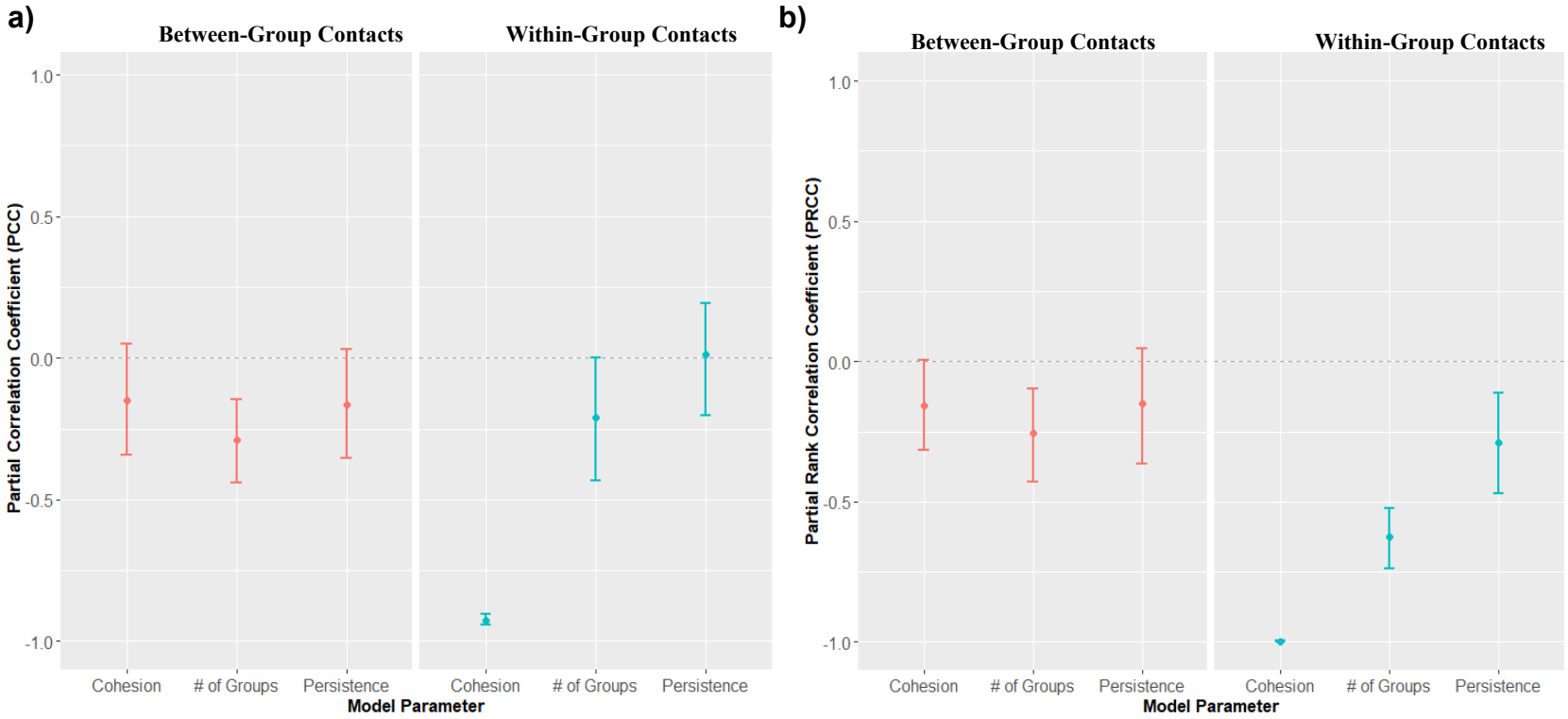

Figure 2.6. Sensitivity plots for population between- and within-group contact metrics. For a, partial correlation coefficient is displayed on the y-axis, indicating sensitivity, whereas the test parameters of group cohesion, number of groups, and movement persistence are on the x-axis. For b, partial rank correlation coefficient, looking for non-linear effects, is displayed on the y-axis, indicating sensitivity, whereas the test parameters of group cohesion, number of groups, and movement are on the x-axis. Confidence intervals were obtained via bootstrapping.

Chapter 3: Artificial Attractants: Fatal Attraction or Management Tool?

Introduction

Anthropogenic activities on landscapes can create natural and artificial hotspots of wildlife activity that drive the spread of emerging diseases. Supplemental feeding, baiting, and unintentional attractants, such as haybales and grain bags, are common for ungulates in North America (Sorensen et al. 2014, Milner et al. 2014). Supplemental feeding sites are designed to attract large herbivores for viewing or hunting, to reduce herbivory on plantings or vehicle collisions on roads, or to influence population dynamics by supplying additional food resources (Sorensen et al. 2014). Unintentional feeding includes depredation on agricultural crops, such as grain and canola, when they are growing or in storage units in the field of origin or clustered around farms (Plummer et al. 2018, Jerina 2012, Andreassen et al. 2005, Felton et al. 2017). Economic losses to farmers from depredation on stored crops and hay were nearly a quarter-million dollars total in damage in 1989 in the United States, with costs as high as hundreds of dollars per hectare (Austin et al., 1998; Menichetti et al., 2019; Wywialowski, 1994). Most jurisdictions pay some level of compensation to farmers for crop damage or provide materials to fence out ungulates to prevent depredation on stored crops (Gooding and Brook, 2014; Menichetti et al., 2019), but these programs depend on farmers following acceptable storage practices, such as erecting fencing and using repellants, to minimize depredation (Lemieux et al., 2000; Mysterud et al., 2021; Mysterud and Rolandsen, 2019). Nevertheless, aggregation of ungulates in winter due to improperly stored grains or accidental spillage remains a key problem in most agricultural areas (Mysterud et al., 2021; Sorensen et al., 2015).

In addition to the economic losses, aggregation of ungulates in winter at stored crops can lead to higher disease transmission. High use of artificial attractants (AA), such as grain bins, stored hay bales, and grain bags, facilitates direct transmission by increasing direct interactions among individuals at a site or indirect contacts where diseases are transmitted environmentally (Escobar et al., 2020; Oja et al., 2017; Sorensen, 2014; Thompson et al., 2008). For example, individual deer have been shown to stay 1.36 to 1.69 times longer at AA depending on the layout of the feed, and increase between-group contacts compared to natural feeding areas (Cross et al., 2013; Sorensen, 2014; Thompson et al., 2008). White-tailed deer spent the highest amount of time at sites where grain was spread out, followed by sites where the grain was in a pile, both of which were higher than at natural areas (Miller et al., 2003; Thompson et al., 2008). Infected animals can also contact individuals along travel routes to and from AA and, if infective agents are dropped or excreted along the routes, can spread a disease within the nearby home ranges of other individuals (Benavides et al., 2012). The role that AA play in disease transmission in an area will depend on the extent to which ungulates use AA, which in turn is contingent on the number of AA available, their spatial distribution relative to deer movement patterns, and the availability of other natural, high quality forages (Miller et al., 2003; White et al., 2018b).

One disease of cervids where AA may be influencing the transmission and spread of the disease is chronic wasting disease (CWD, Rivera et al., 2019; Sorensen, 2014; Western Association of Fish and Wildlife Agencies, 2018). CWD is a 100% fatal prion disease in cervids that has limited vertical transmission but horizontal transmission occurs both directly through contact between individuals and indirectly through the environment (Williams and Miller, 2003). CWD was first detected in a research facility in Colorado in 1967 and is now found in wild cervid populations in 3 Canadian provinces and 26 states (Miller and Williams, 2004; Smolko et

al., 2021; U.S. Geological Survery, 2022). It was transported into Saskatchewan via farmed elk in 1996, before being detected in wild deer in Saskatchewan in 2000, and in Alberta in 2005 (Miller and Williams, 2004; Smolko et al., 2021). After finding CWD in Alberta, the Alberta government initiated a herd reduction program within a CWD control area in 2005 that was stopped after 3 years (Smolko et al. 2021). Alberta has continued a hunter-harvest surveillance program since 1996 that shows CWD is spreading from east to west and prevalence province-wide is now at 14.8% in mule deer and 5% in white-tailed deer (https://www.alberta.ca/chronic-wasting-disease-updates.aspx). When local CWD prevalence levels reaches ~25% or higher, modelling studies indicate evidence for population decline (DeVivo et al., 2017; Edmunds et al., 2016). Because there is no vaccine for CWD, the most common management approach for addressing CWD has focused on manipulating harvest strategies (Conner et al., 2021; Mysterud and Edmunds, 2019; Potapov et al., 2016; Rivera et al., 2019). However, if AA play a significant role in CWD transmission, particularly in agricultural areas, additional research is needed to provide guidelines for best practices in reducing AA (Heberlein, 2004; Peterson et al., 2002; Western Association of Fish and Wildlife Agencies, 2018).

A first step to assessing the influence of AA on CWD transmission and devising guidelines for their management is modelling how the density and configuration of AA may influence deer behavior and potential contact rates. Assuming deer are attracted to AA, then AA density and certain general AA arrangements or their relationship to preferred habitats may indicate non-linear increases in the rate of contact among individuals or with unique AA sites, which points to where management efforts to reduce AA may be most effective. For example, while a very low number of AA may result in few contacts, as numbers of AA increase individuals may be attracted to more and different AA, increasing contacts with multiple,

potentially infected groups that use a site. However, as the number of AA continues to increase, individuals may be exposed to fewer numbers of potentially infected groups or sites if they use only local, nearby AA and share sites with fewer other groups (Becker et al., 2018; Sah et al., 2018). Therefore, I may see the highest contact rates at an intermediate AA density, with peak contact rates that may be contingent on the configuration of AA or their proximity to preferred habitat. For example, in the prairie-parklands of Alberta's CWD zone, woody cover is key to the space use and movement behavior of deer (Habib et al., 2011; Nobert et al., 2016; Chapter 2). Thus, guidelines for limiting densities and where AA are located may differ between regions.

In this chapter, I address the effects of non-intentional feeding sites associated with the storage of foods that attract deer (i.e., AA) in winter and in a modelling framework assess the influence that density and configuration of AA may have on potential contact rates, reflecting the potential for the transmission of CWD. In Alberta, hay bales, grain bags, and grain bins where grain spills occur are the most commonly reported types of non-intentional attractants for cervids (Ewald, pers. comm.; Government of Alberta unpublished data, 2021; Mejía-Salazar et al., 2018). I focus on mule deer because they have the highest prevalence of CWD in Alberta (Smolko et al., 2021), and on winter because more aggregation at AA occurs then, most commonly in agricultural areas (Mejía-Salazar et al., 2018; Mysterud et al., 2021). I use the individual-based model (IBM) developed in Chapter 2 to simulate the influence of AA density, arrangement, and proximity to woody cover on metrics of per capita dyad and site contact rates in a landscape representative of the habitat conditions in a portion of WMU 234 in central-eastern Alberta (Fig. 1). I hypothesize that if mule deer modify their movement in relation to AA (i.e., are attracted to AA), there will be a non-linear relationship between total contact rates and AA density, whose shape is influenced by both the landscape arrangement of AA and their

proximity to woody cover. More specifically, I predict that the highest per capita contact rates and site use among deer will occur at intermediate AA densities because, as the number of AA increase, deer will be attracted to more sites initially, but eventually high local density of AA will result in fewer contacts with unique deer. Further, I expect that the general arrangement of AA and, in particular relative to preferred habitat (i.e., woody cover), will influence the number of unique AA sites any individual would visit, implying a potential influence of environmental transmission as overall prevalence increases. If thresholds in contact rates exist, they may be an important consideration in guiding future regulations for how to effectively manage AA to minimize transmission of CWD and other diseases.

Methods

Study Area

The focus of this study was a 1440-km^2 area representative of eastern Alberta (Fig. 1). The area consists of rolling hills with an elevation of 553 to 782 m. The area is within the parkland ecosystem (Meijer and Karpuk, 1999) and consists of agricultural cropland (48%), grassland and pastures (18.9%), and woody cover (24%) consisting of deciduous tree stands (*Populus* spp., 20.1%), and tall shrubland (*Elaeagnus commutata*, *Salix* spp., *Prunus* spp., and *Amelancier alnifolia,* 3.9%). The area has no major river drainages, but has multiple creeks and streams, including Ribstone creek, the most major drainage in the area. In the 2006-2009 data period, winter temperatures ranged between ~ -20 and ~10^o C (based on Lloydminter weather data) while in the later 2019-2020 period it ranged from -34.3 – 15.2° C ($\overline{x}$ = -6.13, based on Edgerton AGCM station). In the earlier period monthly snow depth ranged from 0 – ~45 cm, while in the later period monthly snowfall ranged between 12.0 and 22.8 cm. Land use consists primarily of agricultural use and cattle farming as well as oil and gas extraction throughout the area. Farm

sites were located based on buildings designated on the plat maps for Wainwright and Provost areas (The Municipal District of Provost No. 52, 2019; The Municipal District of Wainwright No. 61, 2020), which assumed all buildings selected were farms (Figure 3.1). Ruggedness in the area ranged from 0 to 36.

Deer Movement Model and Attraction to AA

Individual deer moved in groups in 2-hour timesteps responding to landscape covariates at a 30 by 30 m scale. The centroid of a group of deer was initially located according to the predicted values from a home-range resource selection function (RSF) as described in Chapter 2, and the set of centroids used was invariant. Mule deer group size was ~6.6 deer with the composition within the group being 70:30 females to males.

Individual deer were moved according to a sex-specific integrated step selection function (iSSF) with movement being biased toward a home range centroid, influenced by social grouping, and biased toward AA when they came within a 6-km buffer of the AA. The iSSFs were derived from movements of GPS-collared male (n = 25) and female (n = 52) mule deer in the study area, with sex-specific step length distributions fitted to the empirical distributions of step lengths and a turning angle distribution that was a modified Von Mises. The Von Mises distribution of turn angles was modified to produce home range behaviour by incorporating bias towards a home range centroid via the consensus method in Duchesne et al. (2015). Direction of movement of individuals within a group was influenced by a group leader selected randomly at each time step with group members following the leader by constraining their movement direction to be within 30^{o} of the leader's turn angle. For further details on these movements see Chapter 2. When deer were within 6 km of an AA, attraction to AA was incorporated into

weighting function of the iSSFs with a negative beta coefficient of 0.001 so that weighting values are higher for cells closer to AA (smaller distance value, Appendix L).

Contact Simulations

We simulated deer movement and recorded sex-specific contacts of deer dyads, number of unique deer contacts, number of unique AA contacted by a deer, and number of unique deer using an AA during a 144-day winter period under 6 AA configurations and 6 AA densities. The 6 spatial configurations represented two different agricultural practices of storing feed that potentially attract deer: grain bags and hay bales left within the fields where they were harvested (hereafter field AA) and grain bins (where grain spillage can occur) and hay storage units that typically are in proximity to farm sites (hereafter farm AA). Field AA were randomly distributed within agricultural areas across the study area. Farm sites were located based on buildings designated on the plat maps for Wainwright and Provost area (The Municipal District of Provost No. 52, 2019; The Municipal District of Wainwright No. 61, 2020), which assumed all buildings selected were farms sites (Fig. 1). Farm placement was restricted to areas that were more than 400 m from the simulation area edge to ensure AA around the farm were not placed outside the study area. AA were located around each farm centroid based on a bivariate normal spatial probability distribution, with a standard deviation of 200 m. I allocated AA to farm sites used using a Neyman-Scott process that identified farm centroids as 'parent' points, and then placed the approximately equal number of 'daughter' AA.

The 6 AA densities ranged from 0 AA to 1 AA/km^2, by 0.2 AA/km^2. Varying densities of AA were derived by placing the maximum number of AA according to the above

configurations, and then removing a set number of AA using different strategies for the field and farm AA scenarios.

For the field AA, I reduced AA randomly and by proximity to wood cover. The latter approach was used because woody cover provides security cover/other resources for deer and deer are closely associated with woody cover in this area (Habib et al., 2011; Nobert et al., 2016; Chapter 2). I removed field AA based on a probability function that related the probability of removal to the distance to the nearest woody cover. The relationship used to obtain a probability was an exponential transformation with a decay coefficient of -0.0384 (Appendix M). The function was derived from the distribution of distance to woody cover values at GPS- locations of 25 male and 52 females from 16 December to 9 May as a function of distance to nearest woody cover with data pooled for the sexes during this period. For altering densities of AA at a farm site, I removed either individual AA at a farm, or I removed the entire cluster of AA at a farm. Individual AA or a cluster of AA at a farm site was removed either randomly, or again according to their distance from cover. When removing the entire cluster, I used the average distance of all the AA at a farm site to cover.

We ran 5 iterations of deer moving across the landscape for each density × AA configuration. For all simulations, I kept the density of deer constant at $1/km^2$. I defined a contact as two deer coming within 5 m of each other and classified a contact by dyad type (FF: female-female, MF: male-female, MM: male-male) and whether contacts occurred within or between a deer group.

We recorded 1) number of unique deer using each AA, 2) contact rates at each AA and at the population level, 3) number of unique contacts for each deer, and 4) number of between- and within-group contacts by dyad type (male-male, male-female, female-female). These metrics

were then plotted against AA density to look for relationships between AA reduction and model outputs.

Results

When there are zero AA, average contacts/deer dyad rates were similar across all simulations, because deer were placed in the same initial locations and allowed to move with the same movement rules for 1840 steps. Similarly, average contact rates/deer dyad when comparing random removal strategies to removal by proximity to woody cover are similar at maximum densities of 1 AA/km^2 because these represent the same starting conditions for removal. The number of contacts both within and between groups was highest between females and lowest between males because I assumed a ratio of 70 females and 30 males in the simulations; further, because patterns in contact rates were similar between sex-specific dyads (Appendix K), I present only the patterns of contacts across all dyads (Fig. 3.2).

When AA were distributed broadly, the number of within-group contacts declined as AA density increased, but this was not true with AA that were clustered around farms (Fig. 3.2A). The number of within-group contacts does not appear to change in the farm AA scenarios, but where contacts occur does change because the number of contacts at each AA increases at lower AA density (Figure 3.3). In contrast, the number of between-group contacts decreased as the density of AA increased in most scenarios (Fig. 3.2B). The exception to this pattern was when AA were randomly removed around farms (Fig. 3.2B). When field AA density was decreased by removing AA near woody cover, between-group contacts were higher at low densities compared to when they were removed randomly.

Mean number of unique deer contacted by each individual exhibited a moderate increase at low AA density both in the field and farm-clustered AA scenarios with contacts being slightly higher when AA near woody cover were removed (Figure 3.4). The exception was when AA clustered at farms were removed randomly (Figure 3.4). Further, when AA near woody cover in the field were removed, the number of unique deer contacted by each individual increased more than when removed randomly.

The number of unique AA used by each deer increased with AA density and the relationship showed only minor variation in the linearity of the relationship among scenarios (Fig. 3.5). In contrast, the number of unique deer visiting an AA was highest at low AA density, and, in general, the number of unique deer using a site was higher when AA were removed in clusters around farms (i.e., all AA around a farm) than when randomly removed around farms (Fig. 3.6). There was some evidence that where field AA near woody cover were removed with a higher probability, the number of unique visits declined before increasing.

Discussion

We used empirical data for winter movements and habitat selection of mule deer in a landscape representative of eastern Alberta, Canada to assess the role artificial attractants (AA) may play in the transmission of diseases such as CWD. I found that increasing AA density from none to a density of 0.2 AA/km^2 had the potential to increase contact rates by as much as ~300%. When AA density is relatively low, yet deer still have access to AA (i.e., some AA fall within deer home ranges), the attraction to locations at and near AA (i.e., locations less than 6 km away) results in relatively more deer groups using the area around the few available AA sites; consequently, the number of contacts increased at low AA density (e.g., Figures 3.2 - 3.4). In this case, the iSSF weight, which is affected by the distance to the nearest AA, is more variable

because there is proportionally more area > 6 km from any AA at low AA density. As a result, deer use is concentrated in areas of high iSSF weight areas around few AA, thereby increasing deer contacts. In contrast, as the density of AA increases and proportionally more of the landscape is within 6 km of an AA, the mean iSSF weight value will increase and be less variable (Figure 3.7). As a result, the landscape is more "connected" in the sense that deer are likely to use more of the landscape and deer use around an AA is not as concentrated. Consistent with the increase in total contacts at a site, I found deer had a higher number of contacts with unique deer at lower densities of AA.

As a result of these dynamics, I found some support for my hypothesis that if mule deer were attracted to AA there would be a non-linear relationship between total contact rates and AA density with the highest contact rates at moderate densities of AA. I found that compared to zero AA present, contact rates increased at very low density but then decreased as density increased for the reasons described above. The non-linear rate of change at low densities and a potential threshold might have been clearer if I had modelled densities below 0.2 AA/km^2. How the total number of contacts changed after an initial increase depended on the configuration of AA. A relative decrease in contacts with increasing AA was more evident across scenarios for between-group contacts than within-group contacts. The exception was within-group contacts for field AA, where AA were not clustered around a farm (Figure 3.2A). This could be because when AA were placed in clusters around buildings, the deer could spread out over the nearby AA in the clusters. This does not change when removing entire clusters or individual AA at farms because what remains on the landscape is still clusters of AA. In contrast, field AA were more spread out and reducing the density of AA concentrated deer at fewer individual AA and increased within-group contacts. The fact that, in most cases, the relative responsive to AA densities of direct

between-group contacts was greater than within-group contacts, has important disease implications. For example, although contact rates are typically higher within groups (Schauber et al., 2007), network models used to model disease dynamics have shown that increased connectivity between groups, i.e., more between-group contacts, increases prevalence and is an important determinant in epidemic size and duration (Sah et al., 2018; Silk et al., 2019; White et al., 2017).

The model outputs I present assume that deer were attracted to a site from as far away as 6 km and that attraction to all AA was similar. If deer were attracted to an AA only as they got closer than a 6 km distance, (i.e., had a shorter perceptual range), this likely would have decreased the number of total contact rates and the unique AA sites visited by deer overall, but this could be constrained by density of the AA. For example, if the perceptual range at which deer were attracted to AA was 1000 m instead of 6000 m, contacts at site would likely decrease because deer would detect (come within 1000 m) and visit fewer AA (Pe'er and Kramer-Schadt, 2008; White et al., 2018b). These results are consistent with those of Pe'er and Kramer-Schadt (2008) who, using an IBM model, found that perceptual range for landscape feature selection had a large impact on animal movements and landscape connectivity (in their model this was ability to immigrate from one forest patch to another), with increased connectivity at higher perceptual range. Further, if deer were attracted to AA differentially, perhaps due to different grain types (Cosgrove et al., 2018) or due to tactics used to scare away deer (Lemieux et al., 2000), I would have expected higher variability across sites and potentially a less connected landscape because deer would not be equally likely to move to every attractant.

Aggregation of deer also may promote disease spread for some diseases such as CWD that are transmitted via the environment. AA potentially can serve as reservoirs of CWD given

the slow degradation of prions in the environment (Plummer et al., 2018; Sorensen, 2014). Indeed, several studies based on remote cameras and direct observations of deer behavior indicate that environmental contacts and intensity of use may be higher at artificial feeding sites than at natural feeding sites (Mejía-Salazar et al., 2018; Thompson et al., 2008). I found that the number of unique AA that a deer visited increased almost linearly with increasing AA density, suggesting that because deer within my model ranged widely, they were able to readily access AA at least within their home range. This may not be the case in reality because deer movements can be constrained by rivers and roads (Northrup et al., 2015). Additionally, I saw more unique visits per AA as density decreased indicating higher potential for environmental contamination at the remaining sites. This indicates that environmental transmission potential may be based on a balance of deer visiting more sites as AA density increases and a higher contamination level of remaining sites at low density. The relative importance of direct animal vs. environmental exposure pathway depends on the probability of transmission given exposure, and this may change depending on the proportion of infected individuals and sites over the disease progression. In fact, previous modelling of CWD indicated that although individual-to-individual animal transmission may be key in the early period of disease transmission, environmental transmission may be the dominate route of transmission as the disease progresses (Almberg et al., 2011). Thus, the role of AA in transmission also may change over time depending on the length of time CWD has been present in the area.

Although artificial attractants during the winter may provide a major route of CWD spread (Western Association of Fish and Wildlife Agencies, 2018), results of this modelling exercise provide several insights for designing management. First, lower density of AA may not necessarily translate into fewer between-group contacts unless there are practically no AA (total

restriction), or they are so sparsely scattered that the constraints of home range movement prevent deer from encountering them. Similarly, the mean number of contacts with unique, individual deer shows the same pattern as between-group contacts, suggesting that reduction in AA to an insufficient amount could actually increase disease transmission. Second, management of AA for disease purposes can be directed not only at the density of AA but where to target the removal of AA. When AA were removed based on their proximity to woody cover, I found similar overall patterns as when removed randomly, i.e., initial increase in between group contacts followed by a decline as AA density increased; however, in cases when AA represented grain bags and hay bales widely distributed in the field, there was evidence for a relative increase in the number of contacts when the remaining AA at low densities were far from woody cover. This is inconsistent with the findings of Miller et al. (2003) that more AA in open areas led to lower bovine tuberculosis risk whereas more AA closer to and in wooded areas increased risk; however, I attributed this to the relative increase in the attraction of deer to AA when woody cover, their preferred habitat was not nearby. Additionally, in the iSSF weights, if the selection for woody cover is much higher, the deer will be more drawn to woody cover and move less far for attractants; however, when the selection for AA is higher, deer will be drawn away from woody cover into areas where AA are present. Further, when managing clusters around farms, removing individual AA did not have as much of an impact on contact rates when compared to removing whole clusters. This difference in response in cluster versus individual removal of AA likely occurred because, removal of farm AA in clusters eliminates some areas where the deer congregate, making more groups congregate at the fewer remaining sites/clusters. The difference in response when removing individual AA versus clusters of AA implies that

removing individual AA at farms may be a lower risk way to reduce density because inadvertently increasing contacts is not as much of a risk.

Further model refinements that may improve my understanding of AA management fall in to three categories. First, further analysis of the impact of model components on results would give us insight into the sensitivity of the model outputs to model assumptions. In particular, the radius within which a deer is attracted is an important parameter because perceptual range is known to have a major influence on movements (Pe'er and Kramer-Schadt, 2008). Also, altering the relative strength of selection for woody cover versus AA would allow us to see the importance of this relationship and its impact on removal strategy results. Lastly, I could have variable attraction amongst sites which would give us insight into the effect of density and configuration when multiple attractant types of varying attractiveness are present.

Second, I could refine the observed patterns by including higher AA densities and finer resolution of densities between 0 and 0.2 AA/km^2 which may indicate a low-density threshold when contacts and unique visits/contacts begin to decrease. I could also vary deer density to examine more of the interplay between deer density and AA densities and distributions. For the current modelling I kept deer densities at 1/km^2 but increasing density could lead to a decrease in contacts with increasing density, because more AA would be required to spread the larger number of deer out on.

Third, I could extend the model to include the probability of transmission at AA (environment) and for direct contacts between deer and keep track of infected individuals. This would allow us to gain insight into the geographic spread of disease and patterns relating to prevalence.

Finally, the IBM developed here could be used to investigate arrangements for vaccine baits, where one is trying to maximize contacts with a site instead of trying to minimize them. It could also be used for different areas and for different types of attractants, providing insight into more management scenarios.

Chapter 3 Figures

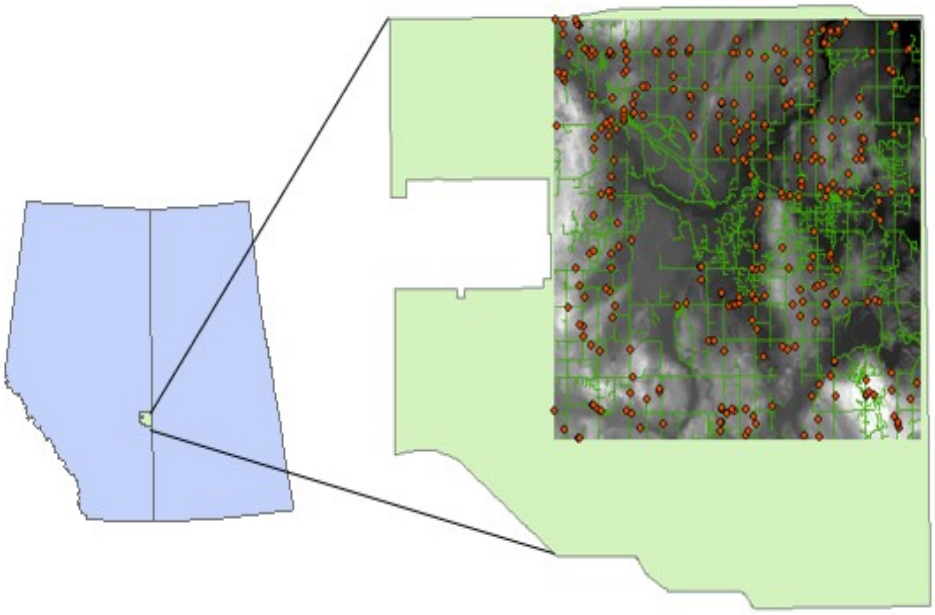

Figure 3.1. Location of simulation area in eastern Alberta, with wildlife management unit 234 represented by the green polygon. Within the depiction of the simulation area, the background is elevation, roads are displayed in green, and building sites are represented by brown points (Altalis, 2020, 2018; The Municipal District of Provost No. 52, 2019; The Municipal District of Wainwright No. 61, 2020).

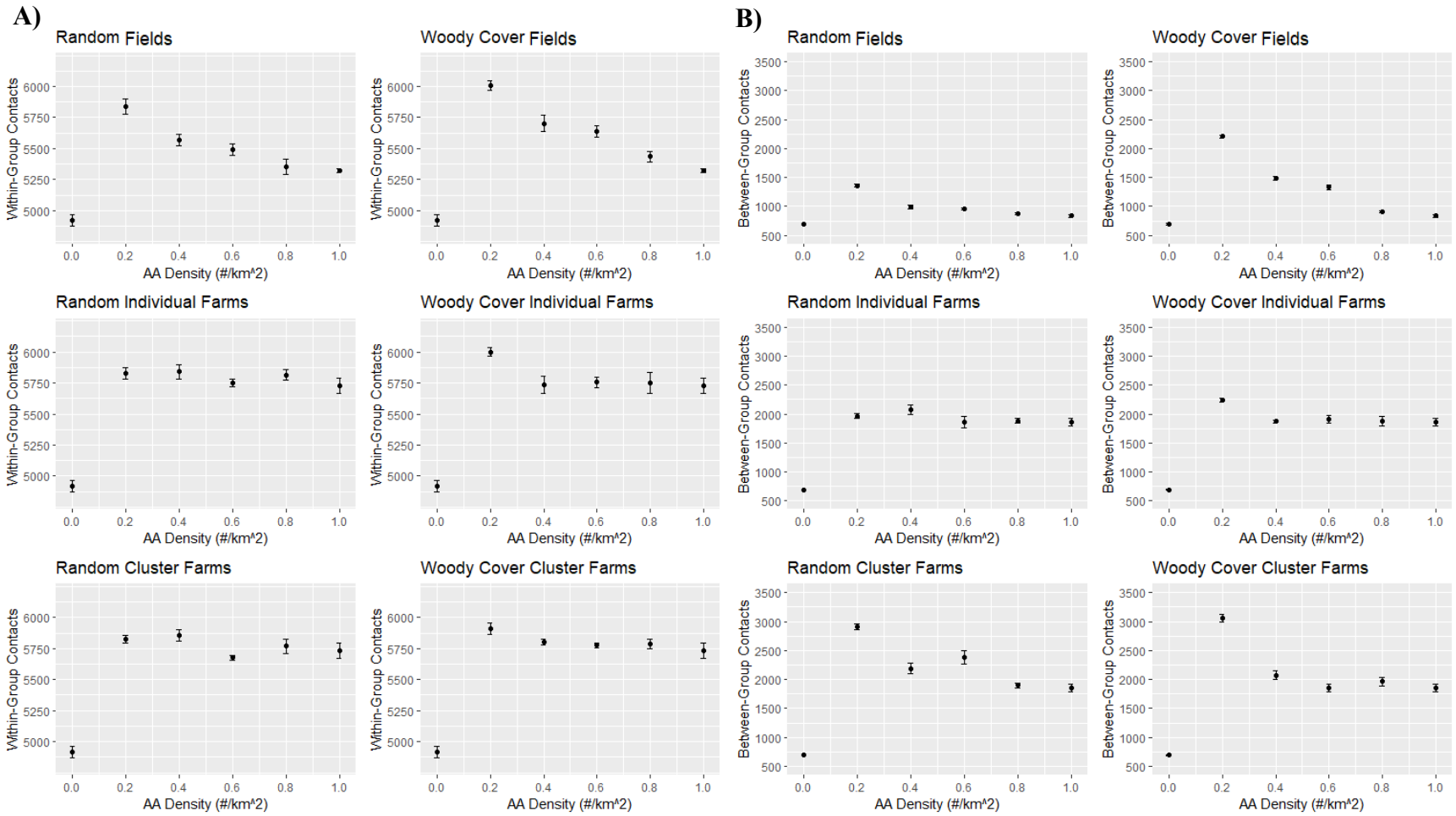

Figure 3.2. Mean number of A) total within-group contacts and B) total between-group contacts for all dyad types, averaged across 5 random seeds for each attractant density. Error bars represent standard error. 'Random' scenarios refer to when density decrease was due to random removal of artificial attractants (AA) whereas 'Woody Cover' scenarios refer to when AA were removed based on proximity to woody cover. 'Individual Farms' scenarios refer to when AA at farms were removed individually while 'Cluster Farms' refers to when entire clusters of AA at farms were removed. Note: y-axis scales differ between panels A and B.

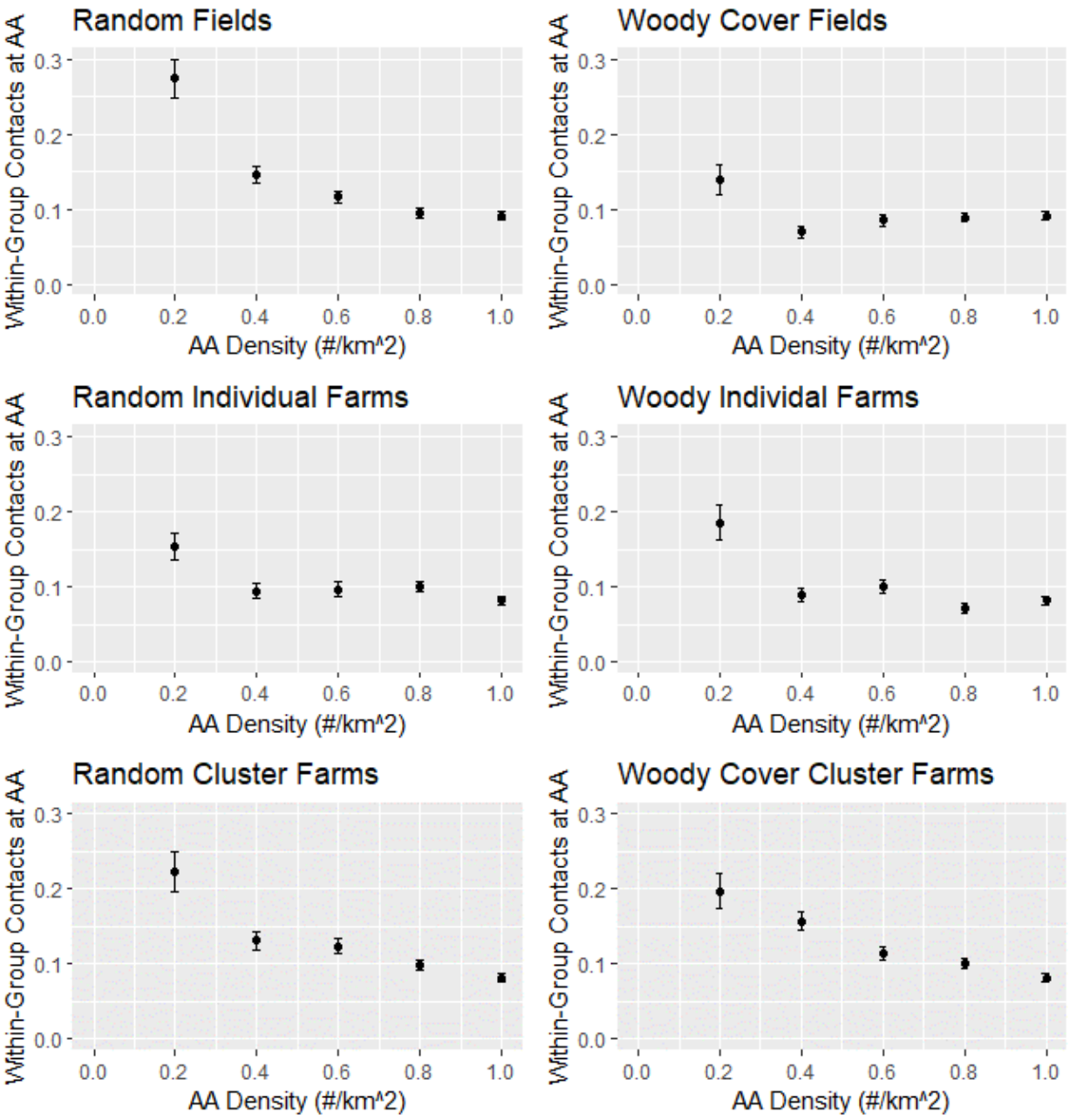

Figure 3.3. Mean within-group contacts at each attractant + the eight neighbouring cells averaged across 5 random seeds for each attractant density and across all attractants. Error bars represent standard error.

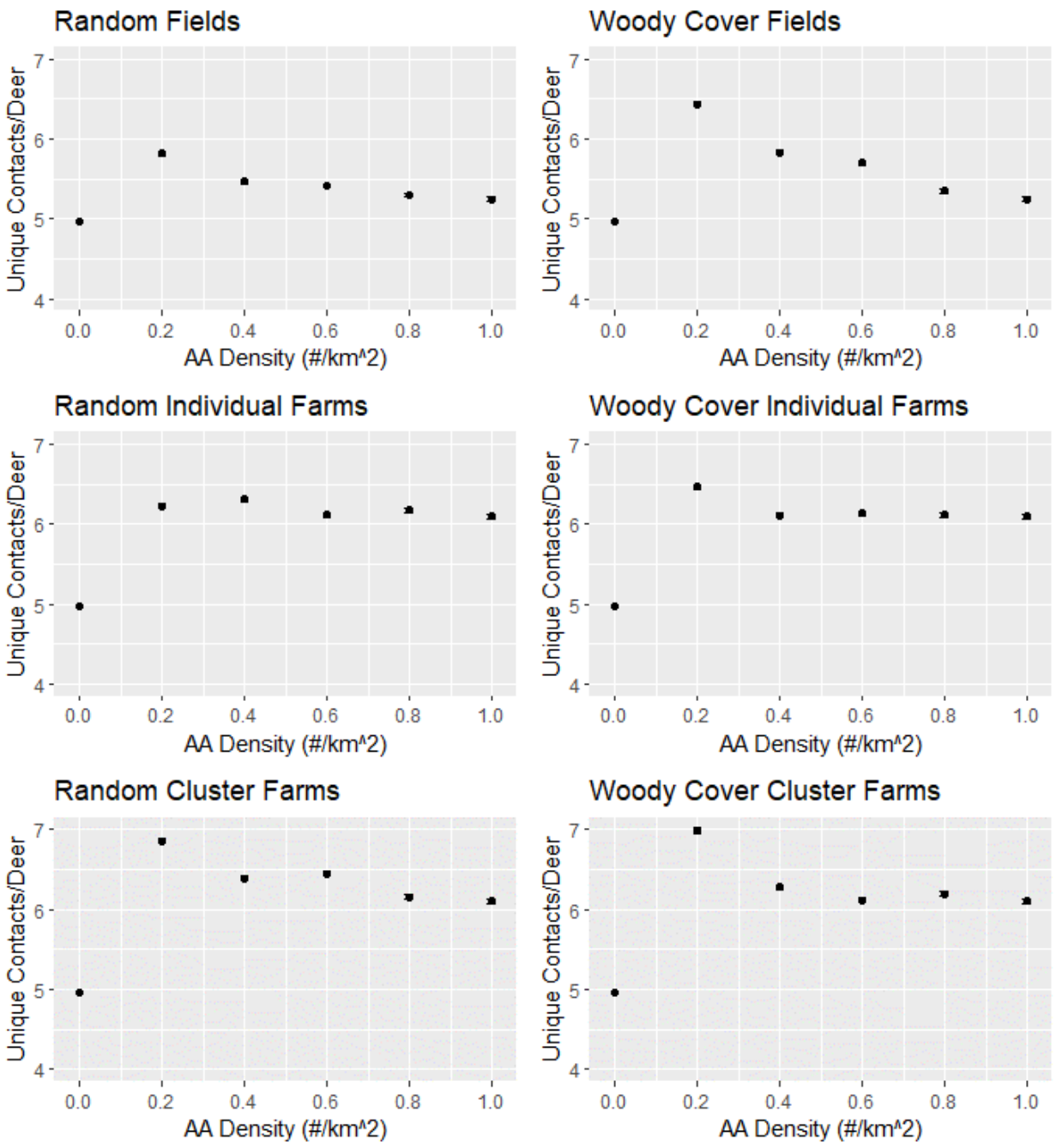

Figure 3.4. Mean number of unique deer contacted by each individual, averaged across 5 random seeds for each attractant density and across all deer in each simulation. Error bars represent standard error.

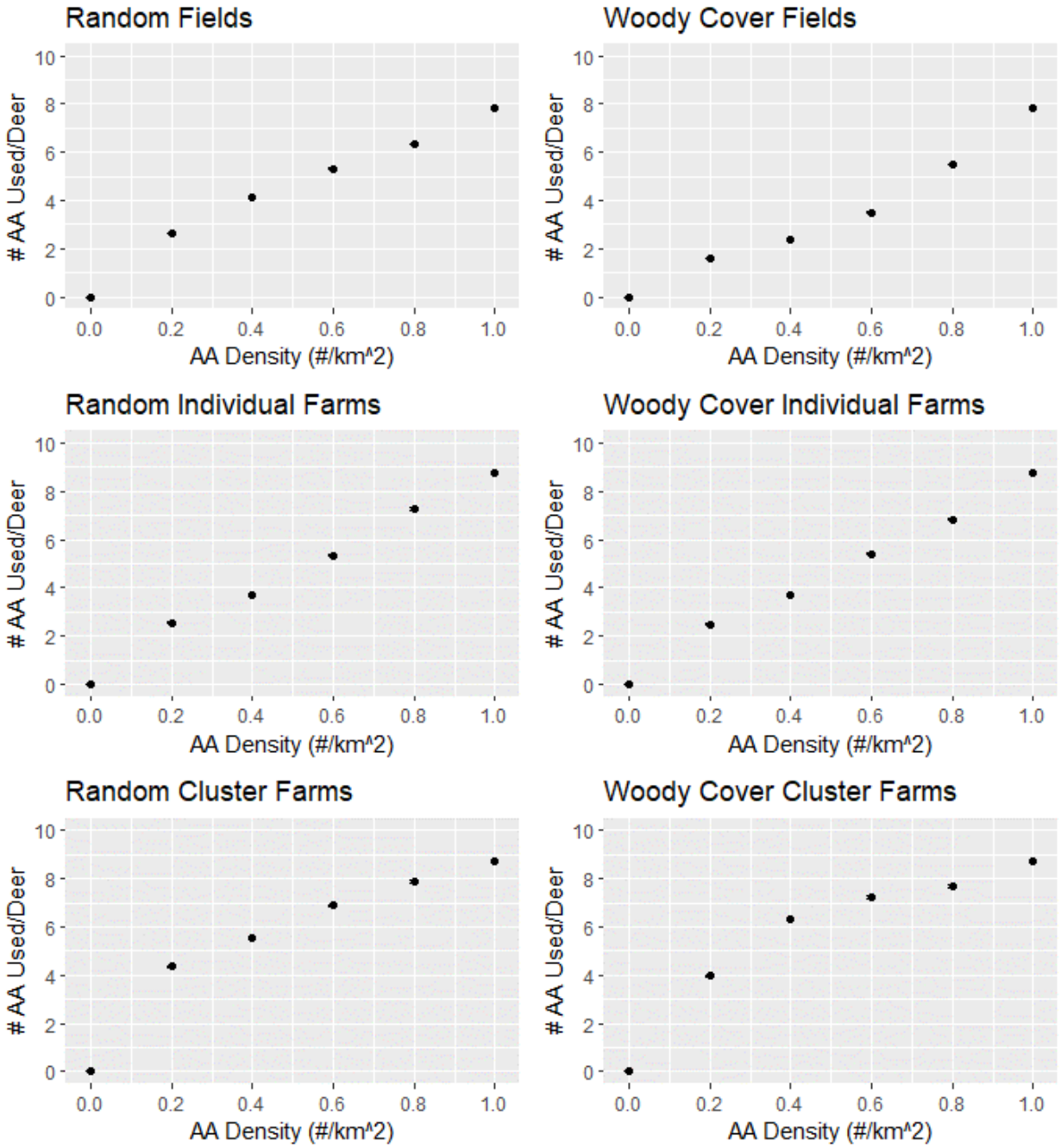

Figure 3.5. Mean number of unique artificial attractants used by each deer, averaged across 5 random seeds and across all deer in the simulation for each artificial attractant density for field and farm distributions under 6 different management removal scenarios (random removal in fields, random removal around farms, random cluster removal of farms, and removal by woody cover proximity instead of random for the same three scenarios). Error bars represent standard error.

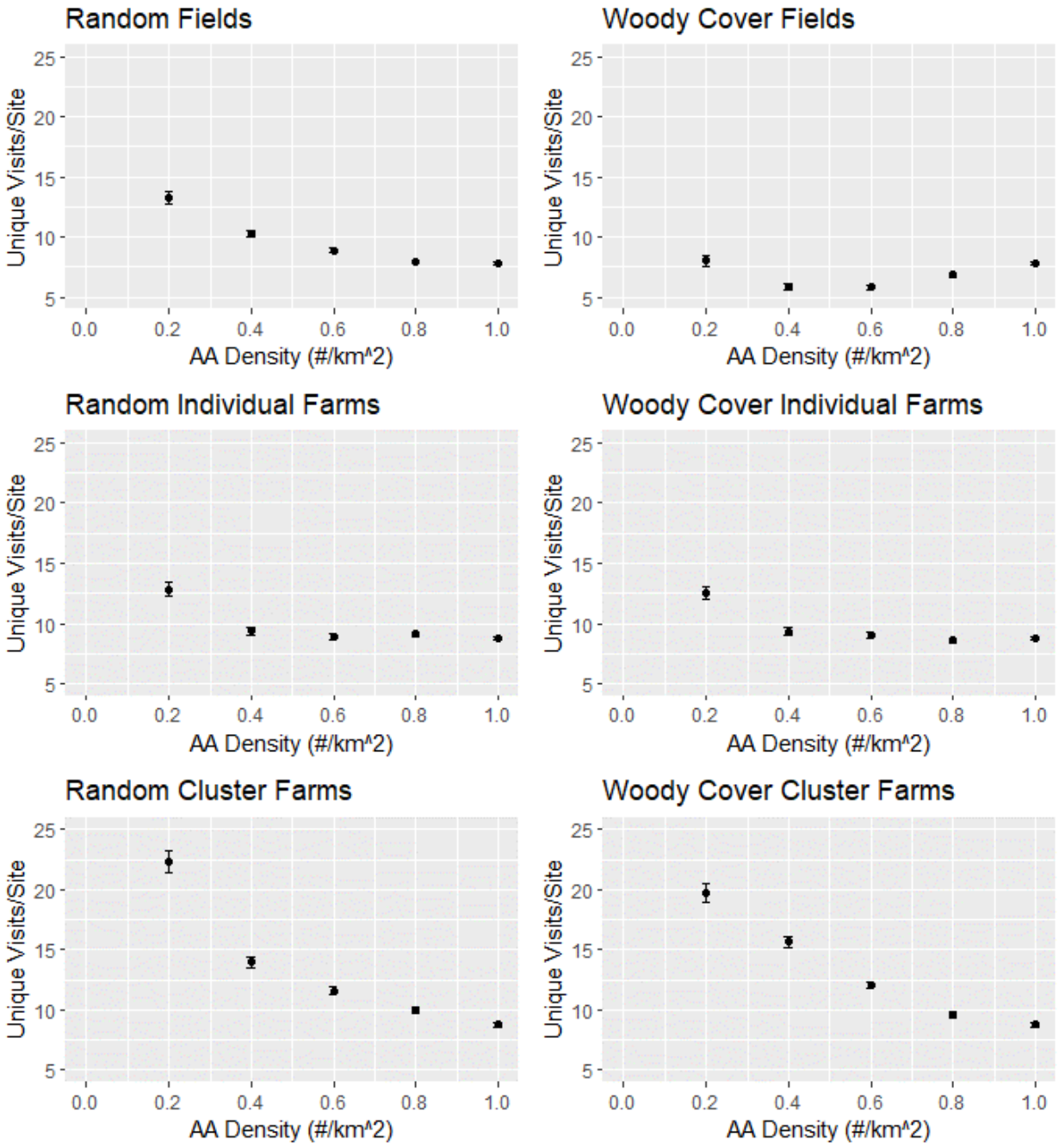

Figure 3.6. Mean number of unique deer that visited each attractant averaged across 5 random seeds for each attractant density and across all attractants for each simulation. Error bars represent standard error.

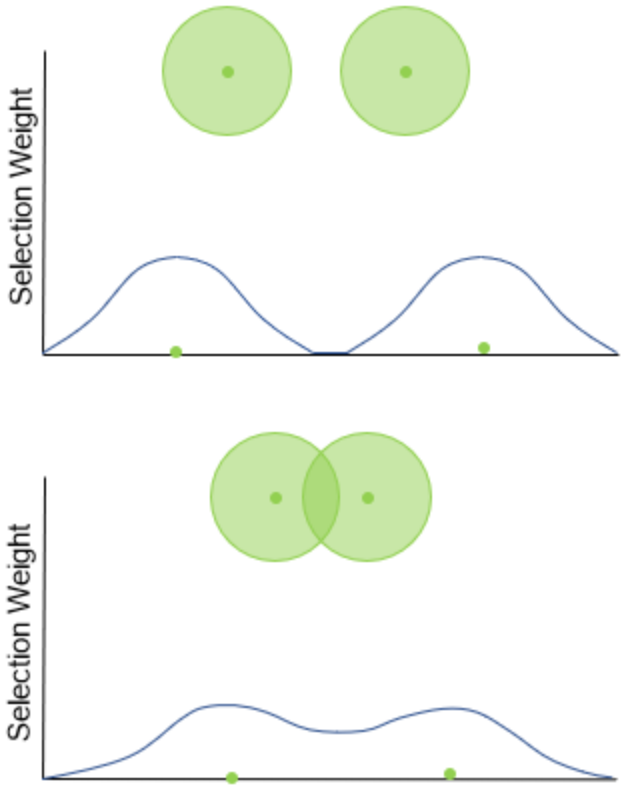

Figure 3.7. Relative selection weight for two different landscape arrangements of attractants. Selection weight decreases less between attractants that overlap because the distance to nearest attractant does not get as large.

Chapter 4: Summary and Conclusions

In this thesis I developed an IBM that simulated deer movement and contacts between dyads of mule deer in a heterogeneous landscape and used it to address how rates of contact (i.e., two deer within 5 m) were influenced by the density and configuration of artificial attractants such as hay bales and grain bags. The movement model incorporated home range, grouping, and resource selection behaviours in an attempt to simulate realistic deer movement. I used empirical data from 81 GPS-collared mule deer in the parkland systems of eastern Alberta to develop sex-specific iSSFs, and found woody cover had the most influential effect on deer movements.

The model assumed group leadership could be by either sex, deer can sense their environment at the end of any drawn step, and group membership stayed constant throughout winter (i.e., no fission or fusion). From the sensitivity analysis of model parameters, I found that within-group contacts are more sensitive than between-group contacts. Within-group contacts were particularly sensitive to group cohesiveness and the number of groups on the landscape indicating that tighter and larger groups could increase contacts.

I had a unique opportunity to compare the relative distribution of where contacts occurred from simulations to the relative probability of contact, predicted from a statistical model derived by Dobbin (2022) using contact locations of GPS-collared deer. I found good correspondence between the output of my simulation and the statistical predictions based on a t-test comparison of average relative contact probability at contact and random locations. The exception was a poor correspondence in the winter within-group male-male contacts and this was attributed to the fact that upon validation of the RCP model, this was the worst performing model and did not outperform randomness (Dobbin, 2022).

Within the context of managing chronic wasting disease in eastern Alberta, I used the deer IBM to assess the influence of artificial attractants (AA) on contact rates in winter as a surrogate to disease transmission. AA have been identified by a consortium of wildlife agencies as one source of potentially high disease transmission (Western Association of Fish and Wildlife Agencies, 2018), and regulations on feeding deer and government programs to abate unintentional feeding government vary by agency. I focused on winter because this has been identified as one of the most important and high-use seasons for AA (Mejía-Salazar et al., 2018; Mysterud et al., 2021). My objective was to provide insight on how AA density and configurations influence total contact rates and contacts with unique deer representing potential animal to animal contact, and the number of AA used by each deer and number of unique visits per AA as a surrogate for exposure to environmental transmission. I used two strategies for distributing AA that represented common practices in Alberta of hay bales and grain bags left in fields, and agricultural storage, including hay and grain bins, at farms. I assumed deer were attracted to AA when within 6 km of an AA (McRae et al., 2020). Sensitivity analysis on this distance and on relative strength of woody cover and AA attraction, are yet to be conducted.

The simulations revealed that reducing density of AA can actually increase rates of contact because there are few AA that more deer are attracted to and use. Generally, changes in within-group contacts were less sensitive to changes in AA density than between-group contacts. To reduce overall contact rates, densities would need to be so low that few deer would have AA within or adjacent to their winter ranges. I would need to conduct further simulations to determine the threshold density of AA where this would occur under the assumptions of my model. AA density reduction decreased the number of AA used by each deer and increased the unique number of deer using each site. A balance of these effects of deer using fewer potentially

contaminated sites or contaminating fewer sites, and a greater number of deer at each site to potentially contaminate the environment will impact the amount of environmental transmission. Additionally, configuration had an effect as removal strategy at farms, individual or by cluster, impacted patterns seen as removing individually had far less of an effect. Furthermore, only removal of field AA appeared to impact within-group contacts. Removal by proximity to woody cover increased between-group contacts more than random removal for field AA, indicating that method of removal can make a difference on the magnitude of the impact.

Our IBM model of mule deer movements is one of several IBMs built to explore management of CWD (Belsare et al., 2020; Kjær, 2010), but none of these models have been applied to assessing the influence of AA on contacts rates as their potential roles in disease spread. The model could be extended to include different levels of disease transmission from individual animal contacts and from visits to AA, as well as to discern how the patterns I observed might change at different deer densities. It could also be used in other applications such as identifying the most efficient distribution of oral vaccines in baits, were vaccines available for CWD. Nonetheless, as among the first explorations of how AA influence key processes in disease transmission I make the following management recommendations based on the current results:

- Decreasing AA by ≥65% as recommended by the Western Association of Fish and Wildlife Agencies (2018) may not be an effective management strategy unless the density of AA is already very low. Management should be an all or none response, not aiming to simply reduce AA numbers, but to eliminate or nearly eliminate them as insufficient reduction, to 0.2 AA/km^2 for example, could increase contacts. This implies that strong restrictions, such as mandatory fencing of bales and bags in fields, with the aim of nearly

eliminating AA, as occurs in jurisdictions like in Norway, is likely necessary for CWD management.

- Targeting regulations and the removal of AA that are broadly distributed or entire clusters of AA at locations such as farms is risky if densities are not sufficiently lowered because this could increase between-group contacts and removing by cluster also could increase unique visits per site more than other strategies. Additionally reducing field AA by distance to woody cover may result in larger increases in contact rates than if removed randomly.
- Reducing the density of AA reduces the number of the AA an individual deer visits, which may limit exposure to contaminated sites. At the same time, it is more likely the AA they visit are contaminated because the number of animal-to-animal contacts, as well as the number of unique deer visiting a site, increases at low densities of AA. To better understand these trade-offs, further investigation of the dynamics of these interactions would likely need to be studied in the context of actual disease transmission before the best course of action in limiting the role of AA in CWD progression could be identified.

References

Accolla, C., Vaugeois, M., Grimm, V., Moore, A.P., Rueda-Cediel, P., Schmolke, A., Forbes, V.E., 2021. A Review of Key Features and Their Implementation in Unstructured, Structured, and Agent-Based Population Models for Ecological Risk Assessment. Integrated Environmental Assessment and Management 17, 521–540. https://doi.org/10.1002/ieam.4362

Aiello, C., 2018. A multi-level study of disease dynamics in desert tortoise (Gopherus agassizii) with implications for translocation risk assessment. ThePennsylvania State University.

Aiello, C.M., Esque, T.C., Nussear, K.E., Emblidge, P.G., Hudson, P.J., 2018. Associating sex-biased and seasonal behaviour with contact patterns and transmission risk in Gopherus agassizii. Behav. 155, 585–619. https://doi.org/10.1163/1568539X-00003477

Alberta Energy Regulator, 2020. ST37: List of Wells in Alberta.

Almberg, E.S., Cross, P.C., Johnson, C.J., Heisey, D.M., Richards, B.J., 2011. Modeling Routes of Chronic Wasting Disease Transmission: Environmental Prion Persistence Promotes Deer Population Decline and Extinction. PLoS ONE 6, e19896. https://doi.org/10.1371/journal.pone.0019896

Altalis, 2020. Access.

Altalis, 2018a. Hydrography.

Altalis, 2018b. 25m Raster DEM.

An, L., Grimm, V., Turner II, B.L., 2020. Editorial: Meeting Grand Challenges in Agent-Based Models. JASSS 23, 13.

Aureli, F., Schaffner, C.M., Asensio, N., Lusseau, D., 2012. What is a subgroup? How socioecological factors influence interindividual distance. Behavioral Ecology 23, 1308–1315. https://doi.org/10.1093/beheco/ars122

Austin, D.D., Urness, P.J., Duersch, D., 1998. Alfalfa Hay Crop Loss Due to Mule Deer Depredation. Journal of Range Management 51, 29. https://doi.org/10.2307/4003559

Avgar, T., Potts, J.R., Lewis, M.A., Boyce, M.S., 2016. Integrated step selection analysis: bridging the gap between resource selection and animal movement. Methods in Ecology and Evolution 7, 619–630. https://doi.org/10.1111/2041-210X.12528

Bartlett, G., Pardee, J., Thiede, K., 2003. Environmental impact statement on rules to eradicate chronic wasting disease in Wisconsin's free-ranging white-tailed deer herd.

Bates, D., Bolker, B., Maechler, M., Walker, S., 2015. Fitting Linear Mixed-Effects Models Using lme4. Journal of Statistical Software 67, 1–48.

Becker, D., Snedden, C.E., Altizer, S., Hall, R.J., 2018. Host dispersal responses to resource supplementation determine pathogen spread in wildlife metapopulations. The American naturalist 192, 503–517. https://doi.org/10.1086/699477

Belsare, A.V., Gompper, M.E., Keller, B., Sumners, J., Hansen, L., Millspaugh, J.J., 2020. An agent-based framework for improving wildlife disease surveillance: A case study of chronic wasting disease in Missouri white-tailed deer. Ecological Modelling 417, 108919. https://doi.org/10.1016/j.ecolmodel.2019.108919

Benavides, J., Walsh, P.D., Meyers, L.A., Raymond, M., Caillaud, D., 2012. Transmission of Infectious Diseases En Route to Habitat Hotspots. PLOS ONE 7, e31290. https://doi.org/10.1371/journal.pone.0031290

Body, G., Weladji, R.B., Holand, Ø., Nieminen, M., 2015. Fission-fusion group dynamics in reindeer reveal an increase of cohesiveness at the beginning of the peak rut. acta ethol 18, 101–110. https://doi.org/10.1007/s10211-014-0190-8

Bonnell, T.R., Sengupta, R.R., Chapman, C.A., Goldberg, T.L., 2010. An agent-based model of red colobus resources and disease dynamics implicates key resource sites as hot spots of disease transmission. Ecological Modelling 221, 2491–2500. https://doi.org/10.1016/j.ecolmodel.2010.07.020

Bowyer, R., McCullough, D., Belovsky, G., 2001. Causes and consequences of sociality in mule deer. Alces. Alces 37, 371–402.

Boyce, M.S., Vernier, P.R., Nielsen, S.E., Schmiegelow, F.K.A., 2002. Evaluating resource selection functions. Ecological Modelling 157, 281–300. https://doi.org/10.1016/S0304-3800(02)00200-4

Burnham, K.P., Anderson, D.R., 2004. Multimodel Inference: Understanding AIC and BIC in Model Selection. Sociological Methods & Research 33, 261–304. https://doi.org/10.1177/0049124104268644

Burnham, K.P., Anderson, D.R. (Eds.), 2002. Model Selection and Multimodel Inference: A Practical Information-Theoretic Approach, in: Model Selection and Multimodel Inference: A Practical Information-Theoretic Approach. Springer, New York, NY, pp. 49–97. https://doi.org/10.1007/978-0-387-22456-5_2

Burnham, K.P., Anderson, D.R., Huyvaert, K.P., 2011. AIC model selection and multimodel inference in behavioral ecology: some background, observations, and comparisons. Behav Ecol Sociobiol 65, 23–35. https://doi.org/10.1007/s00265-010-1029-6

Calenge, C., 2006. The package adehabitat for the R software: tool for the analysis of space and habitat use by animals. Ecological Modelling 197, 1035.

Cariboni, J., Gatelli, D., Liska, R., Saltelli, A., 2007. The role of sensitivity analysis in ecological modelling. Ecological Modelling 203, 167–182. https://doi.org/10.1016/j.ecolmodel.2005.10.045

Comer, C.E., Kilgo, J.C., D'Angelo, G.J., Glenn, T.C., Miller, K.V., 2005. Fine-scale genetic structure and social organization in female white-tailed deer. Journal of Wildlife Management 69, 332–344. https://doi.org/10.2193/0022-541X(2005)069<0332:FGSASO>2.0.CO;2

Conner, M.M., Wood, M.E., Hubbs, A., Binfet, J., Holland, A.A., Meduna, L.R., Roug, A., Runge, J.P., Nordeen, T.D., Pybus, M.J., Miller, M.W., 2021. The relationship between harvest management and chronic wasting disease prevalence trends in western mule deer (Odocoileus hemionus) herds. Journal of Wildlife Diseases 57, 831–843. https://doi.org/10.7589/JWD-D-20-00226

Cosgrove, M.K., O'Brien, D.J., Ramsey, D.S.L., 2018. Baiting and Feeding Revisited: Modeling Factors Influencing Transmission of Tuberculosis Among Deer and to Cattle. Frontiers in Veterinary Science 5, 306. https://doi.org/10.3389/fvets.2018.00306

Cotterill, G.G., Cross, P.C., Middleton, A.D., Rogerson, J.D., Scurlock, B.M., Toit, J.T. du, 2018. Hidden cost of disease in a free-ranging ungulate: brucellosis reduces mid-winter pregnancy in elk. Ecology and Evolution 8, 10733–10742. https://doi.org/10.1002/ece3.4521

Croft, S., Massei, G., Smith, G.C., Fouracre, D., Aegerter, J.N., 2020. Modelling Spatial and Temporal Patterns of African Swine Fever in an Isolated Wild Boar Population to Support Decision-Making. Front. Vet. Sci. 7. https://doi.org/10.3389/fvets.2020.00154

Crooks, A., Castle, C., Batty, M., 2008. Key challenges in agent-based modelling for geo-spatial simulation. Computers, Environment and Urban Systems, GeoComputation: Modeling with spatial agents 32, 417–430. https://doi.org/10.1016/j.compenvurbsys.2008.09.004

Cross, P.C., Creech, T.G., Ebinger, M.R., Manlove, K., Irvine, K., Henningsen, J., Rogerson, J., Scurlock, B.M., Creel, S., 2013. Female elk contacts are neither frequency nor density dependent. Ecology 94, 2076–2086. https://doi.org/10.1890/12-2086.1

Cross, P.C., Johnson, P.L.F., Lloyd-Smith, J.O., Getz, W.M., 2007. Utility of R0 as a predictor of disease invasion in structured populations. Journal of The Royal Society Interface 4, 315–324. https://doi.org/10.1098/rsif.2006.0185

Cross, P.C., Lloyd-Smith, J.O., Johnson, P.L.F., Getz, W.M., 2005. Duelling timescales of host movement and disease recovery determine invasion of disease in structured populations. Ecology Letters 8, 587–595. https://doi.org/10.1111/j.1461-0248.2005.00760.x

DeVivo, M.T., Edmunds, D.R., Kauffman, M.J., Schumaker, B.A., Binfet, J., Kreeger, T.J., Richards, B.J., Schätzl, H.M., Cornish, T.E., 2017. Endemic chronic wasting disease causes mule deer population decline in Wyoming. PLoS ONE 12, e0186512. https://doi.org/10.1371/journal.pone.0186512

Dion, E., Lambin, E.F., 2012. Scenarios of transmission risk of foot-and-mouth with climatic, social and landscape changes in southern Africa. Applied Geography 35, 32–42. https://doi.org/10.1016/j.apgeog.2012.05.001

Dion, E., VanSchalkwyk, L., Lambin, E., 2011. The landscape epidemiology of foot-and-mouth disease in South Africa: A spatially explicit multi-agent simulation. Ecological Modelling 222, 2059–2072. https://doi.org/10.1016/j.ecolmodel.2011.03.026

Dobbin, M., 2022. Analysis of direct contacts between mule deer (*Odocoileus hemionus*) (Masters Thesis). University of Alberta.

Duchesne, T., Fortin, D., Rivest, L.-P., 2015. Equivalence between Step Selection Functions and Biased Correlated Random Walks for Statistical Inference on Animal Movement. PloS one 10, e0122947. https://doi.org/10.1371/journal.pone.0122947

Edmunds, D.R., Albeke, S.E., Grogan, R.G., Lindzey, F.G., Legg, D.E., Cook, W.E., Schumaker, B.A., Kreeger, T.J., Cornish, T.E., 2018. Chronic wasting disease influences activity and behavior in white-tailed deer. Jour. Wild. Mgmt. 82, 138–154. https://doi.org/10.1002/jwmg.21341

Edmunds, D.R., Kauffman, M.J., Schumaker, B.A., Lindzey, F.G., Cook, W.E., Kreeger, T.J., Grogan, R.G., Cornish, T.E., 2016. Chronic Wasting Disease Drives Population Decline of White-Tailed Deer. PLOS ONE 11, e0161127. https://doi.org/10.1371/journal.pone.0161127

Escobar, L.E., Pritzkow, S., Winter, S.N., Grear, D.A., Kirchgessner, M.S., Dominguez-Villegas, E., Machado, G., Townsend Peterson, A., Soto, C., 2020. The ecology of chronic wasting disease in wildlife. Biological Reviews 95, 393–408. https://doi.org/10.1111/brv.12568

Evans, J.S., 2020. spatialEco.

Fortin, D., Beyer, H., Boyce, M., Smith, D., Duchesne, T., Mao, J., 2005. Wolves influence elk movements: Behavior shapes a trophic cascade in Yellowstone National Park. Ecology 86, 1320–1330. https://doi.org/10.1890/04-0953

Gooding, R.M., Brook, R.K., 2014. Modeling and mitigating winter hay bale damage by elk in a low prevalence bovine tuberculosis endemic zone. Preventive Veterinary Medicine 114, 123–131. https://doi.org/10.1016/j.prevetmed.2014.01.005

Governement of Saskatchewan, 2019. Saskatchewan Upgraded Road Network.

Governement of Saskatchewan, 2015. Vertical Wells.

Government of Alberta, 2021. Wildlife Damage Complaints. Government of Alberta.

Government of Canada, 2017. Lakes and rivers in Canada - CanVec – Hydro Features.

Government of Canada, 2016. Canada Digital Elevation Model.
Grimm, V., Berger, U., Bastiansen, F., Eliassen, S., Ginot, V., Giske, J., Goss-Custard, J., Grand, T., Heinz, S.K., Huse, G., Huth, A., Jepsen, J.U., Jørgensen, C., Mooij, W.M., Müller, B., Pe'er, G., Piou, C., Railsback, S.F., Robbins, A.M., Robbins, M.M., Rossmanith, E., Rüger, N., Strand, E., Souissi, S., Stillman, R.A., Vabø, R., Visser, U., DeAngelis, D.L., 2006. A standard protocol for describing individual-based and agent-based models. Ecological Modelling 198, 115–126. https://doi.org/10.1016/j.ecolmodel.2006.04.023
Grimm, V., Berger, U., DeAngelis, D.L., Polhill, J.G., Giske, J., Railsback, S.F., 2010. The ODD protocol: A review and first update. Ecological Modelling 221, 2760–2768. https://doi.org/10.1016/j.ecolmodel.2010.08.019
Gustine, D.D., Parker, K.L., Lay, R.J., Gillingham, M.P., Heard, D.C., 2006. Interpreting Resource Selection at Different Scales for Woodland Caribou in Winter. wild 70, 1601–1614. https://doi.org/10.2193/0022-541X(2006)70[1601:IRSADS]2.0.CO;2
Habib, T.J., Merrill, E.H., Pybus, M.J., Coltman, D.W., 2011. Modelling landscape effects on density–contact rate relationships of deer in eastern Alberta: implications for chronic wasting disease. Ecological Modelling 222, 2722–2732.
Heberlein, T.A., 2004. "Fire in the Sistine Chapel": How Wisconsin Responded to Chronic Wasting Disease. Human Dimensions of Wildlife 9, 165–179. https://doi.org/10.1080/10871200490479954
Helton, J.C., Davis, F.J., 2003. Latin hypercube sampling and the propagation of uncertainty in analyses of complex systems. Reliability Engineering & System Safety 81, 23–69. https://doi.org/10.1016/S0951-8320(03)00058-9
Herrera, J., Nunn, C.L., 2019. Behavioural ecology and infectious disease: implications for conservation of biodiversity. Philosophical transactions. Biological sciences 374, 20180054. https://doi.org/10.1098/rstb.2018.0054
Holsman, R.H., Petchenik, J., Cooney, E.E., 2010. CWD After "the Fire": Six Reasons Why Hunters Resisted Wisconsin's Eradication Effort. Human Dimensions of Wildlife 15, 180–193. https://doi.org/10.1080/10871201003718029
Hurford, A., 2009. GPS Measurement Error Gives Rise to Spurious 180° Turning Angles and Strong Directional Biases in Animal Movement Data. PLoS ONE 4, e5632. https://doi.org/10.1371/journal.pone.0005632
Joly, D.O., Samuel, M.D., Langenberg, J.A., Blanchong, J.A., Batha, C.A., Rolley, R.E., Keane, D.P., Ribic, C.A., 2006. Spatial epidemiology of chronic wasting disease in Wisconsin white-tailed deer. Journal of Wildlife Diseases 42, 578–588. https://doi.org/10.7589/0090-3558-42.3.578
Kerr, C.C., 2019. Is epidemiology ready for Big Software? Pathogens and Disease 77. https://doi.org/10.1093/femspd/ftz006
Kjær, L., 2010. Indivdual-based modeling of white-tailed deer (Odocoileus virginanus) movements and epizootiology (Doctor of Philosophy). Southern Illinois University Carbondale, Illinois.
Kjær, L.J., Schauber, E.M., Nielsen, C.K., 2008. Spatial and temporal analysis of contact rates in female white-tailed deer. The Journal of Wildlife Management 72, 1819–1825. https://doi.org/10.2193/2007-489
Ladle, A., Galpern, P., Doyle-Baker, P., 2018. Measuring the use of green space with urban resource selection functions: An application using smartphone GPS locations. Landscape and Urban Planning 179, 107–115. https://doi.org/10.1016/j.landurbplan.2018.07.012

Latifovic, R., 2019. 2015 Land Cover of Canada.
Lele, S.R., Merrill, E.H., Keim, J., Boyce, M.S., 2013. Selection, use, choice and occupancy: clarifying concepts in resource selection studies. Journal of Animal Ecology 82, 1183–1191. https://doi.org/10.1111/1365-2656.12141
Lemieux, N., Maynard, B.K., Johnson, W.A., 2000. A Regional Survey of Deer Damage Throughout Northeast Nurseries and Orchards. Journal of Environmental Horticulture 18, 1–4. https://doi.org/10.24266/0738-2898-18.1.1
Leuthold, W., Leuthold, B.M., 1975. Patterns of social grouping in ungulates of Tsavo National Park, Kenya. Journal of Zoology 175, 405–420. https://doi.org/10.1111/j.1469-7998.1975.tb01408.x
Ligmann-Zielinska, A., Siebers, P.-O., Magliocca, N., Parker, D.C., Grimm, V., Du, J., Cenek, M., Radchuk, V., Arbab, N.N., Li, S., Berger, U., Paudel, R., Robinson, D.T., Jankowski, P., An, L., Ye, X., 2020. 'One Size Does Not Fit All': A Roadmap of Purpose-Driven Mixed-Method Pathways for Sensitivity Analysis of Agent-Based Models. JASSS 23, 6. https://doi.org/10.18564/jasss.4201
Lingle, S., 2003. Group composition and cohesion in sympatric white-tailed deer and mule deer. Canadian Journal of Zoology 81, 1119–1130. https://doi.org/10.1139/z03-097
Maloney, M., Merkle, J.A., Aadland, D., Peck, D., Horan, R.D., Monteith, K.L., Winslow, T., Logan, J., Finnoff, D., Sims, C., Schumaker, B., 2020. Chronic wasting disease undermines efforts to control the spread of brucellosis in the Greater Yellowstone Ecosystem. Ecological Applications 30, e02129. https://doi.org/10.1002/eap.2129
Manjerovic, M.B., Green, M.L., Mateus-Pinilla, N., Novakofski, J., 2014. The importance of localized culling in stabilizing chronic wasting disease prevalence in white-tailed deer populations. Preventive Veterinary Medicine 113, 139–145. https://doi.org/10.1016/j.prevetmed.2013.09.011
Manlik, O., Lacy, R.C., Sherwin, W.B., 2018. Applicability and limitations of sensitivity analyses for wildlife management. Journal of Applied Ecology 55, 1430–1440. https://doi.org/10.1111/1365-2664.13044
Manlove, K.R., Cassirer, E.F., Plowright, R.K., Cross, P.C., Hudson, P.J., 2017. Contact and contagion: Probability of transmission given contact varies with demographic state in bighorn sheep. Journal of Animal Ecology 86, 908–920. https://doi.org/10.1111/1365-2656.12664
Manly, B.F.J., 2002. Resource selection by animals : statistical design and analysis for field studies., 2nd ed. ed. Kluwer Academic Publishers.
Mateus-Pinilla, N., Weng, H.Y., Ruiz, M.O., Shelton, P., Novakofski, J., 2013. Evaluation of a wild white-tailed deer population management program for controlling chronic wasting disease in Illinois, 2003-2008. Preventive veterinary medicine 110, 541–548. https://doi.org/S0167-5877(13)00074-3 [pii]
McCallum, H., Jones, M., Hawkins, C., Hamede, R., Lachish, S., Sinn, D.L., Beeton, N., Lazenby, B., 2009. Transmission dynamics of Tasmanian devil facial tumor disease may lead to disease-induced extinction. Ecology 90, 3379–3392. https://doi.org/10.1890/08-1763.1
McRae, J.E., Schlichting, P.E., Snow, N.P., Davis, A.J., VerCauteren, K.C., Kilgo, J.C., Keiter, D.A., Beasley, J.C., Pepin, K.M., 2020. Factors Affecting Bait Site Visitation: Area of Influence of Baits. Wildl. Soc. Bull. 44, 362–371. https://doi.org/10.1002/wsb.1074
Meijer, M., Karpuk, E., 1999. Dillberry Lake Provincial Park biophysical inventory.

Mejía-Salazar, M.F., Waldner, C.L., Hwang, Y.T., Bollinger, T.K., 2018. Use of environmental sites by mule deer: a proxy for relative risk of chronic wasting disease exposure and transmission. Ecosphere 9, e02055. https://doi.org/10.1002/ecs2.2055

Menichetti, L., Touzot, L., Elofsson, K., Hyvönen, R., Kätterer, T., Kjellander, P., 2019. Interactions between a population of fallow deer (Dama dama), humans and crops in a managed composite temperate landscape in southern Sweden: Conflict or opportunity? PLOS ONE 14, e0215594. https://doi.org/10.1371/journal.pone.0215594

Merrill, E.H., Pybus, M.J., Nobert, B.R., Habib, T.J., Brownrigg, E., Jones, P., Garrett, C., Bertrand, A., Wachowski, J., Stevens, J., Flaig, C., 2013. Alberta Chronic Wasting Disease: North Border Deer Study 1–76.

Miller, M.W., Williams, E.S., 2004. Chronic Wasting Disease of Cervids, in: Harris, D.A. (Ed.), Mad Cow Disease and Related Spongiform Encephalopathies. Springer Berlin Heidelberg, Berlin, Heidelberg, pp. 193–214. https://doi.org/10.1007/978-3-662-08441-0_8

Miller, R., Kaneene, J.B., Fitzgerald, S.D., Schmitt, S.M., 2003. Evaluation of the influence of supplemental feeding of white-tailed deer (Odocoileus virginianus) on the prevalence of bovine tuberculosis in the Michigan wild deer population. Journal of Wildlife Diseases 39, 84–95. https://doi.org/10.7589/0090-3558-39.1.84

Moorter, B., Visscher, D., Benhamou, S., Börger, L., Boyce, M., Gaillard, J.-M., 2009. Memory keeps you at home: A mechanistic model for home range emergence. Oikos 118, 641–652. https://doi.org/10.1111/j.1600-0706.2008.17003.x

Mortensen, L.O., Chudzinska, M.E., Slabbekoorn, H., Thomsen, F., 2021. Agent-based models to investigate sound impact on marine animals: bridging the gap between effects on individual behaviour and population level consequences. Oikos n/a. https://doi.org/10.1111/oik.08078

Murphy, K.J., Ciuti, S., Kane, A., 2020. An introduction to agent-based models as an accessible surrogate to field-based research and teaching. Ecology and Evolution 10, 12482–12498. https://doi.org/10.1002/ece3.6848

Mysterud, A., Edmunds, D.R., 2019. A review of chronic wasting disease in North America with implications for Europe. European Journal of Wildlife Research 65, 26. https://doi.org/10.1007/s10344-019-1260-z

Mysterud, A., Rolandsen, C.M., 2019. Fencing for wildlife disease control. Journal of Applied Ecology 56, 519–525. https://doi.org/10.1111/1365-2664.13301

Mysterud, A., Skjelbostad, I.N., Rivrud, I.M., Brekkum, Ø., Meisingset, E.L., 2021. Spatial Clustering by Red Deer and Its Relevance for Management of Chronic Wasting Disease. Animals (Basel) 11, 1272. https://doi.org/10.3390/ani11051272

Mysterud, A., Viljugrein, H., Solberg, E.J., Rolandsen, C.M., 2019. Legal regulation of supplementary cervid feeding facing chronic wasting disease. The Journal of Wildlife Management 83, 1667–1675. https://doi.org/10.1002/jwmg.21746

Nielsen, S.E., Cranston, J., Stenhouse, G.B., 2009. Identification of Priority Areas for Grizzly Bear Conservation and Recovery in Alberta, Canada. Journal of Conservation Planning 5, 24.

Nobert, B.R., 2012. Landscape ecology of mule deer (Odocoileus hemionus) and white-tailed deer (O. virginianus) with implications for chronic wasting disease (PhD Thesis). https://doi.org/10.7939/R3BC95

Nobert, B.R., Merrill, E.H., Pybus, M.J., Bollinger, T.K., Hwang, Y.T., 2016. Landscape connectivity predicts chronic wasting disease risk in Canada. J Appl Ecol 53, 1450–1459. https://doi.org/10.1111/1365-2664.12677

Northrup, J.M., Anderson, C.R., Wittemyer, G., 2015. Quantifying spatial habitat loss from hydrocarbon development through assessing habitat selection patterns of mule deer. Glob Change Biol 21, 3961–3970. https://doi.org/10.1111/gcb.13037

O'Brien, D.J., Schmitt, S.M., Fitzgerald, S.D., Berry, D.E., 2011. Management of bovine tuberculosis in Michigan wildlife: Current status and near term prospects. Veterinary Microbiology 151, 179–187. https://doi.org/10.1016/j.vetmic.2011.02.042

O'Brien, D.J., Schmitt, S.M., Fitzgerald, S.D., Berry, D.E., Hickling, G.J., 2006. Managing the wildlife reservoir of Mycobacterium bovis: The Michigan, USA, experience. Veterinary Microbiology, 4th International Conference on Mycobacterium bovis 112, 313–323. https://doi.org/10.1016/j.vetmic.2005.11.014

Oja, R., Velström, K., Moks, E., Jokelainen, P., Lassen, B., 2017. How does supplementary feeding affect endoparasite infection in wild boar? Parasitology Research 116, 2131–2137. https://doi.org/10.1007/s00436-017-5512-0

Pe'er, G., Kramer-Schadt, S., 2008. Incorporating the perceptual range of animals into connectivity models. Ecological Modelling 213, 73–85. https://doi.org/10.1016/j.ecolmodel.2007.11.020

Peterson, M.J., Samuel, M.D., Nettles, V.F., Wobeser, G., Hueston, W.D., 2002. Review of chronic wasting disease management policies and programs in Colorado (Report).

Plummer, I.H., Johnson, C.J., Chesney, A.R., Pedersen, J.A., Samuel, M.D., 2018. Mineral licks as environmental reservoirs of chronic wasting disease prions. PloS one 13, e0196745. https://doi.org/10.1371/journal.pone.0196745

Potapov, A., Merrill, E., Pybus, M., Coltman, D., Lewis, M.A., 2013. Chronic wasting disease: Possible transmission mechanisms in deer. Ecological Modelling. https://doi.org/10.1016/j.ecolmodel.2012.11.012

Potapov, A., Merrill, E., Pybus, M., Lewis, M.A., 2016. Chronic Wasting Disease: Transmission Mechanisms and the Possibility of Harvest Management. PLoS ONE 11, e0151039. https://doi.org/10.1371/journal.pone.0151039

Potapov, A., Merrill, E., Pybus, M., Lewis, M.A., 2015. Empirical Estimation of R0 for Unknown Transmission Functions: The Case of Chronic Wasting Disease in Alberta. PLOS ONE. https://doi.org/10.1371/journal.pone.0140024

Prieto, K., Ibarguen-Mondragon, E., 2019. Parameter estimation, sensitivity and control strategies analysis in the spread of influenza in Mexico. J. Phys.: Conf. Ser. 1408, 012020. https://doi.org/10.1088/1742-6596/1408/1/012020

Rakowski, F., Gruziel, M., Bieniasz-Krzywiec, Ł., Radomski, J.P., 2010. Influenza epidemic spread simulation for Poland — a large scale, individual based model study. Physica A: Statistical Mechanics and its Applications 389, 3149–3165. https://doi.org/10.1016/j.physa.2010.04.029

Ramsey, D.S.L., Efford, M.G., 2010. Management of bovine tuberculosis in brushtail possums in New Zealand: predictions from a spatially explicit, individual-based model: Spatially explicit model of Tb in possums. Journal of Applied Ecology 47, 911–919. https://doi.org/10.1111/j.1365-2664.2010.01839.x

Ramsey, D.S.L., O'Brien, D.J., Cosgrove, M.K., Rudolph, B.A., Locher, A.B., Schmitt, S.M., 2014. Forecasting Eradication of Bovine Tuberculosis in Michigan White-Tailed Deer. The Journal of Wildlife Management 78, 240–254.
Real, L.A., Biek, R., 2007. Spatial dynamics and genetics of infectious diseases on heterogeneous landscapes. J. R. Soc. Interface. 4, 935–948. https://doi.org/10.1098/rsif.2007.1041
Rifkin, J.L., Nunn, C.L., Garamszegi, L.Z., 2012. Do Animals Living in Larger Groups Experience Greater Parasitism? A Meta-Analysis. The American Naturalist 180, 70–82. https://doi.org/10.1086/666081
Riley, S.J., DeGloria, S.D., Elliot, R., 1999. A terrain ruggedness index that quantifies topographic heterogeneity. Intermountain Journal of Sciences 5, 23–27.
Rivera, N.A., Brandt, A.L., Novakofski, J.E., Mateus-Pinilla, N.E., 2019. Chronic Wasting Disease In Cervids: Prevalence, Impact And Management Strategies. Vet Med (Auckl) 10, 123–139. https://doi.org/10.2147/VMRR.S197404
Rodgers, P.A., Sawyer, H., Mong, T.W., Stephens, S., Kauffman, M.J., 2021. Sex-Specific Behaviors of Hunted Mule Deer During Rifle Season. The Journal of Wildlife Management 85, 215–227. https://doi.org/10.1002/jwmg.21988
Ruckstuhl, K.E., Neuhaus, P., 2000. Sexual Segregation in Ungulates: A New Approach. Behaviour 137, 361–377.
Sah, P., Mann, J., Bansal, S., 2018. Disease implications of animal social network structure: A synthesis across social systems. J Anim Ecol 87, 546–558. https://doi.org/10.1111/1365-2656.12786
Salecker, J., Sciaini, M., Meyer, K., Wiegand, K., 2019. The nlrx r package: A next-generation framework for reproducible NetLogo model analyses. Methods in Ecololgy and Evolution 00, 2041–210X.
Schauber, E.M., Storm, D.J., Nielsen, C.K., 2007. Effects of joint space use and group membership on contact rates among white-tailed deer. The Journal of Wildlife Management 71, 155–163. https://doi.org/10.2193/2005-546
Scherer, C., Radchuk, V., Franz, M., Thulke, H.-H., Lange, M., Grimm, V., Kramer-Schadt, S., 2020. Moving infections: individual movement decisions drive disease persistence in spatially structured landscapes. Oikos 129, 651–667. https://doi.org/10.1111/oik.07002
Seagle, S.W., 2003. Can ungulates foraging in a multiple-use landscape alter forest nitrogen budgets? Oikos 103, 230–234. https://doi.org/10.1034/j.1600-0706.2003.12287.x
Signer, J., Fieberg, J., Avgar, T., 2019. Animal movement tools (amt): R package for managing tracking data and conducting habitat selection analyses. Ecology and Evolution 9, 880–890.
Silbernagel, E., 2010. Factors affecting movement patterns of mule deer (Odocoileus hemionus) (Master Thesis). Landscape. University of Saskatchewan.
Silbernagel, E.R., Skelton, N.K., Waldner, C.L., Bollinger, T.K., 2011. Interaction among deer in a chronic wasting disease endemic zone. The Journal of Wildlife Management 75, 1453–1461. https://doi.org/10.1002/jwmg.172
Silk, M.J., Hodgson, D.J., Rozins, C., Croft, D.P., Delahay, R.J., Boots, M., McDonald, R.A., 2019. Integrating social behaviour, demography and disease dynamics in network models: applications to disease management in declining wildlife populations. Phil. Trans. R. Soc. B 374, 20180211. https://doi.org/10.1098/rstb.2018.0211

Smith, M.J., Telfer, S., Kallio, E.R., Burthe, S., Cook, A.R., Lambin, X., Begon, M., 2009. Host-pathogen time series data in wildlife support a transmission function between density and frequency dependence. Proceedings of the National Academy of Sciences 106, 7905–7909. https://doi.org/10.1073/pnas.0809145106

Smolko, P., Seidel, D., Pybus, M., Hubbs, A., Ball, M., Merrill, E., 2021. Spatio-temporal changes in chronic wasting disease risk in wild deer during 14 years of surveillance in Alberta, Canada. Preventive Veterinary Medicine 197, 105512. https://doi.org/10.1016/j.prevetmed.2021.105512

Sorensen, A., 2014. Habitat selection by sympatric ungulates in an agricultural landscape : implications for disease transmission and human-wildlife conflict. Masters Thesis University of Saskatchewan.

Sorensen, A.A., van Beest, F.M., Brook, R.K., 2015. Quantifying overlap in crop selection patterns among three sympatric ungulates in an agricultural landscape. Basic and Applied Ecology 16, 601–609. https://doi.org/10.1016/j.baae.2015.05.001

Storm, D.J., Samuel, M.D., Rolley, R.E., Shelton, P., Keuler, N.S., Richards, B.J., Deelen, T.R.V., 2013. Deer density and disease prevalence influence transmission of chronic wasting disease in white-tailed deer. Ecosphere 4, art10. https://doi.org/10.1890/ES12-00141.1

ten Broeke, G., van Voorn, G., Ligtenberg, A., 2016. Which Sensitivity Analysis Method Should I Use for My Agent-Based Model? JASSS 19, 5.

The Municipal District of Provost No. 52, 2019. Ownership Map M.D. of Provost No. 52.

The Municipal District of Wainwright No. 61, 2020. Ownership Map M.D. of Wainwright No. 61.

Thompson, A., Samuel, M., Deelen, T.V., 2008. Alternative feeding strategies and potential disease transmission in Wisconsin white-tailed deer. Journal of Wildlife Management 72, 416–421. https://doi.org/10.2193/2006-543

Thulke, H.-H., Eisinger, D., 2008. The strength of 70%: revision of a standard threshold of rabies control. Developments in biologicals 131, 291.

Thurfjell, H., Ciuti, S., Boyce, M.S., 2014. Applications of step-selection functions in ecology and conservation. Movement Ecology 2, 1–12. https://doi.org/10.1186/2051-3933-2-4

Tosa, M.I., Schauber, E.M., Nielsen, C.K., 2015. Familiarity breed contempt: Combining proximity loggers and GPS reveals female white-tailed deer (Odocoileus virginianus) avoiding close contact with neighbors. Journal of Wildlife Diseases 51, 79. https://doi.org/10.7589/2013-06-139

U.S. Geological Survery, 2022. Distribution of Chronic Wasting Disease in North America | U.S. Geological Survey [WWW Document]. URL https://www.usgs.gov/media/images/distribution-chronic-wasting-disease-north-america-0 (accessed 1.7.22).

Vander Wal, E., Laforge, M.P., McLoughlin, P.D., 2014. Density dependence in social behaviour: home range overlap and density interacts to affect conspecific encounter rates in a gregarious ungulate. Behav Ecol Sociobiol 68, 383–390. https://doi.org/10.1007/s00265-013-1652-0

VerCauteren, K.C., Hygnstrom, S.E., 2004. White-tailed Deer, in: Wishart, D.J. (Ed.), Encyclopedia of the Great Plains. University of Nebraska Press.

von Neumann, J., 1951. Various Techniques Used in Connection With Random Digits, in: Monte Carlo Method. US Government Printing Office, Washington, DC, pp. 36–38.

Walter, W.D., Baasch, D.M., Hygnstrom, S.E., Trindle, B.D., Tyre, A.J., Millspaugh, J.J., Frost, C.J., Boner, J.R., VerCauteren, K.C., 2011. Space use of sympatric deer in a riparian ecosystem in an area where chronic wasting disease is endemic. wbio 17, 191–209. https://doi.org/10.2981/10-055

Wells, K., Hamede, R.K., Jones, M.E., Hohenlohe, P.A., Storfer, A., McCallum, H.I., 2019. Individual and temporal variation in pathogen load predicts long-term impacts of an emerging infectious disease. Ecology 100, e02613. https://doi.org/10.1002/ecy.2613

Western Association of Fish and Wildlife Agencies, 2018. Recommendations for Adaptive Management of Chronic Wasting Disease in the West. Western Association of Fish and Wildlife Agencies, Edmonton, AB, Canada and Fort Collins, Colorado, USA.

White, L.A., Forester, J.D., Craft, M.E., 2018a. Dynamic, spatial models of parasite transmission in wildlife: Their structure, applications and remaining challenges. Journal of Animal Ecology 87, 559–580. https://doi.org/10.1111/1365-2656.12761

White, L.A., Forester, J.D., Craft, M.E., 2018b. Disease outbreak thresholds emerge from interactions between movement behavior, landscape structure, and epidemiology. Proceedings of the National Academy of Sciences of the United States of America 115, 7374–7379. https://doi.org/10.1073/pnas.1801383115

White, L.A., Forester, J.D., Craft, M.E., 2017. Using contact networks to explore mechanisms of parasite transmission in wildlife. Biological Reviews 92, 389–409. https://doi.org/10.1111/brv.12236

Wilensky, U., 1999. Netlogo. Center for Connected Learning and Computer-Based Modeling, Northwestern University, Evanston, IL.

Williams, E., Miller, M., 2003. Prion disease horizontal prion transmission in mule deer. Nature 425, 35–36. https://doi.org/10.1038/425035a

Williams, E., Young, S., 1982. Spongiform Encephalopathy of Rocky Mountain Elk. Journal of Wildlife Diseases 18, 465–471.

Williams, E., Young, S., 1980. Chronic Wasting Disease of Captive Mule Deer: A Spongiform Encephalopathy. Journal of Wildlife Diseases 16, 89–98.

Wywialowski, A.P., 1994. Agricultural Producers' Perceptions of Wildlife-Caused Losses. Wildlife Society Bulletin (1973-2006) 22, 370–382.

Appendices

Appendix A. State variables for the patches and deer in the individual-based model.

Table A.1 State variables for individuals and patches included in the movement IBM

Patches	
proportional-Mweight/ proportional-Fweight	Used to determine whether an individual accepts or rejects a step, calculated by dividing the cell weight (as determined by step-selection function) by the maximum weight across all cells
within-contacts-winter-*XX* / between-contacts-winter-*XX*	Total number of within/between-group contacts that have occurred on that cell between the given dyad type (MF, MM, FF).
Deer	
male?/female?	True/false variables that define the sex of the individual
leader	True/false variable that defines the leader of the group
group	Group number of the individual, defines group membership
leaderangle	[who] (ID) of the deer in group with leader=true
HRX/HRY	x and y coordinates of the home range centre
angle	The turning angle for the deer's step
step-length	The step length for the deer's step
result	A 0/1 parameter, 0 when not accepting step, switches to 1 when step is accepted and breaks the loop in the code
point	The proportional weight value of the cell to which the drawn step sends the individual
sine/cosine	Parameters calculated using the direction of persistence and direction towards the home range centre, used to determine the new heading for the individual
vm-length	Spread parameter for the Von mises turning angle distribution
Within-group-winter-*same or mixed* / between-group-winter-*same or mixed*	The total number of contacts that have occurred for that deer, with deer of the same sex and with deer of the opposite sex (mixed).
Step-within-winter-*same or mixed* /step-between-winter-*same or mixed*	The number of contacts occurring in the current step that are with the same sex or with the opposite sex (mixed).

Appendix B: Model selection and k-fold validation for home range RSFs

Table B.1 Model selection table for home range resource selection functions with top 5 models for each season/sex. * indicates that the confidence interval does not overlap zero.

Sex/ Season	Int	ED_{250}	Rivers	Roads	Rugg	Streams	WC_{250}	WC_{250}^2	Wells	ΔAICc
Female	-4.62		0.45	1.11	0.19		20.67	-18.80	-0.15	
Summer	± 0.65*		± 0.27	± 0.59	± 1.01		± 4.92*	± 5.52*	± 0.39	0
	-4.53						21.09	-19.43		
	± 0.61*						± 4.66*	± 5.17*		1.172
	-4.62		0.45	1.11	0.17	0.028	20.70	-18.83	-0.15	
	± 0.65*		± 0.28	± 0.59	± 1.08	±0.48	± 4.95*	± 5.55*	± 0.39	1.997
	-3.88	1.64								
	± 0.48*	±0.28*								3.501
	-4.01	1.65	0.48	1.05	-0.14	0.15			-0.26	
	± 0.52*	±0.29*	± 0.28	± 0.60	± 1.07	± 0.47			± 0.38	5.221
Male	-2.81			-1.91	3.04		4.52		-0.003	
Summer	± 0.56*			± 1.39	± 1.46*		± 1.32*		± 0.99	0
	-3.03						4.56			
	± 0.51*						± 1.18*			1.790
	-2.82			-1.92	2.91	0.14	4.54		-0.025	
	± 0.57*			± 1.39	± 1.75	±1.08	± 1.34*		± 1.00	1.982
	-2.93		-0.21		3.41	-0.14	4.79			
	± 0.57*		± 0.77		± 1.94*	± 1.03	± 1.30*			3.291
	-3.19						6.85	-2.74		
	± 0.79*						± 8.45	± 9.98		3.714
Female	-3.81	1.58								
Rut	± 0.48*	±0.28*								0
	-4.38						20.37	-19.02		
	± 0.60*						± 4.73*	± 5.32*		0.247
	-4.12	1.74	0.12	0.003	-1.49	1.14			0.087	
	± 0.51*	±0.29*	± 0.29	± 0.60	± 0.97	± 0.47*			± 0.40	3.034
	-4.72		0.052	0.21	-1.24	1.05	21.68	-19.93	0.14	3.367

	± 0.63*	± 0.29	± 0.59	± 0.98	± 0.47*	± 4.86*	± 5.48*	± 0.40	
	-4.56	0.16	0.51	-0.46		21.07	-19.61		
	± 0.62*	± 0.28	± 0.44	± 0.90		± 4.85*	± 5.47*		4.451
Male Rut	-6.36	0.76	-0.75		1.98	8.18		1.44	
	± 0.87*	± 0.60	± 1.63		± 1.35	± 1.62*		± 0.99	0
	-6.04	0.86		-0.94	2.34	7.48			
	± 0.78*	± 0.80		± 2.90	± 1.36	± 1.47*			0.124
	-5.57					6.50			
	± 0.69*					± 1.32*			1.896
	-6.38	0.93	-0.73	-0.88	2.11	8.11		1.43	
	±0.87*	± 0.80	± 1.62	± 2.76	± 1.41	± 1.62*		± 0.99	2.021
	-6.07		-1.24	2.90		7.86		1.62	
	± 0.85*		± 1.53	± 1.85		± 1.65*		± 0.98	2.701
Winter	-4.64	1.21			-1.34	7.48		0.91	
All	± 0.44*	± 0.36*			± 0.65*	± 0.87*		± 0.31*	0
	-5.59	0.97	-0.59	0.91	-1.33	16.94	-10.44	1.09	
	± 0.77*	± 0.41*	± 0.58	± 1.16	± 0.64*	± 5.30*	± 5.70	± 0.41*	0.462
	-4.61	1.18	-0.60		-1.30	7.46		1.17	
	± 0.44*	± 0.36*	± 0.59		± 0.65*	± 0.87*		± 0.40*	0.962
	-4.56	0.94	-0.63	1.22	-1.45	7.53		1.18	
	± 0.45*	± 0.41*	± 0.60	± 1.16	± 0.65*	± 0.88*		± 0.41*	1.865
	-4.19	0.85		1.28	-1.21	6.91			6.953
	± 0.39*	± 0.39*		± 1.16	± 0.62*	± 0.81*			

Table B.2. K-fold results, i.e., number of folds, correlation (r), and standard deviation (σ) for top RSF models for each group type. (WC_{250m} = proportion woody cover and ED_{250m} = woody cover edge density)

Group	Model	# of folds	r	σ
Female Summer	$WC_{250m} + WC_{250m}^2$	5	0.79	0.12
Male Summer	WC_{250m}	3	0.57	0.13
Female Rut WC	$WC_{250m} + WC_{250m}^2$	5	0.84	0.07
Female Rut ED	ED_{250m}	5	0.80	0.10
Male Rut	WC_{250m}	3	0.69	0.01
Winter All	DistWells + DistRivers + DistStreams + WC_{250m}	5	0.82	0.08

Appendix C: Simulation contacts overlaid on relative contact probability maps (Dobbin 2022)

a)

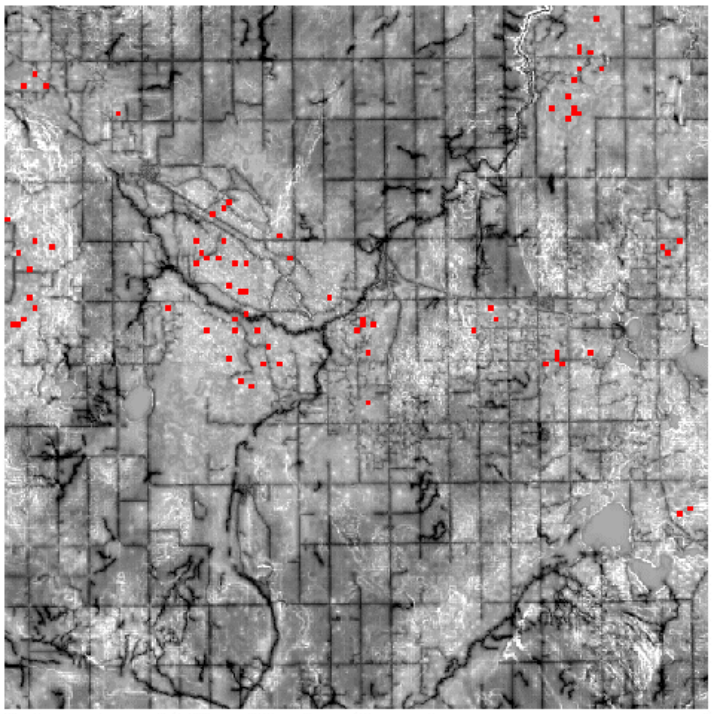

b)

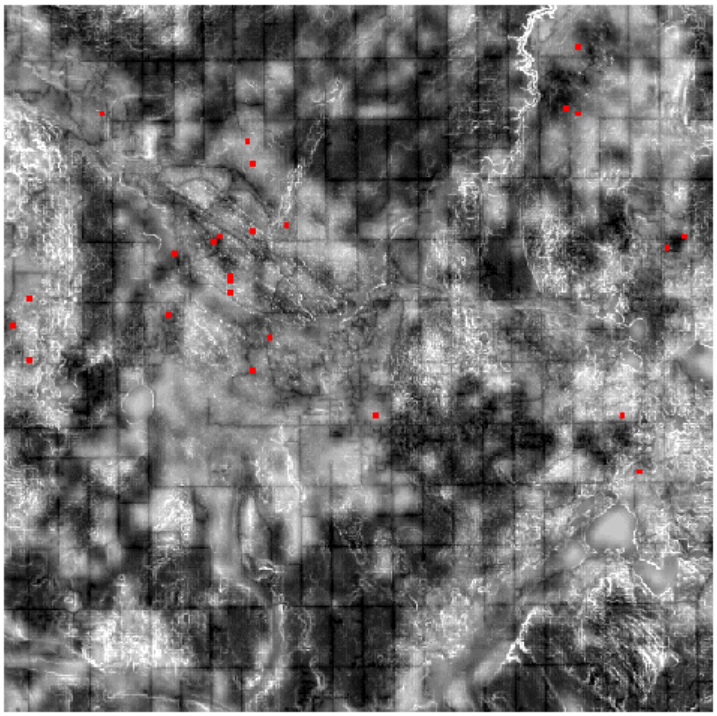

c)

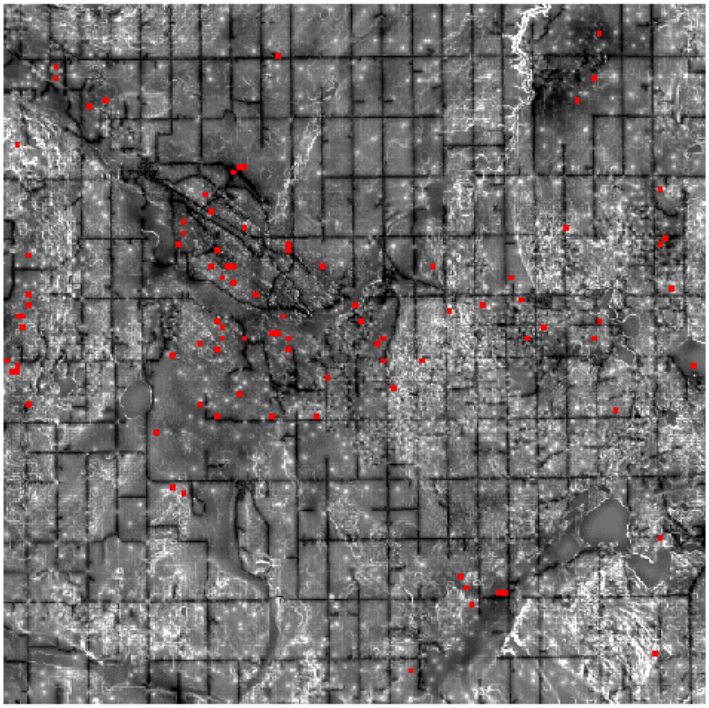

d)

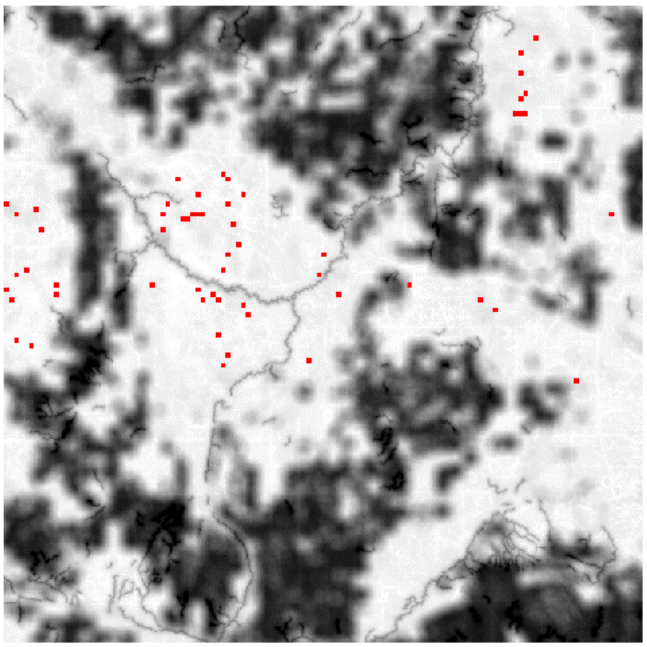

Figure C.1. Contacts overlaid on relative contact probability maps (Dobbin 20022 *in prep*) for Between FF (a), MM Within (b), Within MM (c), and Between MF (d). Simulation contacts were averaged across runs from 10 random seeds and resampled bilinearly to 300 m by 300 m from 30 m by 30 m for visibility. More red is higher contacts while bluer is lower contacts, and no color is no contacts. On the relative contact probability maps, light color is indicative of a higher contact probability.

Appendix D: Contacts as a Function of Parameter for Sensitivity Results

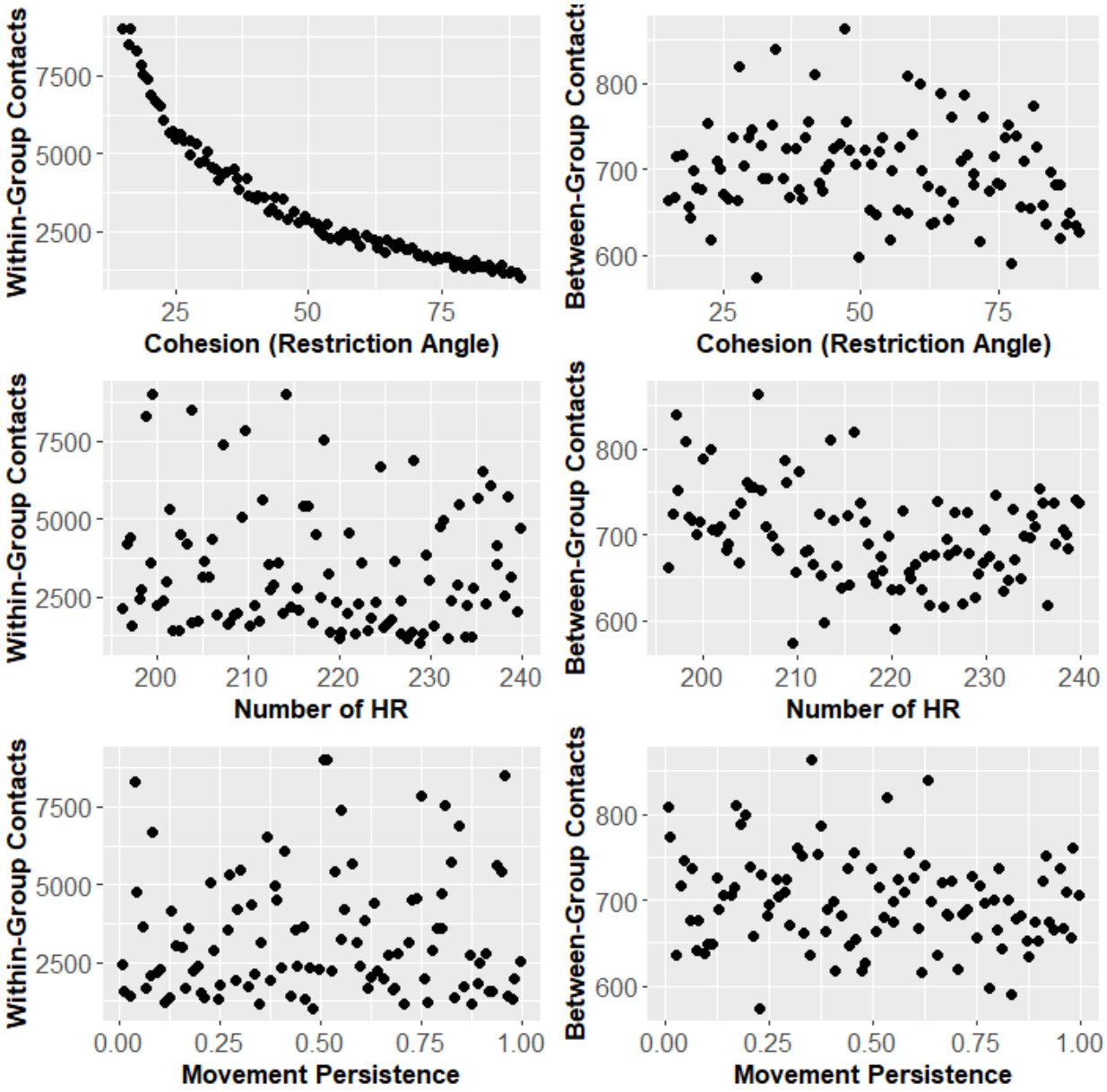

Figure D.1. Total simulation contacts as a function of parameter value. Left panels depict within-group contacts while the right panels depict between-group contacts. The top panels look at the parameter of cohesion, or the restriction angle for the followers. Middle panels look at the number of home ranges on the landscape and therefore also group size since deer density is held contacts. Bottom panels look at the influence of movement persistence (κ_l in turning angle distribution equation). Non-linear relationships can clearly be seen in within-group cohesion.

Appendix E: Inclusion of Individuals in Winter iSSA

Individuals were selected for inclusion in integrated step selection analysis based on the number of observations. For both males and females, the lowest two individuals were removed as outliers and all other individuals were kept (Figure E.1).

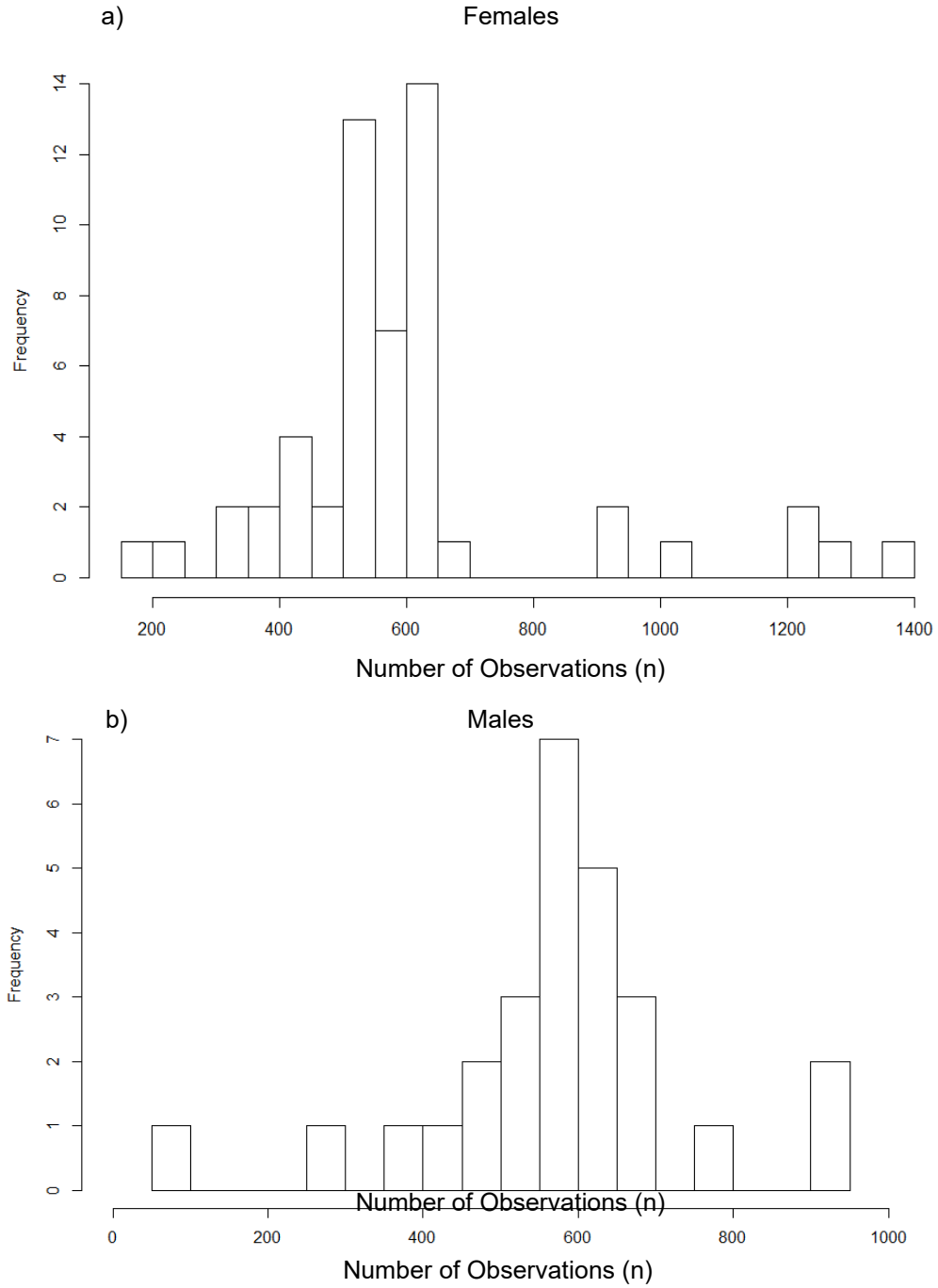

Figure E.1. Histograms of the number of observations obtained from GPS-collared mule deer (54 females (a),27 males (b)) obtained in eastern, Alberta in 2006-2009, and 2017-2020.

Appendix F: Home Range Size Simulation Testing

An experiment was done to determine the relative effect of kappa-1 and kappa-2 on home range size, and which combination gives us the closest to my target home range size of 14.87 km^2, which is based on the median 95% UD area for the winter-spring season. A simulation was run with 6 random seeds and uniform SSF weights, that went through kappa values from 0 to 1 by 0.1 and recorded the distance to home range centre for one of the seven individuals in the group at each timesteps. The 95% quantile was then taken and used to calculate home range size for a given kappa-1, kappa-2 combination. This revealed that the larger the kappa-1: kappa-2 ratio was, the larger the HR size was. This makes sense as kappa-1 controls persistence while kappa-2 control bias towards the HR. In addition to this ratio being important, kappa-2 appears to have an impact on the standard deviation around a point. Therefore, a combination of kappa-1 = 0.4 and kappa-2 = 0.5 was chosen as this combination produced an average HR size of 14.64km^2 with a standard deviation of 2.38km^2. This was the best combination of proximity to the target HR size and low standard deviation

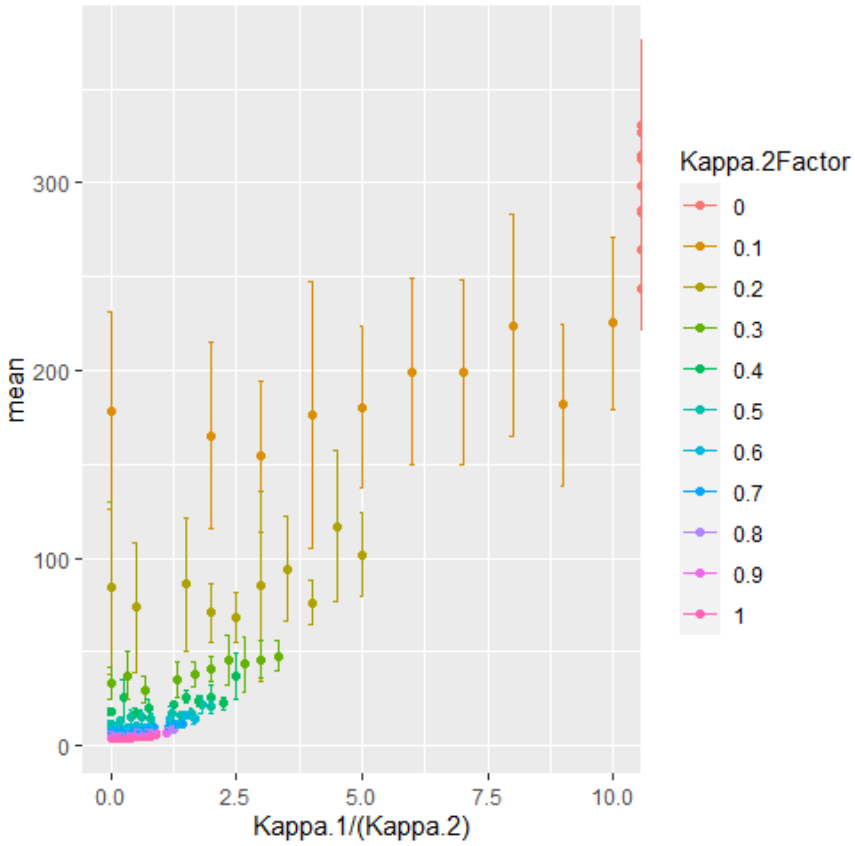

Figure F.1 mean 95% utilization distribution home range size (km^2) as a function of kappa-1 to kappa-2 ratio obtained from simulation with 6 different random seed for each combination. Kappa-1 and kappa-2 were varied from 0 to 1 by 0.1, but were never equal.

Appendix G: Layer Creation Documentation

Hydrology:

Rivers for Saskatchewan were taken from the Government of Canada hydrology layer (Government of Canada, 2017). The North Saskatchewan, South Saskatchewan, and Battle River were taken as the rivers, and all other permanent linear water features were taken as streams. Rivers for Alberta were taken from Altalis and all linear features classified as primary or secondary rivers were included in the rivers layer, whereas all permanent and indefinite streams were included in the streams layer (Altalis, 2018a).

Ruggedness:

Terrain ruggedness index (Riley et al., 1999) was calculated from a digital elevation model in Alberta (Altalis, 2018b) and Saskatchewan (Government of Canada, 2016) that were resampled to 30 m cells. The TRI function in the `spatialEco` R package was then used to transform elevation to terrain ruggedness index (Evans, 2020).

Woody Cover, Agriculture, Edge Density (Dobbin 2022):

To create the percent woody cover, percent agricultural cover and edge density rasters, I used an amalgamation of landcover data produced by Merrill et al. (2013) and the 2015 landcover of Canada (Latifovic, 2019). I primarily used values from Merrill et al. (2013) whenever data was available across WMU 234. Landcover was mapped at 25-meter spatial resolution based on data collected in 2006 using a multi-temporal remote sensing approach, combining Landsat 5 TM satellite imagery and field observations. In areas with no or compromised Landsat imagery (southeast corner of WMU234) I supplemented landcover data with the publicly available 2015 landcover of Canada (Latifovic, 2019). The Canada-wide data was mapped at 30-meter spatial resolution using Operational Land Imager (OLI) Landsat sensor data from 2015. I used nearest neighbor assignment resampling to resize 25-meter cells to 30 meters. To produce woody cover rasters, I defined woody cover (Table H.1.) from both sources and created a binary raster in which cells where delineated between woody cover (1) and no woody cover (0). I then determined the percent woody cover within varying buffer sizes (100, 250, 500, 1000 m). I repeated the same process to produce the percent agricultural cover raster, but created a binary raster that delineated between croplands (1) and non-agricultural landcover types (0). To determine edge density, I used the same binary woody cover raster and created polylines around all clusters of woody cover cells, thereby delineating edge habitat as the boundary between open and covered habitat types. I determined line density of edge habitat within varying buffer sizes (100, 250, 500, 1000 m).

Table G.1. Landcover classifications used to delineate binary rasters for percent woody cover, percent agricultural cover and edge density covariates for Wildlife Management Unit 234. Landcover data from Merrill et al. (2013) derived using a multi-temporal remote sensing approach in 2006 (25x25 m) and from Latifovic (2019) derived using Landsat sensor data from 2015 (30x30 m).

Source	**Landcover Classifications**	
	Woody Cover	**Agriculture**
Merrill et al. 2013	• *Tall shrubland (*Elaeagnus sp.*)* • *Tall shrubland (upland mix)* • *Deciduous* • *Deciduous/Conifer mix*	• *Cultivated/cropland* • *Forage/Moist grassland*
Latifovic 2019	• *Temperate or sub-polar needleleaf forest* • *Mixed forest* • *Temperate or sub-polar broadleaf forest* • *Temperate or sub-polar shrubland*	• *Cropland*

Distance Layers:

We measured the Euclidean distance to the nearest river, well site, road, and stream and then transformed them using a decay function. Decay layers were made using a transformation of exp(-α*distance), with an alpha value of 0.01, as per Nielsen et al. (2009). Testing with univariate models was done to determine the alpha value to be used (Table G.2.). A value of 0.01 was used as it came out as the top model for all but one variable and sex combination. It was decided to use this alpha value for all model layers despite that one outlying combination for the sake of consistency and simplicity.

Table G.2. Univariate model testing results for decay distance layers of wells, roads, rivers, and streams with integrated and non-integrated step-selection functions.

Non-Integrated SSF

Males					**Females**				
AIC									
Alpha	Wells	Roads	Rivers	Streams	Alpha	Wells	Roads	Rivers	Streams
Null	239438.2	239289.8	239438	239417.7	Null	581667.9	581491.5	581658.4	581664
0.006	239393.1	239104.9	239438.1	239428.6	0.006	581590.3	581182.8	581638.3	581643.4
0.007	239386	239089.9	239437.3	239430.5	0.007	581579.6	581150.3	581632.8	581644.4
0.008	239379.8	239077.1	239436	239431.4	0.008	581571.8	581120.8	581627.7	581644.6
0.009	239374.6	239066.1	239434.4	239431.8	0.009	581566.6	581094.1	581622.9	581644.1
0.01	239370.4	239056.9	239432.5	239431.7	0.01	581563.4	581069.8	581618.4	581643.3
Δ AIC									
Alpha	Wells	Roads	Rivers	Streams	Alpha	Wells	Roads	Rivers	Streams
Null	67.8	232.9	5.5	0	Null	104.5	421.7	40	20.7
0.006	22.7	48	5.6	10.9	0.006	26.9	113	19.9	0.1
0.007	15.6	33	4.8	12.8	0.007	16.2	80.5	14.4	1.1
0.008	9.4	20.2	3.5	13.7	0.008	8.4	51	9.3	1.3
0.009	4.2	9.2	1.9	14.1	0.009	3.2	24.3	4.5	0.8
0.01	0	0	0	14	0.01	0	0	0	0

Integrated SSF

Males					**Females**				
AIC									
Alpha	Wells	Roads	Rivers	Streams	Alpha	Wells	Roads	Rivers	Streams
Null	239440.2	239291.4	239440	239419.6	Null	581669.9	581493.5	581660.4	581666
0.006	239395	239105.6	239440	239430.6	0.006	581592.3	581184.5	581640.3	581645.4
0.007	239387.9	239090.6	239439.2	239432.4	0.007	581581.6	581151.9	581634.8	581646.4
0.008	239381.7	239077.7	239438	239433.4	0.008	581573.8	581122.4	581629.7	581646.6
0.009	239376.5	239066.7	239436.4	239433.7	0.009	581568.6	581095.6	581624.9	581646.1
0.01	239372.2	239057.4	239434.5	239433.6	0.01	581565.4	581071.3	581620.4	581645.3
Δ AIC									
Alpha	Wells	Roads	Rivers	Streams	Alpha	Wells	Roads	Rivers	Streams
Null	68	234	5.5	0	Null	104.5	422.2	40	20.7
0.006	22.8	48.2	5.5	11	0.006	26.9	113.2	19.9	0.1
0.007	15.7	33.2	4.7	12.8	0.007	16.2	80.6	14.4	1.1
0.008	9.5	20.3	3.5	13.8	0.008	8.4	51.1	9.3	1.3
0.009	4.3	9.3	1.9	14.1	0.009	3.2	24.3	4.5	0.8
0.01	0	0	0	14	0.01	0	0	0	0

Appendix H: Step-selection function acceptance-rejection method theory

Step-Selection Function Background

The step selection function is a probability density function based on current and previous locations, as well as environmental weightings:

$$f(x_{t+1} \mid x_t, x_{t-1}, Z(x_{t+1}), \psi). \quad (1)$$

In this equation, $x_t \in \Omega \subset \mathbb{R}^2$ represents the position of the animal at time *t*, where Ω is the finite sptatial domain of the animal, and $Z(x) : \Omega \to \mathbb{R}^m$ represents the environmental covariates where *m* is the number of covariates in the model. The vector $\psi \in \mathbb{R}^{m+2}$ represents the parameters in the model where $\psi = (\beta, \alpha, \kappa)$ has components $\beta \in \mathbb{R}^m$ describing covariate weights and $\alpha, \kappa \in \mathbb{R}$ describing step length and turning angle.

The probability density function can be represented by:

$$f(x_{t+1} \mid x_t, x_{t-1}, Z(x_{t+1}), \psi) = \frac{K(x_{t+1}|x_t, x_{t-1}, \kappa, \alpha) w\big(Z(x_{t+1})|\beta\big)}{\int_\Omega K(\xi|x_t, x_{t-1}, \kappa, \alpha) w\big(Z(\xi)|\beta\big) d\xi}. \quad (2)$$

The weighting function $w : \mathbb{R}^m \to \mathbb{R}^+$ describes habitat selection preferences and the numerator represents the location at which a step finishes, x_{t+1}, in terms of the dispersal kernel *K*, and the weighting function *w*. The dispersal kernel itself depends on the locations at the previous two time steps, x_t and x_{t-1}, as well as the step length and turning angle parameters α *and* κ. The denominator ensures that function f is a probability density function, which integrates to 1. The dispersal kernel can be further broken down into a distribution for step length ζ, given by

$$K_1(\zeta \mid \alpha) \quad (3)$$

and a distribution for turning angles, ψ, given by

$$K_2(\psi \mid \kappa). \quad (4)$$

Here the step length is defined by

$$\zeta_t = |x_{t+1} - x_t| \quad (5)$$

and the turning angle is defined as

$$\psi_t = \theta_t - \theta_{t-1} \quad (6)$$

the increment in the bearing where, with $\Delta x_{2t} = x_{2t} - x_{2t-1}$ and $\Delta x_{1t} = x_{1t} - x_{1t-1}$:

$$\theta_t = \tan^{-1}\left(\frac{\Delta x_{2t}}{\Delta x_{1t}}\right) + I(\Delta x_1 < 0) \quad (7)$$

and the components of x_t are given by $x_t = \begin{pmatrix} x_{1t} \\ x_{2t} \end{pmatrix}$ where $I(\Delta x_1 < 0)$ represents the indicator function and is necessary to produce a range spanning the full unit circle due to the symmetry of arctan. Equations 5 to 7 yield the dispersal kernel as

$$K(x_{t+1} \mid x_t, x_{t-1}, \kappa, \alpha) = K_1(\zeta_{t+1} \mid \alpha) K_2(\psi_{t+1} \mid \kappa) \quad (8)$$

where ζ_{t+1} is given in terms of x_{t+1}, x_t by equation 5 and ψ_{t+1} is given in terms of x_{t+1}, x_t, x_{t-1}, and κ by equations 6 and 7

Acceptance-Rejection Method (von Neumann, 1951)

This method simulates via an iterative process of randomly drawing steps until one that is accepted is found and then taking this step. Generating a value for simulation from a probability density function (pdf; *f*) via the rejection-acceptance method requires identifying a pdf, *g*, that is similar to one being simulated, but not identical, and that the ratio $\frac{f}{g}$ is bounded below a constant. When simulating an SSF, the dispersal kernel *K(x)* is taken to be the denominator distribution *g*, while the SSF is the distribution I are simulating from, *f*. This gives us

$$\frac{f(x)}{K(x)} = \frac{w(x)}{\int_{\Omega} K(\xi)w(\xi)d\xi} < c. \tag{9}$$

Rearranged this gives us

$$\frac{f(x)}{K(x)} = \frac{w(x)}{c\int_{\Omega} K(\xi)w(\xi)d\xi} < 1. \tag{10}$$

It is then easily seen that the numerator that will always make this true is when the maximum value of *w* in Ω is used as the denominator constant. For a perspective location, y, one then evaluates equation 11

$$p(y) = \frac{w(y)}{\max\limits_{\xi\in\Omega}\big(w(\xi)\big)} \tag{11}$$

generates a random value, *u*, from uniform(0,1), and then compares the two values. If *u* is less than *p(y)*, then the step is accepted and the individual moves, if not, choose another step and repeat until a step is accepted.

Appendix I: iSSF simulation weight distributions.

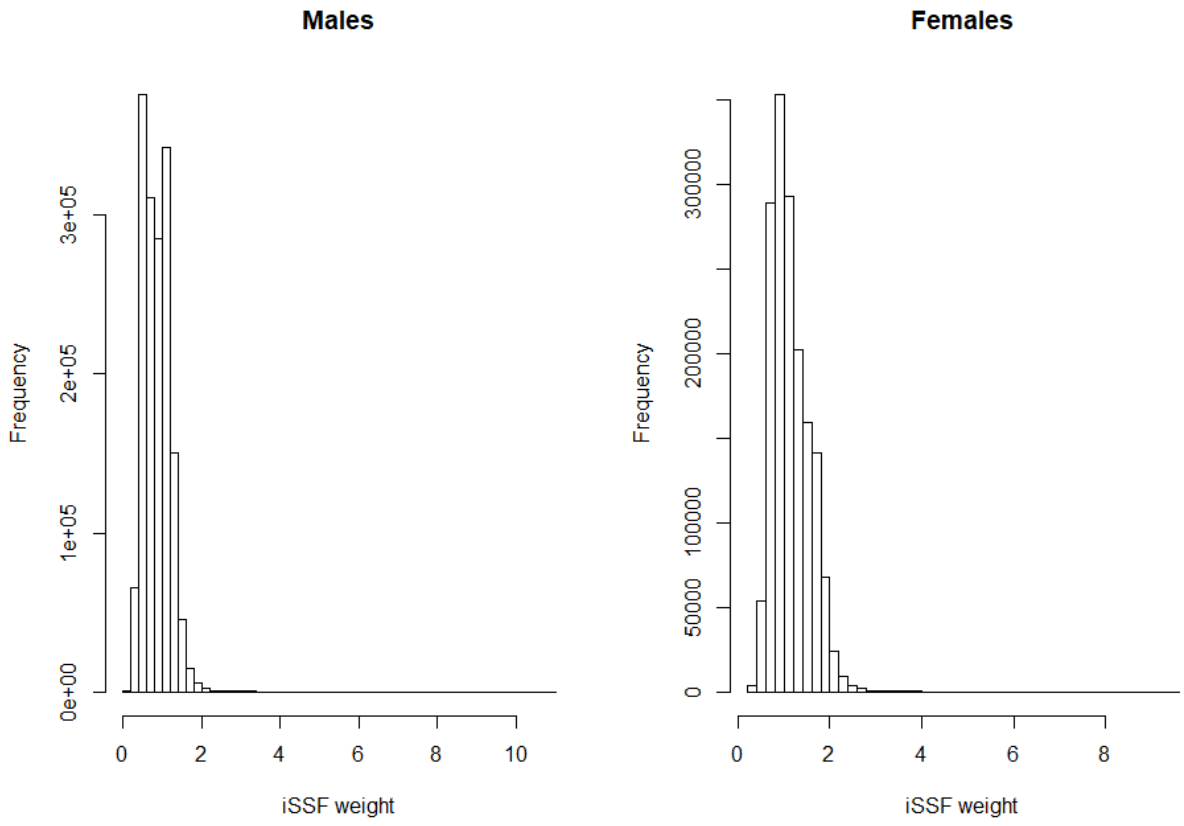

Figure I.1 Distribution of patch iSSF weights for the simulation landscape for males (left) and females (right).

Appendix J: Environmental Layers for Simulation Area

a) Agriculture:

b) Edge:

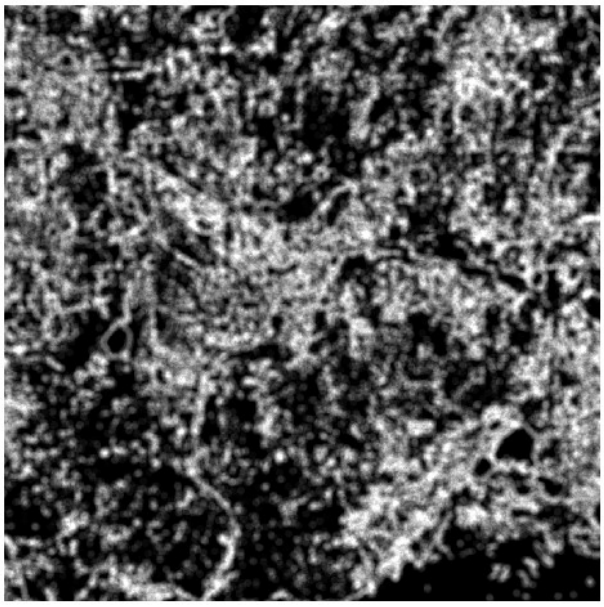

c) Roads:

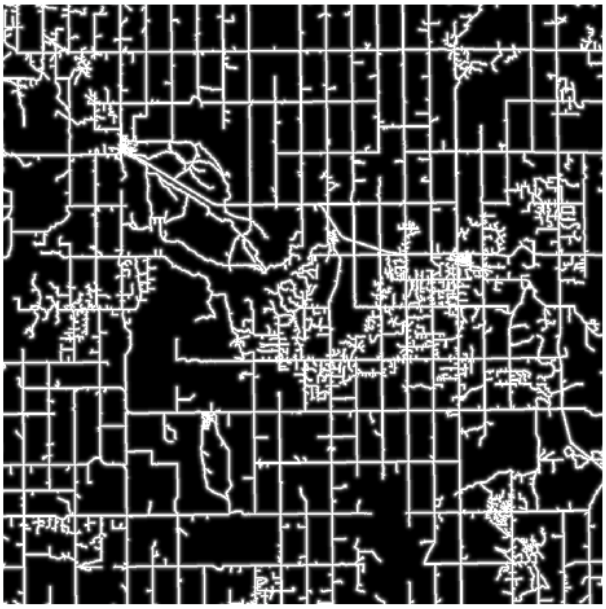

d) Ruggedness:

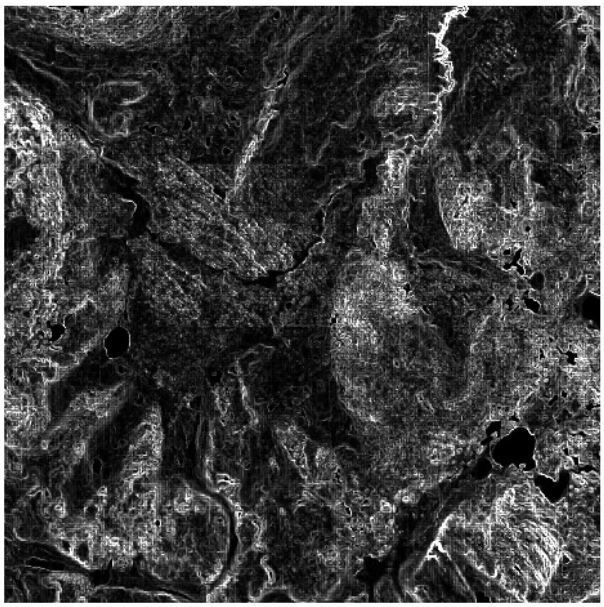

e) Streams:

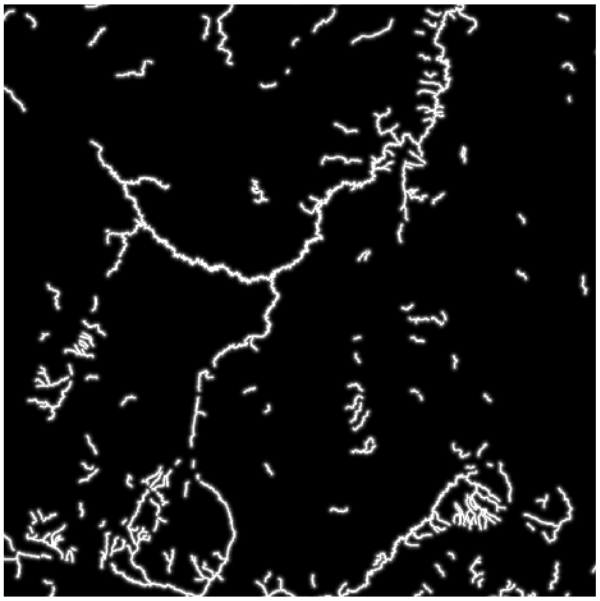

f) Woody Cover:

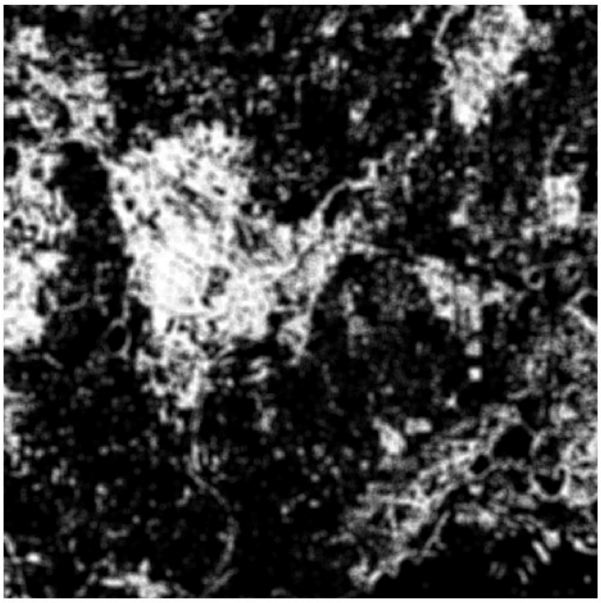

g) Woody Cover Squared:

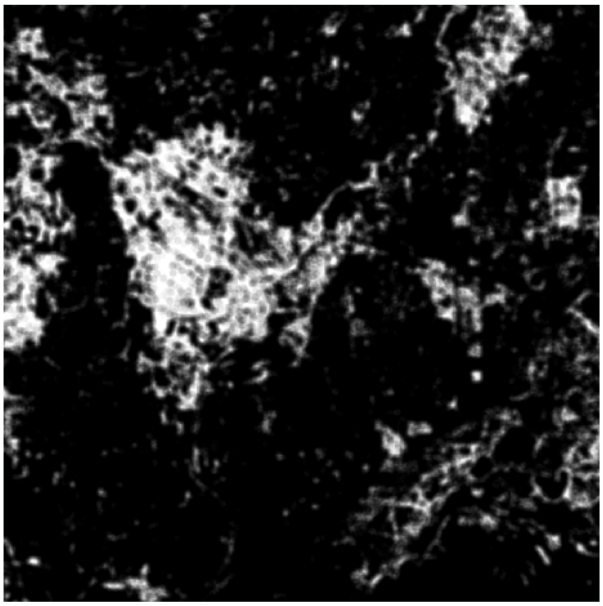

h) Wells:

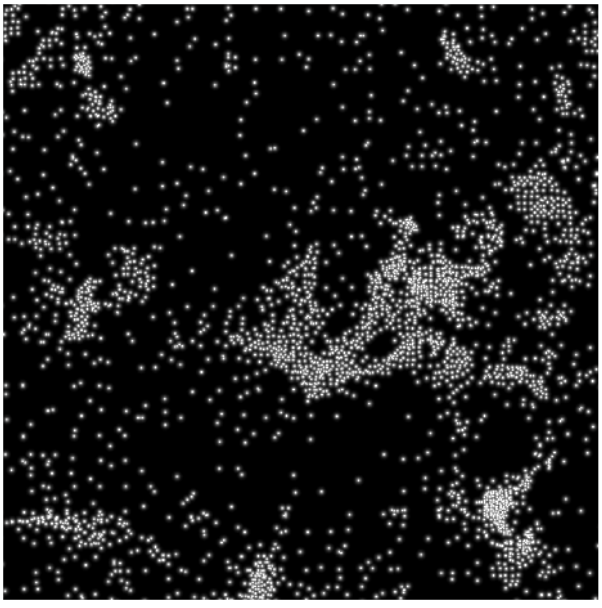

Figure J.1 Simulation area layers for a) proportion agriculture, b) edge density, c) distance to roads, d) terrain ruggedness, e) distance to streams, f) proportion woody cover, g) proportion woody cover squared, and h) distance to wells. Distance to rivers is not included as there is not any variation in my study area.

Appendix K: Within- and Between-Group Contacts by Dyad Type.

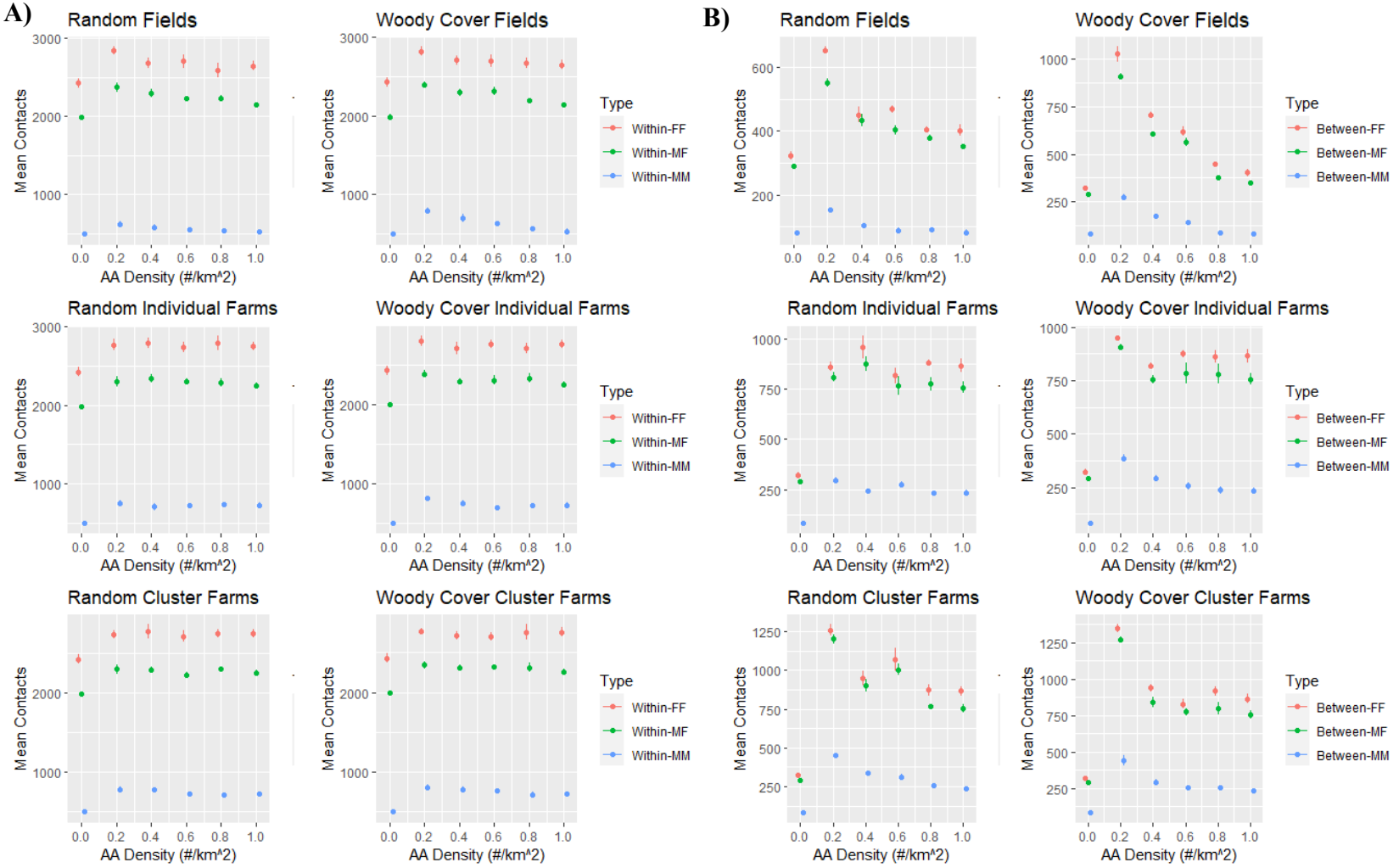

Figure K.1. Mean number of A) within-group contacts and B) between-group contacts for 3 dyad types (FF: female-female, MM: male-male, and MF: male-female) averaged over 5 different random seeds for each attractant density. Error bars represent standard error.

Appendix L: Relationship between Distance to AA and Selection Weight

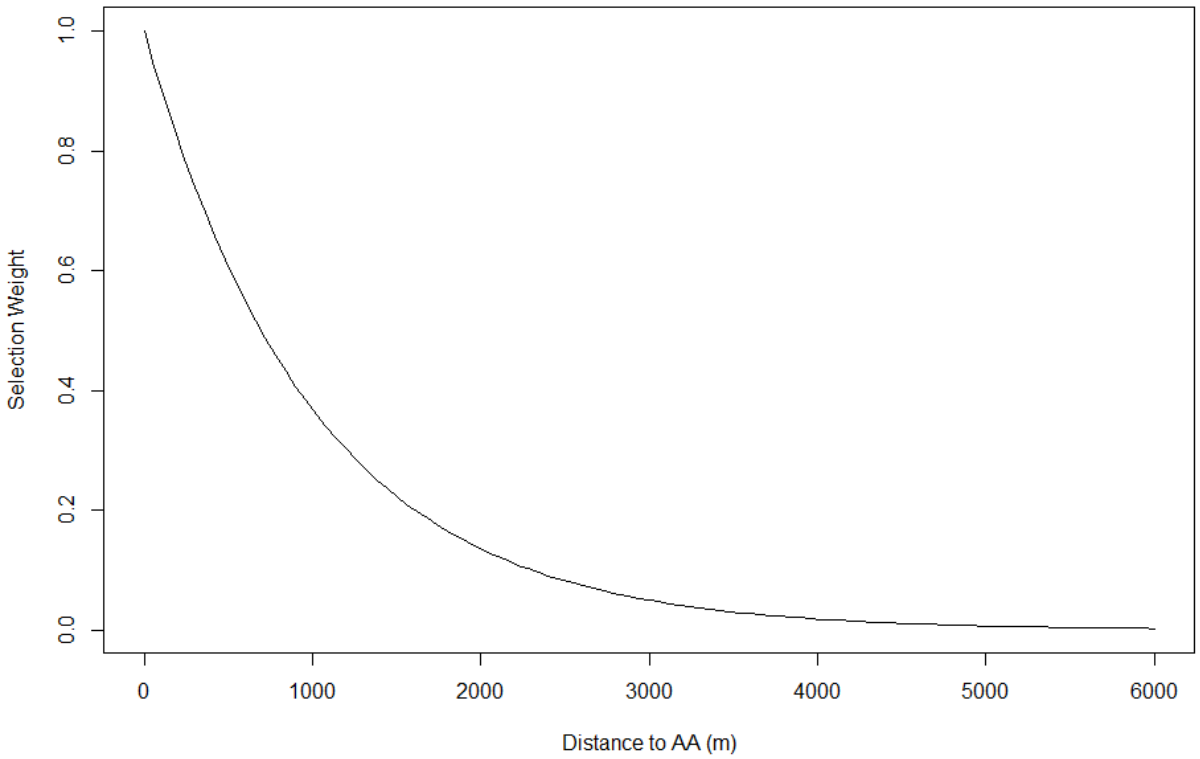

Figure L.1. Statistical relationship between iSSF selection weight and distance to AA (m), using a beta coefficient of -0.001.

Appendix M: Empirical data and fitted relationship for distance to Woody Cover

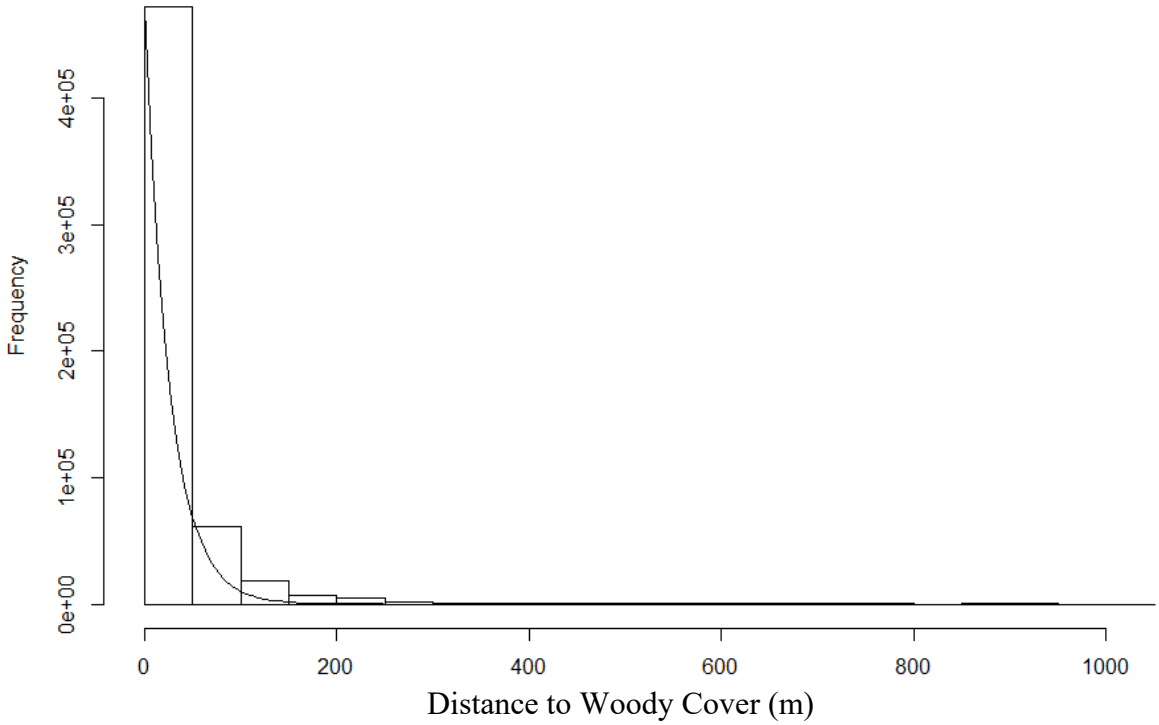

Figure M.1. Relationship between distance to woody cover and frequency GPS observations used to obtain decay coefficient for exponential distribution (-0.0384) used to calculate probability of removed for an AA.